PSFC/RR-01-3

KN1D: A 1-D Space, 2-D Velocity, Kinetic Transport Algorithm For Atomic and Molecular Hydrogen in an Ionizing Plasma

B. LaBombard

August 2001

Plasma Science and Fusion Center
Massachusetts Institute of Technology
Cambridge, MA 02139 USA

This work was supported by the U.S. Department of Energy, Cooperative Grant No. DE-FC02-99ER54512. Reproduction, translation, publication, use and disposal, in whole or in part, by or for the United States government is permitted.

KN1D: A 1-D Space, 2-D Velocity, Kinetic Transport Algorithm for Atomic and Molecular Hydrogen in an Ionizing Plasma

B. LaBombard

Massachusetts Institute of Technology, Plasma Science and Fusion Center,
175 Albany St., Cambridge, MA 02139 USA

Abstract

A set of numerical procedures have been written in IDL[1] to compute the neutral atomic and molecular hydrogen (or deuterium) distribution functions (f_n, f_{H_2}) in a slab-like spatial geometry with specified plasma profiles. This paper reports detailed information about the numerical algorithms and the atomic and molecular physics employed by the code. The top-level numerical procedure (**KN1D**) sets up the model geometry, numerical grid, and boundary conditions and principally calls two sub-programs, one which handles the spatial evolution of the molecular distribution function and the resultant velocity space source of atomic hydrogen (**Kinetic_H2**) and one which handles the spatial evolution of the atomic distribution function (**Kinetic_H**). The model geometry in **KN1D** consists (in increasing values of *x*) of a wall surface, a local limiter shadow and plasma scrape-off layer (SOL) region, a global SOL region, and a core plasma. The input parameters are: the 1-D geometric dimensions (limiter, SOL, and core), plasma profiles (density, ion and electron temperature) and the molecular neutral pressure at the wall. This geometry simulates plasma-neutral interaction that might be expected in the main-chamber of a tokamak with a magnetic divertor or a primary limiter that is remote from the local limiter. If desired, the sub-program units can be run independently by appropriately specifying the plasma profiles, numerical grid, boundary conditions, source profiles, and the other 'unknown' distribution (f_n or f_{H_2}) as input. The numerical algorithm includes charge exchange collisions, electron-impact ionization and dissociation, elastic self-collisions (atomic and molecular), and a variety of elastic cross-collisions (atom-ion, atom-molecule, molecule-ion). Output parameters include: f_n, f_{H_2} and fluid moments, molecular dissociation rate profiles, and molecular ion density and temperature profiles. A number of numerical consistency checks are performed in the code involving mesh size limitations and errors associated with discrete representation of ion and neutral distribution functions. Optionally, the numerical accuracy of f_n and f_{H_2} is checked by direct substitution into the Boltzmann equation and reported at each location on the computational mesh. The source code is entirely written in IDL and is freely available to the community.

Section 1 - KN1D

1.0 Overview

KN1D
Kinetic Neutral 1-D Transport Code

1-D space, 2-D velocity, kinetic transport code for molecular and atomic hydrogen (written in IDL®)

Geometry

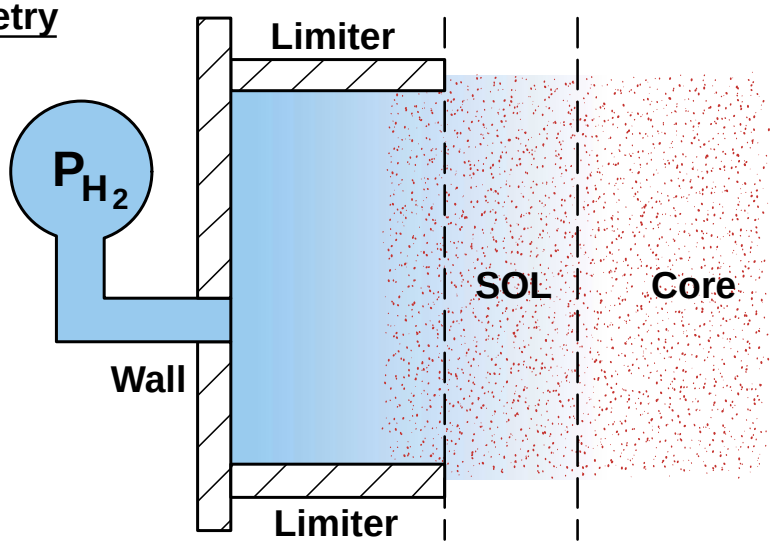

Input

Plasma Backgound (Core, SOL, limiter shadow), 'midplane' neutral pressure, 1D geometry

Boundary Conditions

Zero mass flux onto 'wall' and 'limiter' sides, limiter recycling, RT molecules from wall, 'Black' core plasma

Output

Self-consistent velocity space distributions [$f_{H_2}(v_r,v_x,x)$, $f_H(v_r,v_x,x)$], molecular dissociation, fluid moments, molecular ion density and temperature profiles.

Options Included

Self collisions, cross-collisions: D^+, D_2, D^0, D_2^+ collisions with 'limiter sides'

Fig. 1.1 - Overview of Model Geometry, Input and Output, and Collision Options

1.1 Computational Domain, Inputted Conditions

The primary parameters to be computed are the neutral atomic and molecular distribution functions, f_n, f_{H_2}, and the resultant velocity space source function, S_{H^0}, of neutral hydrogen (or deuterium) atoms over the spatial region $[x_a, x_b]$. Here x_a is the edge of the 'wall' and x_b is some distance into the 'core' region where the neutral flux traveling in the $-x$ direction is negligible. Explicit details of the numerical algorithms used to compute f_n and f_{H_2} can be found in the remaining sections of this report. Background plasma conditions that are specified over the spatial region $[x_a, x_b]$ include:

$n(x)$ - plasma density profile
$T_e(x)$ - electron temperature profile
$T_i(x)$ - ion temperature profile
$v_{xi}(x)$ - plasma ion fluid velocity profile in x-direction ($-x$ is toward the 'wall')

The pressure of room temperature molecular hydrogen at the 'wall' is specified. This results in a Maxwellian distribution function boundary condition on f_{H_2} for positive v_x at the location, $x = x_a$. (Note, deuterium may be specified as the working species in all that follows.) Plasma in the region between the local 'limiter' surfaces is assumed to flow along field lines onto the sides of the limiters, leading to the production of molecular hydrogen. The molecular source at this surface is introduced in the 1-D computation as a room-temperature isotropic Maxwellian distribution function, at rest in the lab frame. As a result, the distance along magnetic field lines (from local limiter surface to local limiter surface) is required for the computation:

$LC(x)$ - connection length to nearest limiters
Zero values of *LC* are treated as infinite (i.e., no limiter at this x location).

The plasma flow to the limiter surface is taken to be proportional to the local sound speed velocity divided by *LC*. The spatial integral of the plasma flow to the limiter sides is scaled so as to achieve a 100% recycling condition (zero net mass flux to/from the limiters and wall). See section 1.2 below.

The effect of molecules and atoms striking the 'side walls' formed by the limiters and/or the pipe connecting to the pressure gauge (see Fig.1) is also optionally included. When an atom or molecule strikes the side walls, it is replaced by a balancing source of molecules with a room-temperature isotropic Maxwellian distribution function, at rest in the lab frame. The rate at which the atoms or molecules are

converted this way is equal to their velocity perpendicular to x divided by 1/2 an effective 'pipe' diameter. This parameter is specified as a profile:

$D(x)$ - effective pipe diameter (optional)

Zero values of *D* are treated as infinite (i.e., no 'pipe' at this x location).

The following elastic and charge-exchange collision options are available by setting these parameters to the value 1 in a common block:

H2_H2_EL -	$H_2 \rightarrow H_2$	elastic self collisions
H2_P_EL -	$H_2 \rightarrow H^+$	elastic collisions
H2_H_EL -	$H_2 \leftrightarrow H$	elastic collisions
H2_HP_CX -	$H_2 \rightarrow H_2^+$	charge exchange collisions
H_H_EL -	$H \rightarrow H$	elastic self collisions
H_P_CX -	$H \rightarrow H^+$	charge exchange collisions
H_P_EL -	$H \rightarrow H^+$	elastic collisions

Explicit details of how these collisions are treated by the algorithm can be found in the description of **Kinetic_H2** and **Kinetic_H** in the sections 2 and 3 of this report.

1.2 Organization of Numerical Algorithm

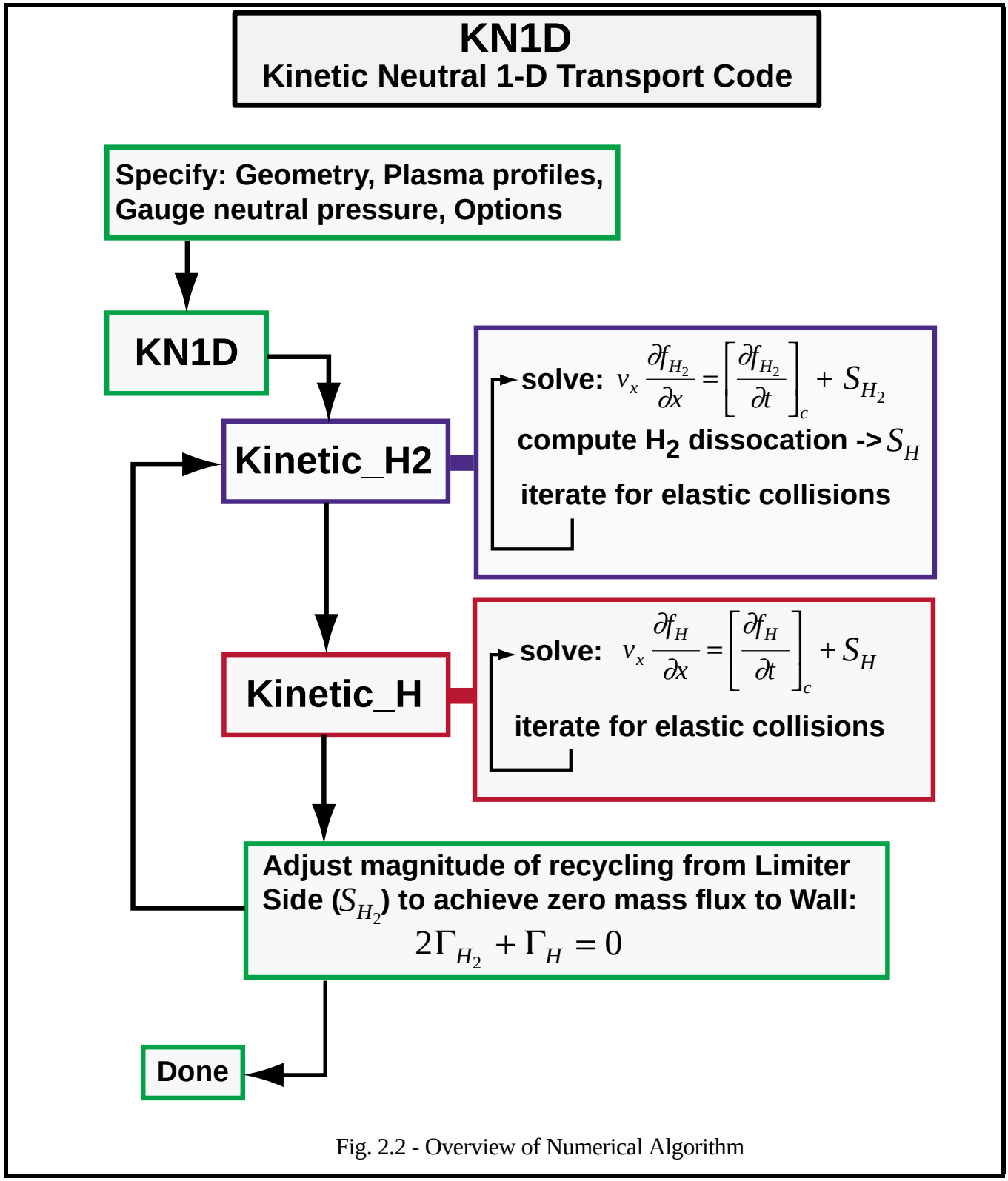

Fig. 2.2 - Overview of Numerical Algorithm

KN1D iteratively calls routines **Kinetic_H2** and **Kinetic_H** to solve the atomic/molecular neutral transport problem. Iterations internal to **Kinetic_H2** and **Kinetic_H** may also occur as these algorithms resolve the effect of elastic collisions. The magnitude of the total molecular flux evolving from the limiter side surfaces from plasma recycling (with a profile shape that matches the profile of plasma flow to the limiter) is adjusted on each iteration, achieving the condition that the total mass flux to the wall and limiter surfaces is zero (100% recycling). See Appendix C for a detailed discussion of the iteration algorithm that is employed.

1.3 Output Parameters

The following parameters are directly outputted via the argument list of the IDL procedure, **KN1D.pro**. If desired, other output parameters, including f_n, f_{H_2} are available via common blocks in **Kinetic_H2.pro** and **Kinetic_H.pro**.

1.3.1 Molecules

xH2 - cross-field coordinate for outputted molecular quantities (m)
nH2 - neutral molecular density profile (m^{-3})
GammaxH2 - neutral flux profile (m^{-2} s^{-1})
TH2 - molecular neutral temperature profile (m^{-3})
qxH2_total - molecular neutral heat flux profile (W m^{-2})
nHP - molecular ion density profile (m^{-3})
THP - molecular ion temperature profile (eV)
SH - atomic source profile (m^{-3} s^{-1})
SP - ion source profile (m^{-3} s^{-1})

1.3.2 Atoms

xH - cross-field coordinate for outputted atomic quantities (m)
nH - neutral atomic density profile (m^{-3})
GammaxH - neutral flux profile (m^{-2} s^{-1})
TH - atomic neutral temperature profile (m^{-3})
qxH_total - atomic neutral heat flux profile (W m^{-2})
NetHSource - net source of atomic neutrals from molecular dissociation and recombination minus ionization (m^{-3})
Sion - atomic ionization rate (m^{-3})
QH_total - net rate of total energy transfer to atomic neutral species (W m^{-3})
SideWallH - atomic neutral sink rate arising from atoms hitting the limiter or 'pipe' side walls (m^{-3} s^{-1}). Wall collisions result in the destruction of atoms. This parameter corresponds to a resulting source of molecular neutrals in Kinetic_H2. (molecular source = 2 times *SideWallH*)
Lyman - Resultant Lyman-alpha emissivity (W m^{-3}) using rate coefficients from collisional-radiative model of L. C. Johnson and E. Hinnov[2]

Balmer - Resultant Balmer-alpha emissivity (W m^{-3}) using rate coefficients from collisional-radiative model of L. C. Johnson and E. Hinnov

1.3.3 Total Mass Flux

GammaHLim - 2 times *GammaxH2* plus *GammaxH* at a spatial location corresponding to the leading edge of the local limiters (m^{-2} s^{-1})

1.4 IDL Program

The complete call to the IDL procedure, **`KN1D.pro`**, is listed below:

```
;+
; KN1D.pro
;
;    Computes the molecular and atomic neutral profiles for inputted profiles
; of Ti(x), Te(x), n(x), and molecular neutral pressure, GaugeH2, at the boundary
; using IDL routines Kinetic_H and Kinetic_H2. Molecular densities, ionization
; profiles, atomic densities and moments of the atomic distribution function, such
; as T0(x), Qin(x), qx0_total(x),... are returned.
;
;     It is assumed that molecular neutrals with temperature equal to the wall
; temperature (~ 1/40 eV) are attacking the plasma at x=x(0).
;
; History: First coding 5/1/2001  -  B. LaBombard
;_____________________________________________________________________________
;
pro  KN1D,x,xlimiter,xsep,GaugeH2,mu,Ti,Te,n,vxi,LC,PipeDia,$
        xH2,nH2,GammaxH2,TH2,qxH2_total,nHP,THP,SH,SP,$
       xH,nH,GammaxH,TH,qxH_total,NetHSource,Sion,QH_total,SideWallH,Lyman,Balmer,$
      GammaHLim,$
       truncate=truncate,refine=refine,File=File,NewFile=NewFile,$
      ReadInput=ReadInput,$
       error=error,compute_errors=compute_errors,$
       plot=plot,debug=debug,debrief=debrief,pause=pause,$
       Hplot=Hplot,Hdebug=Hdebug,Hdebrief=Hdebrief,Hpause=Hpause,$
       H2plot=H2plot,H2debug=H2debug,H2debrief=H2debrief,H2pause=H2pause
;_____________________________________________________________________________
;
; Input:
;       x        - fltarr(nx), cross-field coordinate (meters)
;      xlimiter  - float, cross-field coordinate of limiter edge (meters) (for
;                     graphic on plots)
;       xsep     - float, cross-field coordinate separatrix (meters) (for graphic
;                     on plots)
;       GaugeH2  - float, Molecular pressure (mtorr)
;       mu       - float, 1=hydrogen, 2=deuterium
;       Ti       - fltarr(nx), ion temperature profile (eV)
;       Te       - fltarr(nx), electron temperature profile (eV)
;       n        - fltarr(nx), density profile (m^-3)
;       vxi      - fltarr(nx), plasma velocity profile [negative is towards 'wall'
;                     (m s^-1)]
;       LC       - fltarr(nx), connection length (surface to surface) along field
;                     lines to nearest limiters (meters)
;                  Zero values of LC are treated as LC=infinity.
;      PipeDia   - fltarr(nx), effective pipe diameter (meters)
;                  This variable allows collisions with the 'side-walls' to be
;                     simulated.
;                  If this variable is undefined, then PipeDia set set to zero.
;                     Zero values of PipeDia are ignored (i.e., treated as an infinite
;                     diameter).
;
;   Keyword Input:
;      truncate - float, this parameter is also passed to Kinetic_H and
;                     Kinetic_H2. fH and fH2 are refined by iteration via routines
;                     Kinetic_H2 and Kinetic_H until the maximum change in molecular
;                     neutral density (over its profile) normalized to
;                  the maximum value of molecular density is less than this
;                  value in a subsequent iteration. Default value is 1.0e-3
;
;       refine   - if set, then use previously computed atomic and molecular
;                     distribution functions stored in internal common block (if any)
;                     or from FILE (see below) as the initial 'seed' value'
```

```
;
;          file  - string, if not null, then read in 'file'.kn1d_mesh save set and
;                     compare contents to the present input parameters and
;                     computational mesh. If these are the same
;                  then read results from previous run in 'file'.kn1d_H2 and
;                     'file'.kn1d_H.
;
;       Newfile - if set, then do not generate an error and exit if
;                     'file'.KN1D_mesh or 'file'.KN1D_H2
;                  or 'file'.KN1D_H do not exist or differ from the present input
;                     parameters. Instead, write
;                  new mesh and output files on exiting.
;
;     ReadInput - if set, then reset all input variables to that contained in
;                     'file'.KN1D_input
;
;   Collision options inputted via common block KN1D_collisions (default parameter
;   values are 1 for all collisions):
;
      common KN1D_collisions,H2_H2_EL,H2_P_EL,H2_H_EL,H2_HP_CX,H_H_EL,H_P_EL,$
                             H_P_CX,Simple_CX
;
;               H2_H2_EL - if set, then include H2 -> H2 elastic self collisions
;              H2_P_EL       - if set, then include H2 -> H(+) elastic collisions
;              H2_H_EL       - if set, then include H2 <-> H elastic collisions
;               H2_HP_CX - if set, then include H2 -> H2(+) charge exchange
;                             collisions
;              H_H_EL        - if set, then include H -> H elastic self collisions
;                 H_P_CX - if set, then include H -> H(+) charge exchange
;                             collisions
;                 H_P_EL - if set, then include H -> H(+) elastic collisions
;              Simple_CX - if set, then use CX source option (B): Neutrals are born
;                             in velocity with a distribution proportional to the
;                                local ion distribution function. Simple_CX=1 is default.
;
;  Output:
;    Molecular info
;       xH2       - fltarr(nxH2), cross-field coordinate for molecular quantities
;                      (meters)
;       nH2       - fltarr(nxH2), neutral moleular density profile (m^-3)
;       GammaxH2  - fltarr(nxH2), neutral flux profile (# m^-2 s^-1)
;       TH2       - fltarr(nxH2), molecular neutral temperature profile (m^-3)
;      qxH2_total - fltarr(nxH2), molecular neutral heat flux profile (watts m^-2)
;       nHP       - fltarr(nxH2), molecular ion density profile (m^-3)
;       THP       - fltarr(nxH2), molecular ion temperature profile (eV)
;       SH        - fltarr(nxH2), atomic source profile (m^-3 s^-1)
;       SP        - fltarr(nxH2), ion source profile (m^-3 s^-1)
;
;    Atomic info
;       xH        - fltarr(nxH), cross-field coordinate for atomic quantities
;                      (meters)
;       nH        - fltarr(nxH), neutral atomic density profile (m^-3)
;       GammaxH   - fltarr(nxH), neutral flux profile (# m^-2 s^-1)
;       TH        - fltarr(nxH), atomic neutral temperature profile (m^-3)
;      qxH_total  - fltarr(nxH), atomic neutral heat flux profile (watts m^-2)
;     NetHSource  - fltarr(nxH), net source of atomic neutrals from molecular
;                      dissociation and recomb minus ionization (# m^-3)
;         Sion    - fltarr(nxH), atomic ionization rate (# m^-3)
;         QH_total- fltarr(nxH), net rate of total energy transfer to atomic neutral
;                      species (watts m^-3)
;       SideWallH - fltarr(nxH), atomic neutral sink rate arising from hitting the
;                      'side walls' (m^-3 s^-1)
;                    Unlike the molecules in Kinetic_H2, wall collisions result in
;                      the destruction of atoms.
;                    This parameter is used to specify a resulting source of
;                      molecular
;                    neutrals in Kinetic_H2. (molecular source = 2 times SideWallH)
;         Lyman     - fltarr(nxH), Lyman-alpha emissivity (watts m^-3) using rate
;                      coefficients of L.C.Johnson and E. Hinnov
;         Balmer    - fltarr(nxH), Balmer-alpha emissivity (watts m^-3) using rate
;                      coefficients of L.C.Johnson and E. Hinnov
;
;    Combined
;       GammaHLim - float, 2 times GammaxH2 plus GammaxH at edge of limiter
;                      (# m^-2 s^-1)
;-------------------------------------------------------------------------------
;-
```

Section 2 - Kinetic_H2: A 1-D Kinetic Neutral Transport Algorithm for Hydrogen Molecules in an Ionizing and Dissociating Plasma

The numerical algorithm embodied in **`Kinetic_H2`** is summarized in the following graphic:

Kinetic_H2
1-D Molecular Neutral Transport Code

Solve: $$v_x \frac{\partial f_{H_2}}{\partial x} = \left[\frac{\partial f_{H_2}}{\partial t}\right]_c + S_{H_2}$$

by method of successive collision generations (e.g. [a])

10 Electron-impact reactions included:

$e^- + H_2 \rightarrow e^- + H_2^+ + e^-$ (R1)

$e^- + H_2 \rightarrow e^- + H(1s) + H(1s)$ (R2)

. . . . .

$H_2^+ \leftrightarrow H^+$ **energy equilbration model**

$e^- + H_2^+ \rightarrow e^- + H^+ + H(1s)$ (R7)

. . . . .

$e^- + H_2^+ \rightarrow H(1s) + H^*(n \geq 2)$ (R10)

Multistep corrections to reaction rates based on CR model of Sawada [b] are applied

Velocity space source distribution for H are computed using dissociation energies

Elastic collisions included using a BGK model [c]:

$H_2 + H^+ \rightarrow H_2 + H^+$ (R11)

$H_2 + H \rightarrow H_2 + H$ (R12)

$H_2 + H_2 \rightarrow H_2 + H_2$ (R13)

Collision frequencies set by:

Momentum transfer rate for mixed binary collisions

Temperature isotropization rate for self collisions

Molecular charge exchange is included

$H_2 + H_2^+ \rightarrow H_2^+ + H_2$ (R14)

[a] PFC Report: www.psfc.mit.edu/library/00rr/00RR009

[b] Sawada, K. and Fujimoto, T., Journal of Applied Physics **78** (1995) 2913.

[c] Bhatnagar, P.L., Gross, E.P., and Krook, M., Phys. Rev. **94** (1954) 511.

Fig. 2.1 - Overview of Molecular Neutral Transport Algorithm

2.0 Overview

The IDL procedure **`Kinetic_H2`** computes the neutral molecular hydrogen (or deuterium) distribution function, f_{H_2}, in a slab geometry for inputted plasma profiles (density, ion and electron temperature). The resulting velocity-space source of atomic ground-state hydrogen (or deuterium) is also computed, accounting for Frank-Condon dissociation energies. The distribution functions are described in terms of two velocity components (making use of the rotational symmetry in velocity space about the *x*-axis) and one spatial component (*x*). The neutral molecular flux density entering the edge of the slab and its velocity distribution (positive *x* velocities) are prescribed boundary conditions. The algorithm evolves f_{H_2} in space accounting for elastic and charge exchange collisions, electron-impact ionization, dissociation, and dissociative ionization of the molecules. A spatially distributed source of wall-temperature molecules may be inputted. Reaction rates and hydrogen atom reaction product energies are evaluated using data compiled by Janev [3]. Corrections are applied to the to the production rate of molecular hydrogen ions based on results from the collisional radiative model of Sawada[4], accounting for the influence of multistep electron-impact excitation of electronic and vibrational states of hydrogen molecules. Hydrogen atoms formed initially in excited states are counted as ground-state hydrogen atoms. Thus, multistep ionization processes are not included in the hydrogen atom production rate computation, restricting the background plasma density in the volume of interest to the range where $n_e \leq$ ~10^{19} m^{-3} and $T_e >$ ~5 eV [5] [4]. However, since for $T_e >$ ~5 eV over 90% of the hydrogen atoms are formed directly in the ground-state, this approximation still yields a reliable estimate of the ground-state hydrogen atom velocity source distribution in typical tokamak scrape-off layer plasmas. The output of the computation is $f_{H_2}(v_x, v_r, x)$ and velocity moments of f_{H_2} including molecular neutral density, fluid velocity, temperature, pressure, diagonal elements of the stress tensor, and heat fluxes. In addition, the spatial profiles of the net rate of energy and *x*-directed momentum transfer between unlike species and to the 'side walls' are outputted. A number of numerical consistency checks are performed in the code involving mesh size limitations and errors associated with discrete representation of distribution functions. The accuracy of the numerical solution of f_{H_2} is optionally checked by direct substitution into the Boltzmann equation and reported at each point on the computational mesh.

2.1 Method

2.1.1 Computational Domain, Inputted Conditions

The parameter to be computed is the neutral molecule distribution function, f_{H_2}, and the resultant velocity space source function, S_{H^0}, of neutral hydrogen (or deuterium) atoms over the spatial region $[x_a, x_b]$. It is assumed that all velocity space distribution functions have rotational symmetry about the

v_x axis so that they can be described in terms of two velocity coordinates and one spatial coordinate, e.g., $f_{H_2} = f_{H_2}(v_x, v_r, x)$, with $v_r^2 = v_y^2 + v_z^2$.

The computational domain is specified by input parameters as

$$-v_{x,\max} \le v_x \le v_{x,\max}, \quad v_{r,\min} \le v_r \le v_{r,\max}, \quad x_a \le x \le x_b.$$

The boundary conditions and constraints on the molecular neutral distribution function are:

$f_{H_2}(v_x > 0, v_r, x_a)$ - specified (input)

$f_{H_2}(v_x < 0, v_r, x_b) = 0$

$\frac{\partial f_{H_2}}{\partial x}(v_x = 0, v_r, x)$ - finite

Background plasma conditions are inputted over spatial region $[x_a, x_b]$:

$n(x)$ - plasma density profile

$T_e(x)$ - electron temperature profile

$T_i(x)$ - ion temperature profile

$v_{xi}(x)$ - plasma ion fluid velocity profile in x-direction ($-x$ is towards the 'wall')

A spatially distributed source, S_{H_2}, of wall-temperature molecular hydrogen (or deuterium) may also be specified over the spatial region $[x_a, x_b]$:

$S_{H_2}(x)$- wall-temperature molecular source (optional)

An effective 'pipe diameter', may also be specified to simulate the effect of collisions of molecules with 'side walls'at room temperature that may be present in the actual geometry.

$D(x)$ - effective pipe diameter (optional)

Background atomic hydrogen distribution function is inputted over spatial region $[x_a, x_b]$:

$f_n(v_x, v_r, x)$ - atomic hydrogen distribution function

2.1.2 Atomic and Molecular Physics

2.1.2.1 Electron-Impact Reactions involving Neutral Hydrogen Molecules

The following electron impact ionization and dissociation reactions involving H_2 are included, ordered roughly from most to least importance:

$$e^- + H_2 \rightarrow e^- + H_2^+ + e^- \tag{2.R1}$$

$$e^- + H_2 \rightarrow e^- + H(1s) + H(1s)$$
$$E_{H,\min} = 2, E_{H,\max} = 4.25, \langle E_H \rangle \approx 3\,\text{eV} \tag{2.R2}$$

$$e^- + H_2 \rightarrow e^- + H(1s) + H^*(2s)$$
$$E_{H,\min} = 0.0, E_{H,\max} = 0.55, \langle E_H \rangle \approx 0.3\ \text{eV} \tag{2.R3}$$

$$e^- + H_2 \rightarrow e^- + H^+ + H(1s) + e^-$$
$$E_e \approx 3T_e / 2, \langle E_H \rangle \approx \begin{Bmatrix} 0.5(E_e - 18) & ; & 18 \le E_e < 18.5 \\ 0.25 & ; & 18.5 \le E_e < 26 \\ 0.5(E_e - 26) & ; & 26 \le E_e < 41.6 \\ 7.8 & ; & 41.6 < E_e \end{Bmatrix} \tag{2.R4}$$

$$e^- + H_2 \rightarrow e^- + H^*(2p) + H^*(2s)$$
$$E_{H,\min} = 2.85, E_{H,\max} = 5.85, \langle E_H \rangle \approx 4.85\ \text{eV} \tag{2.R5}$$

$$e^- + H_2 \rightarrow e^- + H(1s) + H^*(n=3)$$
$$E_{H,\min} = 1.25, E_{H,\max} = 3.75, \langle E_H \rangle \approx 2.5\ \text{eV} \tag{2.R6}$$

Figure 2.2 plots the rates for these reactions as a function of electron temperature.

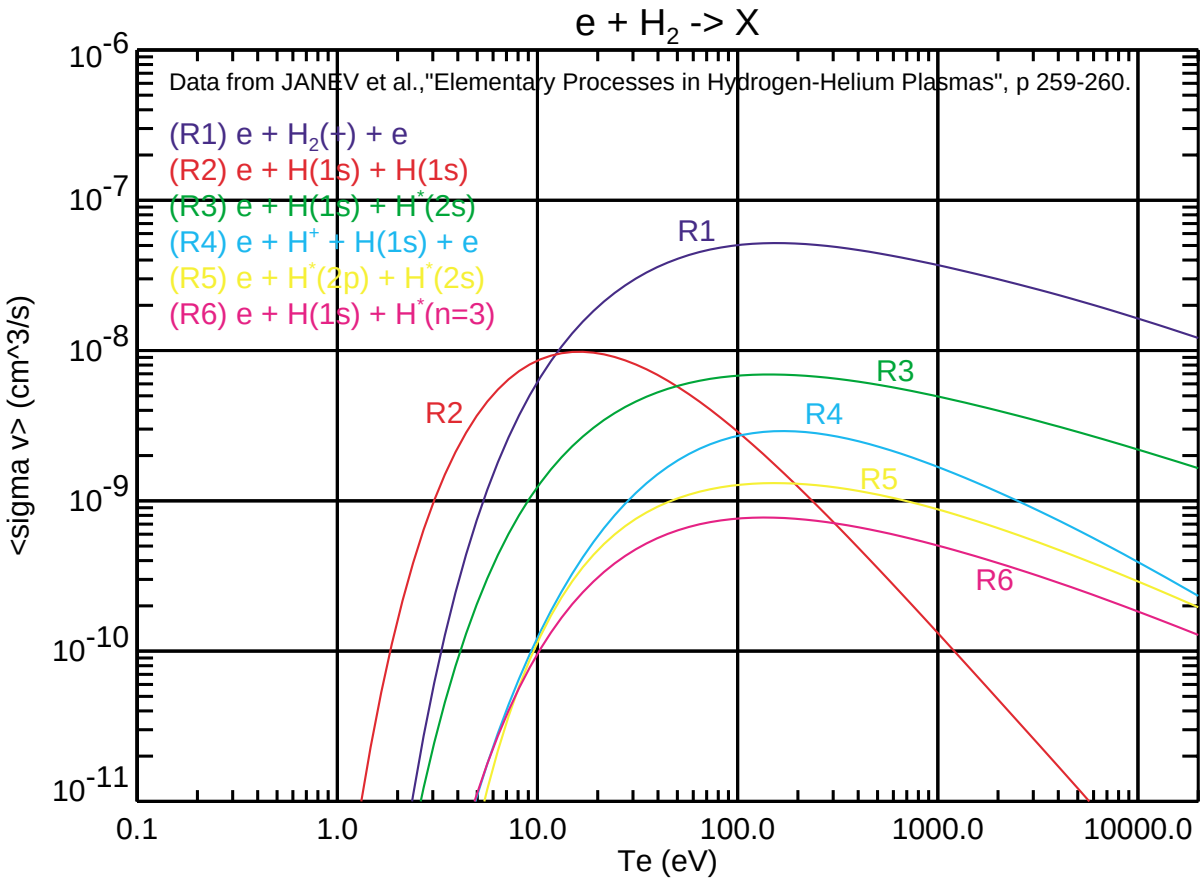

Fig. 2.2 -Electron impact ionization/dissociation ratesfor molecular hydrogen as a function of Te.

All 6 reactions are included in the kinetic transport algorithm. Note that $H^*(2s)$ preferentially converts to $H^*(2p)$ via electron impact rather than ionizes [3]. In plasmas where multistep collisional excitation can be neglected ($n_e \leq \sim 10^{19}$ m^{-3}) [5], this state subsequently decays by radiative transition (L_α) to $H(1s)$ ($A_{2p-1s} = 6.265x10^8 s^{-1}$). Therefore the production of $H^*(2s)$ by reaction R3 and $H^*(2s)$ and $H^*(2p)$ by reaction 2.R5 may be treated as production of $H(1s)$ at the same rate. In the same way, the production of $H^*(n=3)$ from reaction 2.R6 may be treated as production of $H(1s)$ at the same rate. A similar conclusion based on a more detailed analysis was reached by Sawada [4] in analyzing the ground state atomic hydrogen contributions from reactions 2.R3, 2.R5, and 2.R6 (see extended discussion below).

The average energy and energy range of the atomic hydrogen products resulting from the molecular breakup is shown next to the reactions listed above. For the computation of $\langle E_H \rangle$ in reaction 2.R4, the incident energy of the electron is taken to be equal to the average energy in a maxwellian

distribution, $E_e \approx 3T_e / 2$. The reaction products are assumed to have an isotropic velocity distribution function, i.e., the influence of the initial molecular ion velocity (which should be much less than the reaction product velocities, on average) is neglected.

2.1.2.2 Multistep Corrections to Electron-Impact Molecular Hydrogen Reaction Rates

Sawada has published results from a collisional-radiative model for hydrogen molecules in a plasma [4]. The system consists the ground state, stable electronically excited states and the ionic state of the hydrogen molecule. Effective rate coefficients have been computed for the dominate pathways that lead to production of electrons, hydrogen atoms, hydrogen ions, and molecular ions. Using the results from this study, we can examine the influence of multistep processes on the rates of the above reactions 2.R1-2.R6 and the likely fates of their reaction products. The results from the two cases treated in [4] can be considered: (1) 'no v correction', i. e., the initial state of a transition (radiative or collisional) is taken to be in the stable electronic stage that is in the vibrational-rotational ground state, and (2) 'v corrected', i. e., the effects of a distribution of vibrational levels of the initial state, determined by electron-impact excitation, is estimated.

2.R1: $e^- + H_2 \rightarrow e^- + H_2^+ + e^-$

Sawada computed rate coefficients for the direct ionization pathway from the ground state (reaction R1 above, noted as *path I1*) and a multistep pathway accounting for electron-impact electronic excitation of the hydrogen molecule resulting in the increased production of molecular ions (*path I2*):

$$e^- + H_2 \rightarrow H_2^* + e^-;\ e^- + H_2^* \rightarrow\rightarrow H_2^{**} + e^-;\ e^- + H_2^{**} \rightarrow e^- + H_2^+ + e^-$$

The reaction rate for R1 (*path I1*) is unchanged in case (1) of the CR model. For case (2), the reaction increases by a ratio of 3.7/2 for low densities (T_e =20 eV) and then the rate systematically reduces for $n_e > \sim 10^{19}$ m^{-3}, but this trend only results in a 25% reduction (of the 3.7/2 factor) when the density reaches $n_e \sim 10^{20}$ m^{-3}. On the other hand, the multistep pathway (*path I2*) rises dramatically (from essentially zero) with electron density and can be come comparable in contribution to *path I1* at low T_e and high n_e [For case (1), rate of path I2 = path I1 at $T_e \sim 5$ eV and $n_e \sim 6 \times 10^{19}$ m^{-3}]. However, the effect of vibrational levels [case (2)] leads to an overall reduction in the reaction rate of *path I2*. The net effect is that the sum of *path I1* and *path I2* leads to a nearly constant reaction rate that is a factor 3.7/2 times that shown for reaction 2.R1 in Fig. 2.2 above.

Therefore, for this transport model, the constant factor 3.7/2 is applied to the reaction rate, 2.R1, in Fig. 2.2.

2.R2: $e^- + H_2 \rightarrow e^- + H(1s) + H(1s)$

Sawada computed rate coefficients for the direct dissociation pathway from the ground state (reaction 2.R2 above, noted as *path H1*) and a multistep pathway accounting for electron impact excitation of the hydrogen molecule resulting in the increased production of atomic hydrogen dissociation products (*path H2*):

$$e^- + H_2 \rightarrow H_2^* + e^-;\ e^- + H_2^* \rightarrow\rightarrow H_2^{**} + e^-;\ e^- + H_2^{**} \rightarrow\rightarrow e^- + H(1s) + H(1s)$$

The reaction rate for 2.R2 (*path H1*) is unchanged in case (1) and is increased uniformly by ~10% for case (2) of the CR model (T_e =20 eV). For case (1), *path H2* is roughly 0.5 times the reaction rate of *path H1* for a density range $10^{14} < n_e < 10^{17}$ m^{-3} and then falls below this value as the density increases. For case (2) the same relative factor between the rates for *path H1* and *path H2* is seen over the entire density range. Therefore the reaction rates for *path H2* (top number) can be scaled from *path H1* (bottom number) using the following table:

Table 1 - Ratio of reaction rates for *path H2* / *path H1* from Fig. 6 in Sawada [4]

	10^{14} m^{-3}	**10^{17} m^{-3}**	**10^{18} m^{-3}**	**10^{19} m^{-3}**	**10^{20} m^{-3}**	**10^{21} m^{-3}**	**10^{22} m^{-3}**
5 eV	2.2/5.3	2.2/5.3	2.1/5.3	1.9/5.3	1.2/5.3	1.1/5.3	1.05/5.3
20 eV	5.1/10.05	5.1/10.05	4.3/10.05	3.1/10.05	1.5/10.05	1.25/10.05	1.25/10.05
100 eV	1.3/2.1	1.3/2.1	1.1/2.1	0.8/2.1	0.38/2.1	0.24/2.1	0.22/2.1

Therefore, for this transport model, the reaction rate, 2.R2, shown in Fig.1 is multiplied by 1+*H2/H1* where *H2/H1* is obtained from Table 1. For T_e values outside the range in Table 1, the values at 5 eV or 100 eV are used.

2.R3: $e^- + H_2 \rightarrow e^- + H(1s) + H^*(2s)$

2.R5: $e^- + H_2 \rightarrow e^- + H^*(2p) + H^*(2s)$

2.R6: $e^- + H_2 \rightarrow e^- + H(1s) + H^*(n=3)$

Sawada computed rate coefficients for the dissociative excitation processes (2.R3 and 2.R6) leading to the direct production of a hydrogen atom in the ground state,

$$e^- + H_2 \rightarrow e^- + H(1s) + H^*, \qquad (\textit{path H3})$$

and rate coefficients accounting for the likelihood of that the excited hydrogen product reaches the ground state rather than becomes ionized by collisional and radiative processes [accounting for the sum of the cross-sections for production of all excited levels (which is presumed to include reaction 2.R5)],

$$e^- + H_2 \rightarrow e^- + H(1s) + H^*; \quad H^* \rightarrow\rightarrow H(1s). \qquad (\textit{path H4})$$

It was found that for $n_e < \sim 10^{19}$ m^{-3}, essentially all atomic hydrogen formed in the excited state reaches the ground state [for both cases (1) and (2)]. For a density of $n_e = 10^{20}$ m^{-3}, the production of atomic hydrogen by *path H4* is reduced by only 25%. Thus, the procedure used here of counting all hydrogen formed by reactions 2.R3, 2.R5, and 2.R6 as contributing to the ground state populations appears to be justified in the plasmas of interest.

Therefore, for this transport model, the reaction rates for 2.R3, 2.R5 and 2.R6 are used as shown in Fig. 2.2 with the assumption that all hydrogen products in the excited state contribute to the ground state population of atomic hydrogen.

2.R4: $e^- + H_2 \rightarrow e^- + H^+ + H(1s) + e^-$

Sawada considered dissociative ionization from reaction 2.R4 (*path I3* or *path H5*). For case (1), the reaction rate does not change from that shown in Fig. 2.2. However, the effect of vibrational levels [case (2)] leads to an overall increase in the rate of reaction 2.R4, increasing by a factor of 1/0.6 for $n_e < \sim 10^{19}$ m^{-3}, T_e =20 eV. As the density is raised above 10^{19}, the reaction rate falls slightly. A 10% reduction from the factor 1/0.6 is seen at $n_e = 10^{20}$.

Therefore, for this transport model, the reaction rates for 2.R4 shown in Fig. 2.2 is multiplied by a uniform factor of 1/0.6.

2.1.2.3 Electron-Impact Reactions involving Hydrogen Molecular Ions

Reaction 2.R1 leads to a molecular ion which experiences the effect of the magnetic field. In this transport model, it is assumed that the molecular ion remains essentially stationary in the x-coordinate over the time scale between a subsequent electron-impact dissociation collision, but may be 'lost to the side wall' in a characteristic frequency, $\nu_{loss}^{H_2^+}$. The parameter $\nu_{loss}^{H_2^+}$ allows for the possibility of H_2^+ to be

lost by parallel flow along field lines. (For example, $\nu_{loss}^{H_2^+}$ may be ~ C_s / L in a SOL with a collisional presheath. It should be noted that the use of the parameter $\nu_{loss}^{H_2^+}$ is not self-consistent with the idea of all velocity space distribution functions having rotational symmetry about the v_x axis, since the 'parallel flow velocity' of H_2^+ is neglected in the estimate of the atomic hydrogen reaction product source distribution functions.)

The following electron-impact dissociative ionization and dissociative recombination reactions involving H_2^+ are included in the algorithm, ordered roughly from most to least importance in a plasma with T_e > 100 eV:

$$e^- + H_2^+ \rightarrow e^- + H^+ + H(1s)$$
$$\langle E_H \rangle \approx 4.3 \text{ eV} \qquad \text{(2.R7)}$$

$$e^- + H_2^+ \rightarrow e^- + H^+ + H^*(n=2)$$
$$\langle E_H \rangle \approx 1.5 \text{ eV} \qquad \text{(2.R8)}$$

$$e^- + H_2^+ \rightarrow e^- + H^+ + H^+ + e^- \qquad \text{(2.R9)}$$

$$e^- + H_2^+ \rightarrow H(1s) + H^*(n \geq 2)$$
$$E_e \approx 3T_e / 2, \langle E_H \rangle \approx 0.5(E_e - 13.58/n^2) \text{ eV} \qquad \text{(2.R10)}$$

Figure 2.3 shows the rates for these reactions.

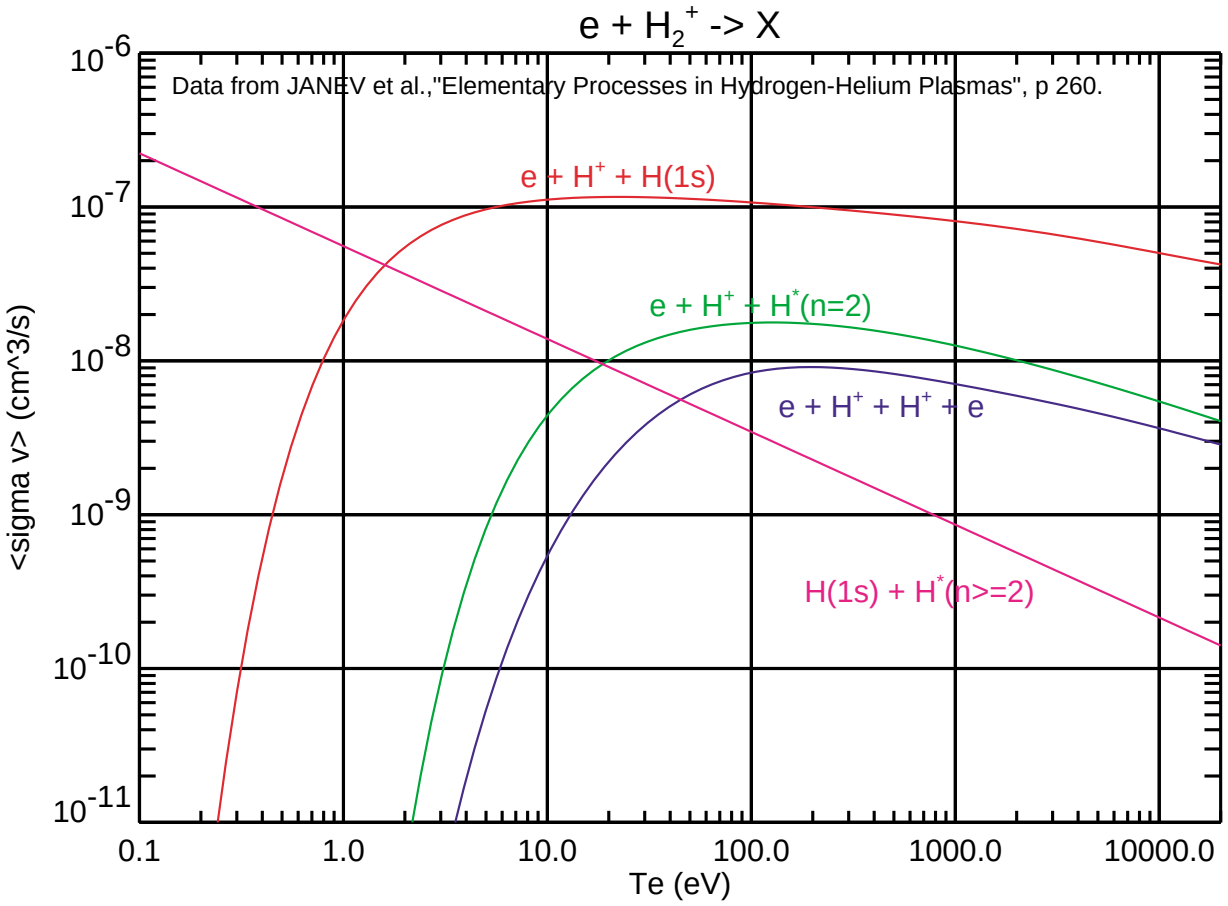

Fig. 2.3 -Electron impact dissociation rates for molecular hydrogen ions as a function of Te.

All 4 reactions are included in the kinetic transport algorithm. Similar to above, multistep ionization is neglected such that the production of $H^*(n \geq 2)$ can be effectively treated as the production of $H(1s)$ at the same rate. The average energy of hydrogen products ($\langle E_H \rangle$) resulting from the molecular ion breakup is shown next to the reactions listed above. These energies correspond to the case that the molecular ions are 'cold' with no thermal distribution of velocities. For the computation of $\langle E_H \rangle$ in reaction 2.R10, the incident energy of the electron is taken as equal to the average energy in a Maxwellian distribution, $E_e \approx 3T_e / 2$.

2.1.2.4 Multistep Corrections to Electron-Impact Molecular Hydrogen Ion Reaction Rates

At present there has been no collisional-radiative treatment of the molecular ion system. Apparently, there is insufficient data available to construct such a system [4]. Therefore, for this transport model, the reaction rates in Fig. 2.3 for 2.R7-2.R10 are used directly.

2.1.2.5 Energy Distribution of Hydrogen Reaction Products in Reactions 2.R7-2.R10

A. Molecular Ion Temperature

It is important to assess the energy distribution of the molecular ions in the plasma, since this can affect the resultant energy distribution of the hydrogen products from reactions 2.R7-2.R10. Through coulomb collisions, the population of molecular ions can begin to thermally equilibrate with the plasma ions. Therefore the effective 'temperature' of the molecular ions will depend on the energy equilibration frequency, $\nu_{eq}^{H_2^+}$, (via coulomb collisions with plasma ions) compared to the larger of the two frequencies: (1) the characteristic frequency of electron-impact dissociation or dissociative ionization of H_2^+ (denoted as $\nu_{dis}^{H_2^+}$) and (2) the characteristic loss frequency of H_2^+ ($\nu_{loss}^{H_2^+}$) by 'parallel transport' to the wall. The frequency $\nu_{dis}^{H_2^+}$ is simply related to the reaction rates,

$$\nu_{dis}^{H_2^+} = n_e[\langle\sigma v\rangle_{R7} + \langle\sigma v\rangle_{R8} + \langle\sigma v\rangle_{R9} + \langle\sigma v\rangle_{R10}].$$

The rate at which H_2^+ gets heated by coulomb collisions with plasma ions is given by[6]

$$\frac{\partial T_{H_2^+}}{\partial t} = \nu_{eq}^{H_2^+}\left(T_{H^+} - T_{H_2^+}\right)$$

with

$$\nu_{eq}^{H_2^+} = 7.7x10^{-7}\frac{n_{H^+}(cm^{-3})}{\sqrt{\mu}\,T_{H^+}^{3/2}} \qquad (s^{-1})$$

for $T_{H_2^+} << T_{H^+}$. (Here μ=1 for hydrogen and 2 for deuterium neutrals/plasma and T_{H^+} is in eV) Using the data in Fig. 2.2, one finds that $\nu_{eq}^{H_2^+}$ can become comparable to $\nu_{dis}^{H_2^+}$ at low temperatures.

In steady state with no heat conduction or convection (other than parallel loss) out of a unit plasma volume, the temperature of the H_2^+ species is determined by a balance between energy gain through coulomb collisions with the bulk plasma and energy loss by flows to the 'wall' and by destruction of the H_2^+ species,

$$\nu_{eq}^{H_2^+}\left(T_{H^+} - T_{H_2^+}\right) = \left(\nu_{loss}^{H_2^+} + \nu_{dis}^{H_2^+}\right)T_{H_2^+}.$$

Here it is also assumed that H_2^+ is formed with negligible temperature since the H_2 species has negligible temperature relative to the plasma. The molecular ion temperature is therefore approximately determined from

$$T_{H_2^+} = T_{H^+} \frac{\nu_{eq}^{H_2^+}}{\nu_{loss}^{H_2^+} + \nu_{dis}^{H_2^+} + \nu_{eq}^{H_2^+}} .$$

B. Model Velocity Distribution for Dissociation Reaction Products

The following function is chosen to represent the velocity space distribution of the hydrogen products for reactions 2.R2-2.R8 and 2.R10, accounting for the Franck-Condon energies and additional velocity spreading due to the finite temperature of the initial molecules (neutral and ionic):

$$f_R(v_x, v_r) \propto \exp\left[-\mu m_H \frac{\left(\sqrt{v_x^2 + v_r^2} - v_{FC} + \frac{3}{2} \frac{T_{FC}}{\mu m_H v_{FC}} \right)^2}{T_{FC} + \frac{1}{2} T_{mol}} \right]$$

with an effective Franck-Condon 'temperature', $T_{FC} = (E_{H,\max} - E_{H,\min})/4$, Franck-Condon 'velocity', $v_{FC} = \sqrt{2\langle E_H \rangle / \mu m_H}$, and the temperature of H_2 molecules (neutral or ionic), T_{mol}. This function is isotropic in velocity space and can be converted to a distribution in particle energy using the relationships: $E = \frac{1}{2} \mu m_H v^2, v^2 = v_x^2 + v_r^2, f_R(E) \partial E = f_R(v) 2\pi v^2 \partial v,$

$$f_R(E) \propto v \exp\left[-\mu m_H \frac{\left(v - v_{FC} + \frac{3}{2} \frac{T_{FC}}{\mu m_H v_{FC}} \right)^2}{T_{FC} + \frac{1}{2} T_{mol}} \right].$$

From this expression, one can see that the model function, $f_R(v_x, v_r)$, has the following desirable characteristics:

A. For $\frac{1}{2} T_{mol} << T_{FC},$ the particle velocity corresponding to the most probable reaction product energy, found by setting $\partial [v^2 f_R(E)] / \partial v = 0,$

$$\frac{\partial[v^2 f_R(E)]}{\partial v} = 3v^2 \exp[...] - \frac{2\mu m_H}{T_{FC}}(v - v_{FC} + \frac{3}{2}\frac{T_{FC}}{\mu m_H v_{FC}})v^3 \exp[...] = 0,$$

occurs when $v = v_{FC}$. Thus the energy-weighted reaction product distribution peaks at the velocity corresponding to the average Franck-Condon energy.

B. For $\frac{1}{2}T_{mol} >> T_{FC} \sim \frac{2}{3}\mu m_H v_{FC}^2$, the velocity distribution becomes

$$f_R(v_x, v_r) \propto \exp\left[-2\mu m_H \frac{\left(v - v_{FC} + \frac{3}{2}\frac{T_{FC}}{\mu m_H v_{FC}}\right)^2}{T_{mol}}\right] \sim \exp\left[-\frac{2\mu m_H v^2}{T_{mol}}\right]$$

which leads to a velocity distribution for the reaction products that approaches a Maxwellian distribution with the average velocity equal to 1/2 the averge velocity of a Maxwellian molecular distribution at temperature, T_{mol}. This is the appropriate situation for when the Franck-Condon energies are negligible relative to the thermal energy of the molecules.

It should be noted that the model function for the reaction product velocity distribution, $f_R(v_x, v_r)$, does not take into account the average x velocity of the inital population of dissociating molecules. Implicitly then, we are assuming that this velocity is negligible relative to v_{FC} or $\sqrt{T_{mol}/\mu m_H}$.

2.1.2.6 Elastic Scattering

The following elastic scattering events are included in the computation of f_{H_2}.

$$H_2 + H^+ \rightarrow H_2 + H^+ \qquad \text{(2.R11)}$$

$$H_2 + H \rightarrow H_2 + H \qquad \text{(2.R12)}$$

$$H_2 + H_2 \rightarrow H_2 + H_2 \qquad \text{(2.R13)}$$

Figure 2.4 shows the momentum transfer cross sections (mt) for these reactions as reported in Janev[7]. The viscosity cross section (vis) for self-collisions of molecular hydrogen is taken to be equal to the momentum transfer cross-section. Note that these cross-sections apply for deuterium using the scaling relationships: $\sigma^{mt}_{el,D}[E_D] \leftrightarrow \sigma^{mt}_{el,H}[E_D/2]$ and $\sigma^{vis}_{el,D}[E_D] \leftrightarrow \sigma^{vis}_{el,H}[E_D]$ [7].

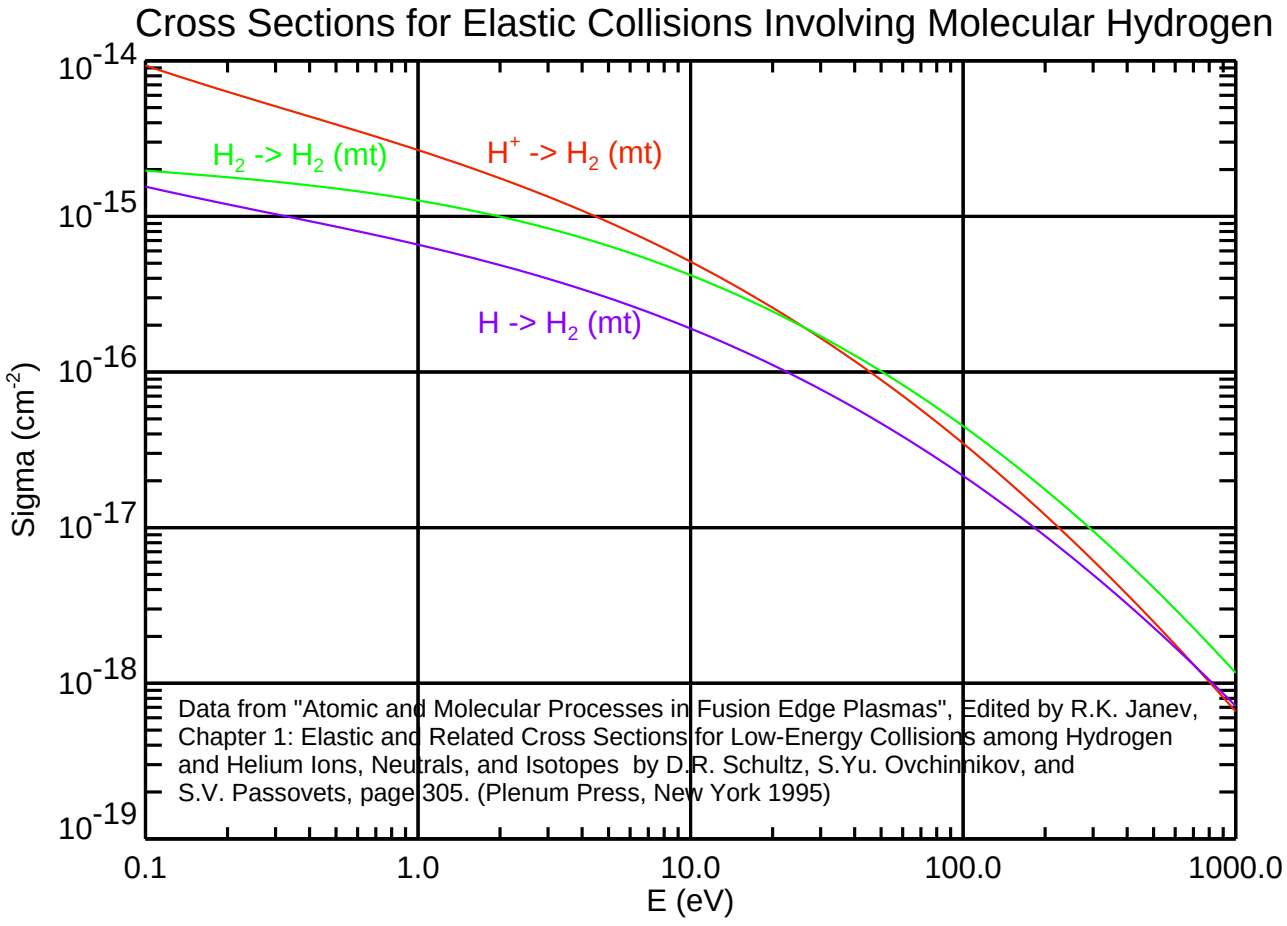

Fig. 2.4 -Momentum transfer cross-sections n as a function of projectile energy, E.

2.1.2.7 Molecular Charge Exchange

Molecular charge exchange is included in the transport algorithm.

$$H_2 + H_2^+ \rightarrow H_2^+ + H_2 \qquad \text{(2.R14)}$$

Figures 2.5 and 2.6 show the molecular charge exchange rates and cross-sections that are used.

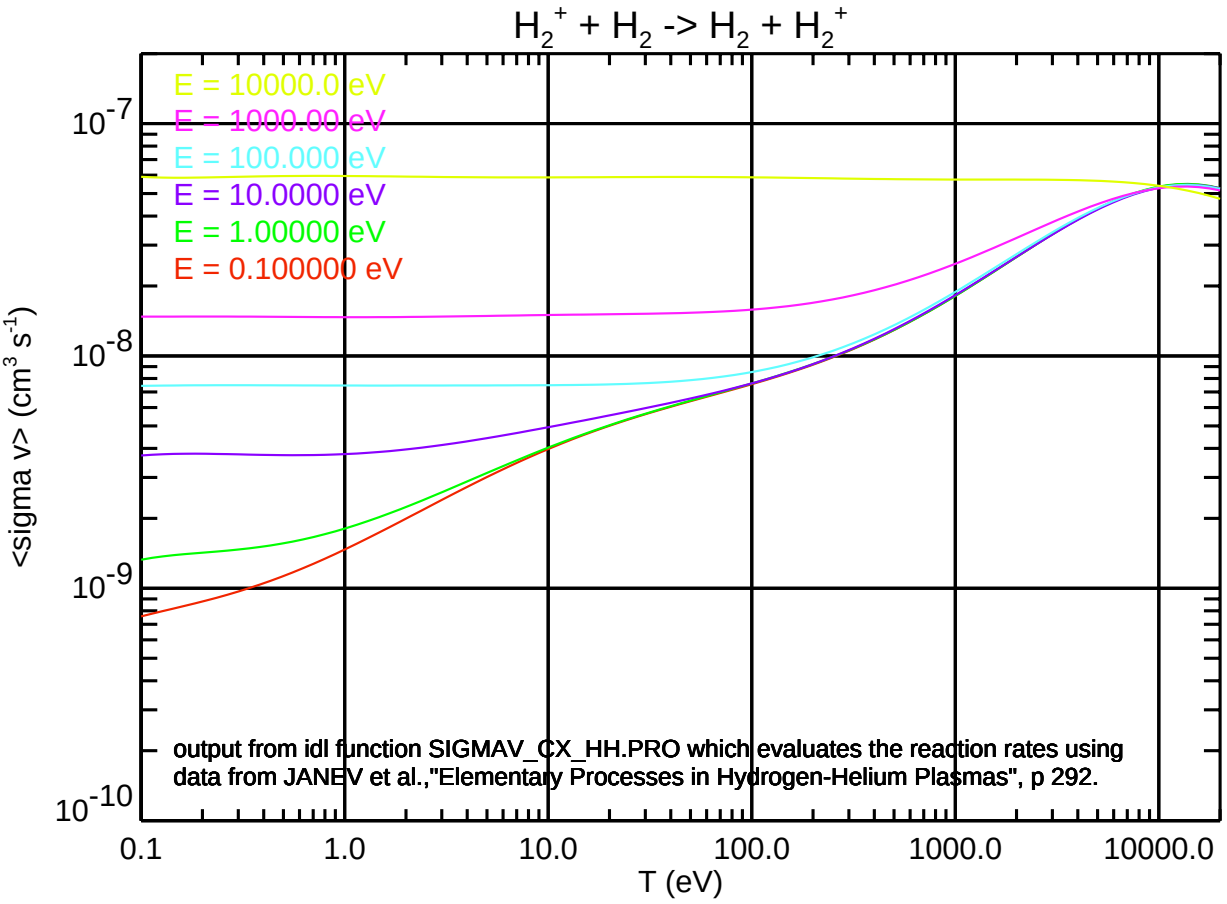

Fig. 2.5 – Molecular charge exchange rate as a function of ion temperature and neutral energy

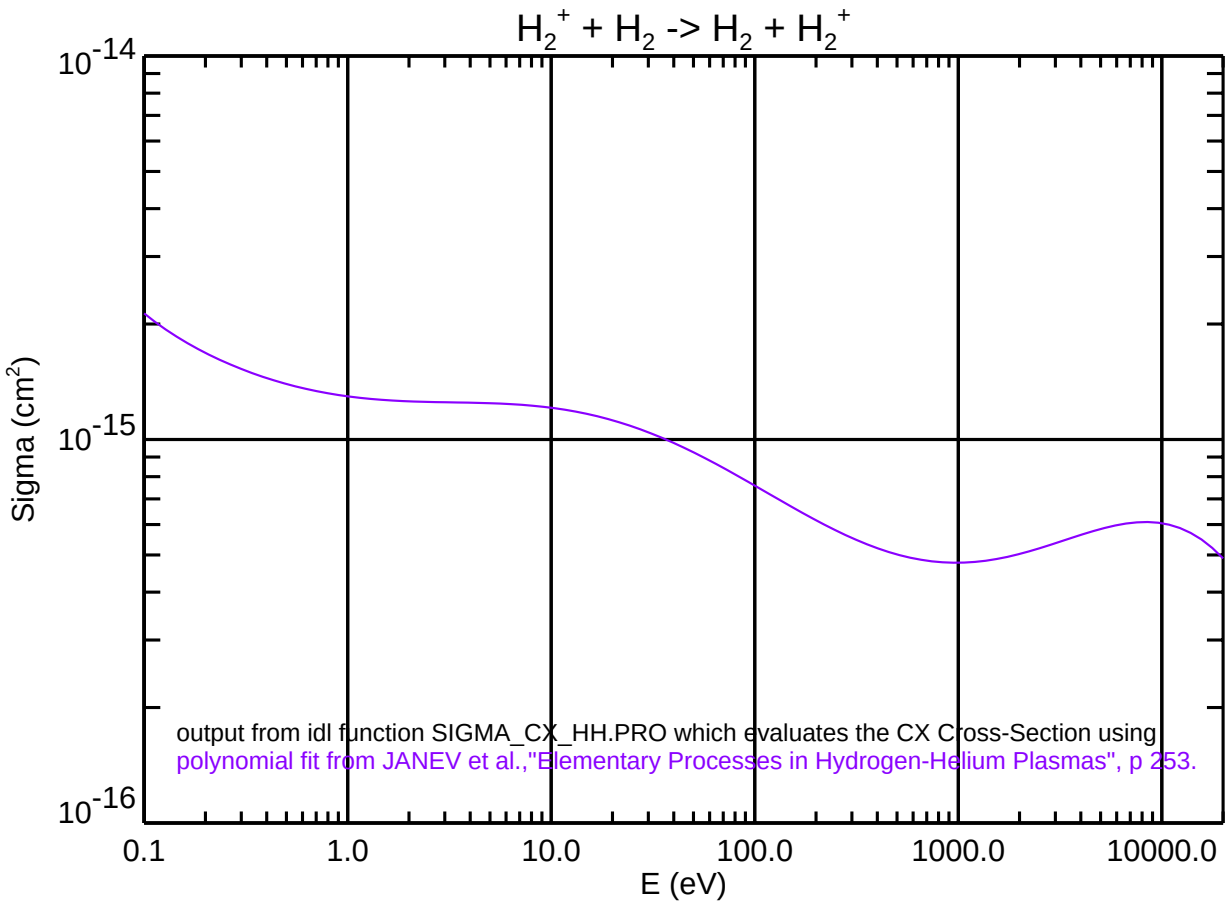

Fig. 2.6 – Molecular charge exchange cross section as a function of relative particle energy

2.1.2.8 Other Reactions

It should be noted that inelastic collisions with protons are ignored. This is generally a good approximation over the range of plasma temperatures considered here. However, it has been pointed out that the ion conversion reaction

$$H_2(v) + H^+ \rightarrow H_2^+ + H \qquad \text{(2.R15)}$$

involving vibrationally excited molecules can contribute to the production of H_2^+ at low electron temperatures [8, 9]. At T_e ~10 eV, the effect is small (< 10% correction to effective H_2 ionization) but for T_e ~5 eV, the effective H_2 ionization can be increased by a factor of 2.

2.1.3 Overview of Computation

The background plasma profiles of density, electron temperature and ion temperature is specified. The distribution function of atomic hydrogen, $f_n(v_x, v_r, x)$, is optionally specified. If self-collisions of the molecules are to be included, then a first guess or 'seed' molecular distribution function, $f_{H_{2s}}(v_x, v_r, x)$, may also be inputted. (If this input is zero, the result is an increased number of iterations outlined below). The optional source distribution function of wall-temperature molecules is specified. The incident distribution function of molecules, $f_{H_2}(v_x > 0, v_r, x_a)$, attacking plasma is also specified:

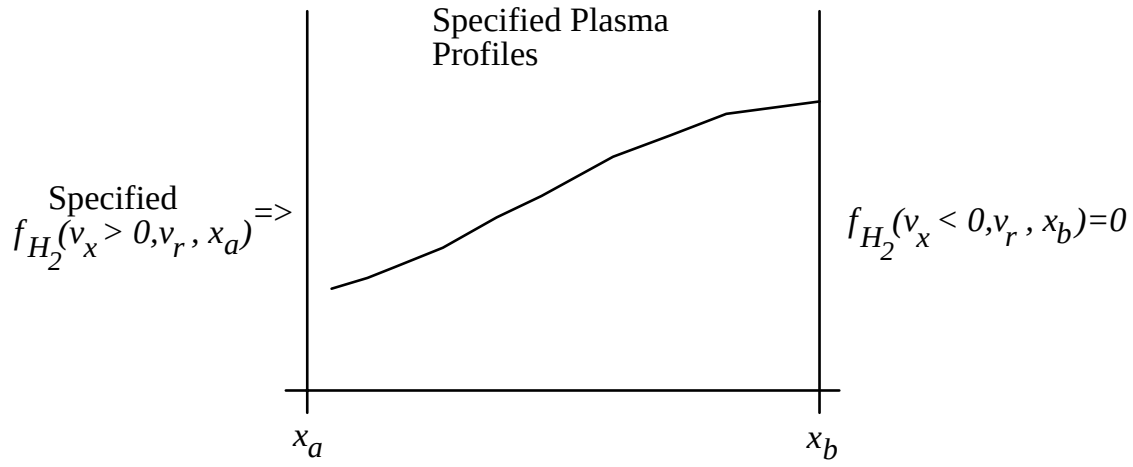

First, the portion of the neutral molecular distribution function which transports through the plasma without ionization, charge exchange, or elastic scattering is computed. This population is designated as $f_{H_2 0}(v_x, v_r, x)$, or the '0th generation'.

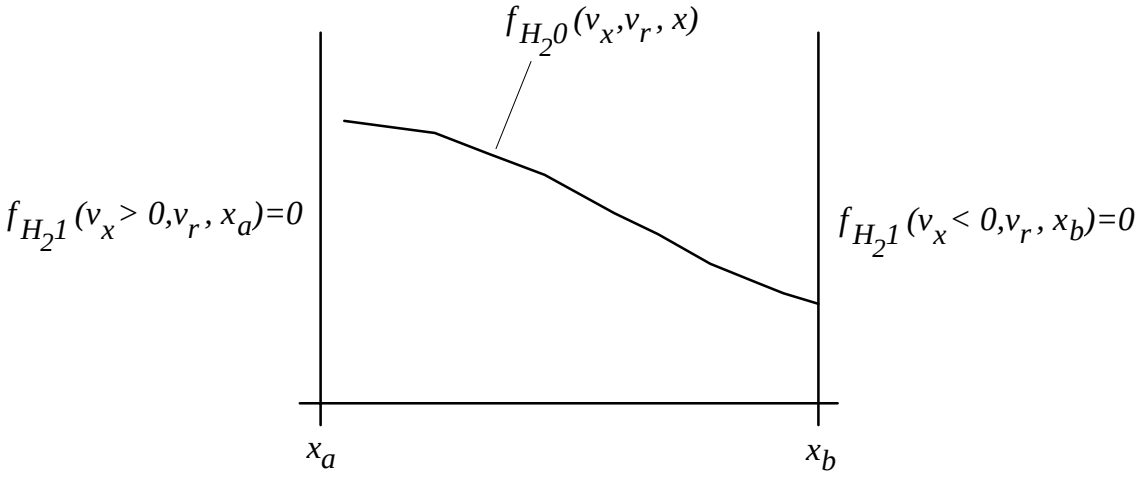

Then the neutral molecular distribution function arising from '1st generation' of charge exchange and elastic scattering, $f_{H_2 1}(v_x, v_r, x)$, is computed by considering the three cases of (A) $v_x > 0$, (B) $v_x < 0$ and (C) $v_x = 0$.

A. $f_{H_2 1}(v_x, v_r, x)$ for $v_x > 0$ is determined by integrating the Boltzmann equation over $[x_a, x]$ and applying the boundary condition of $f_{H_2 1}(v_x > 0, v_r, x_a) = 0$. Here the charge exchange and elastic scattering 'source' terms only include contributions from the previous generation (0^{th} generation).

B. $f_{H_2 1}(v_x, v_r, x)$ for $v_x < 0$ is determined by integrating the Boltzmann equation over $[x, x_b]$ and applying the boundary condition of $f_{H_2 1}(v_x < 0, v_r, x_b) = 0$. Again the charge exchange and elastic scattering 'source' terms only include contributions from the previous generation (0^{th} generation).

C. $f_{H_2 1}(v_x, v_r, x)$ for $v_x = 0$ is computed from the Boltzmann equation for the special case of $v_x = 0$, making use of the 'regularity condition' $\frac{\partial f_{H_2}}{\partial x}(v_x = 0, v_r, x)$ - finite

The above calculations are repeated for subsequent generations, $f_{H_2 2}(v_x, v_r, x)$, $f_{H_2 3}(v_x, v_r, x)$, …The total neutral distribution function in the plasma is then computed by summing over a finite number of generations:

$$f_{H_2}(v_x, v_r, x) = \sum_j f_{H_2 j}(v_x, v_r, x)$$

This distribution function is then compared to $f_{H_2 s}(v_x, v_r, x)$. If the difference between $f_{H_2}(v_x, v_r, x)$ and $f_{H_2 s}(v_x, v_r, x)$ is found to exceed an inputted tolerance range, then $f_{H_2 s}(v_x, v_r, x)$ is set equal to $f_{H_2}(v_x, v_r, x)$ and the computation for $f_{H_2}(v_x, v_r, x)$ is repeated again until the tolerance is met.

The velocity space source functions of ground-state neutral hydrogen (or deuterium) atoms (S_{H^0}) and ions (S_{H^+}) are evaluated using the following method:

D. Normalized source distribution functions, $S_{FCRn}(v_x, v_r, x)$ for n=2-8 and 10, are constructed with velocity distributions corresponding to the hydrogen products in reactions R2-R8 and R10 allowing for finite temperature of H_2^+ and H_2 species (see section 2.1.2.5). S_{FCRn} for reactions R4 and R10 depend on local T_e (through $E_e \approx 3T_e / 2$).

E. S_{H^0} is composed of two parts, $S_{H^0} = S_{H^0}^{H_2} + S_{H^0}^{H_2^+}$, arising from the atomic hydrogen source from the dissociation of neutral and ionized molecules. $S_{H^0}^{H_2}$ is given by

$$S_{H^0}^{H_2} = n_e n_{H_2} \{2\langle\sigma v\rangle_{R2} S_{FC2} + 2\langle\sigma v\rangle_{R3} S_{FC3} + \langle\sigma v\rangle_{R4} S_{FC4} + 2\langle\sigma v\rangle_{R5} S_{FC5} + 2\langle\sigma v\rangle_{R6} S_{FC6}\}$$

F. The H_2^+ density is found by equating the H_2^+ production and destruction rates:

$$n_e n_{H_2} \langle\sigma v\rangle_{R1} = n_{H_2^+} \left(\nu_{dis}^{H_2^+} + \nu_{loss}^{H_2^+}\right)$$

$$n_{H_2^+} = n_{H_2} \frac{n_e \langle\sigma v\rangle_{R1}}{\nu_{dis}^{H_2^+} + \nu_{loss}^{H_2^+}}$$

G. $S_{H^0}^{H_2^+}$ is evaluated from

$$S_{H^0}^{H_2^+} = n_e n_{H_2^+} \{\langle\sigma v\rangle_{R7} S'_{FC7} + \langle\sigma v\rangle_{R8} S'_{FC8} + 2\langle\sigma v\rangle_{R10} S'_{FC10}\}$$

H. The total hydrogen ion source arising from the dissociation of neutral and ionized molecules is given by

$$W_{H^+} = n_e n_{H_2} \langle\sigma v\rangle_{R4} + n_e n_{H_2^+} \{\langle\sigma v\rangle_{R7} + \langle\sigma v\rangle_{R8} + 2\langle\sigma v\rangle_{R9}\}$$

2.2. Formulation

2.2.1 Boltzmann Equation

The neutral molecule distribution function satisfies the Boltzmann equation,

$$
\begin{aligned}
v_x \frac{\partial f_{H_2}}{\partial x} = & -\alpha_{Loss}(x) f_{H_2} + S_{H_2} \hat{f}_w - \gamma_{wall} f_{H_2} + \hat{f}_w \int \gamma_{wall} f_{H_2} \, \partial^3 v' \\
& - f_{H_2} n_{H_2^+} \int \hat{f}'_{H_2^+} |\underline{v} - \underline{v}'| \sigma_{cx}(|\underline{v} - \underline{v}'|) \partial^3 v' \\
& + \hat{f}_{H_2^+} n_{H_2^+} \int f'_{H_2} |\underline{v} - \underline{v}'| \sigma_{cx}(|\underline{v} - \underline{v}'|) \partial^3 v' \\
& + n_i \int\int [f''_{H_2} \hat{f}'''_i - f_{H_2} \hat{f}'_i] |\underline{v} - \underline{v}'| \frac{\delta\sigma^{el}_{H_2:H^+}(|\underline{v} - \underline{v}'|)}{\delta\Omega} \delta\Omega \partial^3 v' \\
& + \int\int [f''_{H_2} f'''_n - f_{H_2} f'_n] |\underline{v} - \underline{v}'| \frac{\delta\sigma^{el}_{H_2:H}(|\underline{v} - \underline{v}'|)}{\delta\Omega} \delta\Omega \partial^3 v' \\
& + \int\int [f''_{H_2} f'''_{H_2} - f_{H_2} f'_{H_2}] |\underline{v} - \underline{v}'| \frac{\delta\sigma^{el}_{H_2:H_2}(|\underline{v} - \underline{v}'|)}{\delta\Omega} \delta\Omega \partial^3 v'
\end{aligned}
\quad , \qquad (2.1)
$$

with the definition

$$
\alpha_{Loss}(x) \equiv n_e \sum_{n=1}^{6} \langle \sigma v \rangle_{Rn} \ . \qquad (2.2)
$$

Spatial symmetries in all distribution functions, $\frac{\partial f}{\partial y} = 0$ and $\frac{\partial f}{\partial z} = 0$ are assumed. $\int \partial^3 v'$ denotes integration over all velocity space and solid angle integration, $\int \partial\Omega$, denotes integration over all scattering angles $\int_0^{2\pi} \int_0^{\pi} \sin\theta \partial\theta \partial\phi$. $\hat{f}_i(\underline{v}, x)$ and $\hat{f}_{H_2^+}(\underline{v}, x)$ are normalized so that $\int \hat{f}(\underline{v}', x) \, \partial^3 v' = 1$. The shorthand notation, $f' = f(\underline{v}', x)$, $f'' = f(\underline{v}'', x)$ and $f''' = f(\underline{v}''', x)$, has been used. It is implicit that the velocity pairs $(\underline{v}, \underline{v}')$ and $(\underline{v}'', \underline{v}''')$ are related to each other through the scattering angles.

The first term on the right hand side (RHS) of Eq. (2.1) corresponds to the loss rate of molecules from electron-impact reactions 2.R1-2.R6. These reaction rates are evaluated according to the scheme outlined in section 2.1.2. The second term corresponds to an optionally specified wall-temperature source of molecules. $\hat{f}_w$ is a normalized Maxwellian distribution of molecules at the wall temperature. The third and fourth terms account for molecules colliding with the walls at a velocity dependent rate,

γ_{wall}. Molecules come back off the wall with the distribution, $\hat{f}_w$. The parameter γ_{wall} is determined from the radial velocity of the molecules and the effective 'pipe diameter' of the walls,

$$\gamma_{wall}(v_r, x) = \frac{2v_r}{D(x)} \tag{2.2b}$$

2.2.2 Charge Exchange Collision Operator

The second integral term on the RHS of Eq. (2.1) depends on the molecular ion temperature and the energy of the molecular neutral species and can be written in the form

$$\int \hat{f}_{H_2^+}(\underline{v}', x)|\underline{v} - \underline{v}'|\sigma_{cx}(|\underline{v} - \underline{v}'|)\,\partial^3 v' = \langle \sigma v \rangle_{cx}[T_{H_2^+}, E_0], \tag{2.3}$$

where $\langle \sigma v \rangle_{cx}[T_{H_2^+}, E_0]$ is the molecular hydrogen charge exchange cross-section averaged over a Maxwellian molecular hydrogen ion distribution (temperature, $T_{H_2^+}$), accounting for the energy of the molecular hydrogen neutral species, E_0, which for a specified velocity, (v_x, v_r), is $E_0 = \frac{1}{2} m_{H_2}\left(v_x^2 + v_r^2\right)$. This reaction rate is evaluated using the data compiled in Fig. 2.5. To evaluate this reaction rate for deuterium, the substitution,

$$\langle \sigma v \rangle_{cx}[T_{H_2/D_2}, E_0] \rightarrow \langle \sigma v \rangle_{cx}[\frac{T_{H_2}}{\mu}, \frac{1}{2} m_{H_2}\left(v_x^2 + v_r^2\right)],$$

is made ($\mu = 2$ for deuterium, $\mu = 1$ for hydrogen). This assumes that the reaction rates for deuterium are identical to hydrogen when the relative velocities between colliding molecules are the same. Similarly, for direct evaluation of $\sigma_{cx}[E_0]$ using tabulated hydrogen data, the relative energy is evaluated using the molecular hydrogen mass for both hydrogen and deuterium cases.

The third integral on the right hand side of Eq. (2.1) is not so readily evaluated in terms of tabulated values. It requires a velocity-space integral to be performed over (v_x', v_r') for each combination of (v_x, v_r), weighted by $f_{H_2}(v_x', v_r', x)$. This integral computes the charge exchange frequency for a specified combination of (v_x, v_r). For large velocity space meshes, this computation can take some time. Therefore two options for computing this integral are included in this algorithm: (A) an 'exact'

integration (using cross section data from Fig. 2.6) and (B) an approximation of the integral. For option (B) the approximation,

$$\begin{aligned} \hat{f}_{H_2^+} n_{H_2^+} \int f_{H_2}(\underline{v}', x)|\underline{v} - \underline{v}'|\sigma_{cx}(|\underline{v} - \underline{v}'|)\partial^3 v' \approx \\ \hat{f}_{H_2^+} n_{H_2^+} \iint \hat{f}_{H_2^+} f_{H_2}(\underline{v}', x)|\underline{v}'' - \underline{v}'|\sigma_{cx}(|\underline{v}'' - \underline{v}'|)\partial^3 v' \partial^3 v'' = \\ \hat{f}_{H_2^+} n_{H_2^+} \int f_{H_2}(\underline{v}', x)\langle\sigma v\rangle_{cx}[T_{H_2^+}, E_0']\partial^3 v' \end{aligned} \quad , \qquad (2.4)$$

is made, replacing the charge exchange frequency for a specified combination of (v_x, v_r) with the velocity-spaced average charge exchange frequency [which is independent of (v_x, v_r)]. In effect, this option assumes that all charge exchange molecules are 'born' with a distribution that is the same as the molecular ion distribution function. As a result, distortions in this source distribution function due to the charge exchange rate being different at different values of relative molecular ion-neutral velocities are not taken into account.

2.2.3 Elastic Collision Operator

The last three collision integrals in Eq. (2.1) compute the change in the molecular distribution function due to elastic scattering reactions, 2.R11-2.R13. The explicit numerical evaluation of these integrals is not practical, even if the differential scattering cross-sections where known. Owing to the 5-dimensional integration space, the computation would require about two orders of magnitude more computer memory and CPU time than that used to solve Eq. (2.1) without these three terms. This problem of evaluating collision integrals routinely arises in kinetic analysis. A reasonable approach, which is very often adopted, is to replace the collision integrals with a simpler kinetic model, such as the BKG [10] model. Reiter [8] recently outlined the algorithm used in the EIRENE Monte-Carlo which approximates elastic collision integrals with a BKG model. A similar method is used here,

$$\begin{aligned} \left[\frac{\partial f_{H_2}}{\partial t}\right]_{elastic} &= \omega^{el}_{H_2:H^+}(M_{H_2:H^+} - f_{H_2}) \\ &+ \omega^{el}_{H_2:H}(M_{H_2:H} - f_{H_2}) \\ &+ \omega^{el}_{H_2:H_2}(M_{H_2:H_2} - f_{H_2}) \end{aligned} \quad , \qquad (2.5)$$

where $\left[\frac{\partial f_{H_2}}{\partial t}\right]_{elastic}$ represents the sum of the three elastic collision integrals on the RHS of Eq. (2.1). The M terms correspond to local drifting Maxwellians and ω^{el} terms correspond to average collision frequencies. It is possible to choose the mixed-collision and self-collision M distributions such that the kinetic model represented by Eq. (2.5) conserves mass, momentum, and energy of the total species mixture for mixed-collisions and conserves mass, momentum, and energy of each species for self-collisions. In the case when the distribution functions of each species are Maxwellians with small drift velocities, there is a single collision frequency (e.g., $\omega^{el}_{H_2:H}$) that characterizes the momentum and energy relaxation rates between each species pair [11]. In this case, cross-collision M distributions can be chosen so as to yield identical momentum and energy relaxation rates as that obtained from the full collision integrals [11, 12]. This choice for the M distributions is

$$\begin{aligned} M_{H_2:H^+} &= n_{H_2}\,\hat{f}_M[m_{H_2}, T_{H_2:H^+}, \underline{U}_{H_2:H^+}] \\ M_{H_2:H} &= n_{H_2}\,\hat{f}_M[m_{H_2}, T_{H_2:H}, \underline{U}_{H_2:H}] \\ M_{H_2} &= n_{H_2}\,\hat{f}_M[m_{H_2}, T_{H_2}, \underline{U}_{H_2}] \end{aligned} \tag{2.6}$$

with $\hat{f}_M[m, T, \underline{U}]$ being a normalized Maxwellian velocity distribution for particles with mass m at temperature T, drifting with velocity $\underline{U}$. The hybrid drift velocities are 'center of mass' velocities given by

$$\begin{aligned} \underline{U}_{H_2:H^+} &= (m_{H_2}\underline{U}_{H_2} + m_{H^+}\underline{U}_{H^+})/(m_{H_2} + m_{H^+}) \\ \underline{U}_{H_2:H} &= (m_{H_2}\underline{U}_{H_2} + m_H\underline{U}_H)/(m_{H_2} + m_H) \end{aligned} \tag{2.7}$$

and the hybrid temperatures are given by

$$\begin{aligned} T_{H_2:H^+} &= T_{H_2} + \frac{2m_{H_2}m_{H^+}}{(m_{H_2} + m_{H^+})^2}\left[(T_{H^+} - T_{H_2}) + \frac{m_{H^+}}{6k}(\underline{U}_{H^+} - \underline{U}_{H_2})^2\right] \\ T_{H_2:H} &= T_{H_2} + \frac{2m_{H_2}m_H}{(m_{H_2} + m_H)^2}\left[(T_H - T_{H_2}) + \frac{m_H}{6k}(\underline{U}_H - \underline{U}_{H_2})^2\right] \end{aligned} \tag{2.8}$$

while $\{T_{H^+}, T_H, T_{H_2}\}$ and $\{\underline{U}_{H^+}, \underline{U}_H, \underline{U}_{H_2}\}$ are the respective kinetic temperatures and drift velocities evaluated from $\{f_i\ , f_n\ , f_{H_2}\}$.

Having chosen the model M distributions, the next task is to determine values for the average collision frequencies (ω^{el}) which yield momentum and/or energy relaxation rates which are consistent with those obtained from the full collision integrals and which best describe the transport physics being studied. One should note that except for the special cases of when (1) the distribution functions of all species are Maxwellians and/or (2) the collision rates are independent of particle velocity [$|\underline{v}-\underline{v}'|\sigma^{el}(|\underline{v}-\underline{v}'|)\sim$ constant] it is not possible to choose ω^{el} such that the BKG collision model yields the same relaxation rates for *all* moments as that obtained from the full collision integral. A reasonable approach for determining ω^{el} is to require that the relaxation rates for the lowest order moments of the BKG collision model yield the same results as the full collision integral. All higher order moments will be only approximately satisfied.

The following procedure is used here: For mixed collisions, the x-directed momentum transfer rate is used to compute a consistent value for ω^{el}. The x-directed momentum transfer rate can be computed from the full collision integral using tabulated values of the momentum transfer cross-sections. For self-collisions, the temperature isotropization rate is used. The temperature isotropization rate can also be computed from the full collision integral using tabulated values of the viscosity cross-sections. Appendix B discusses the basis for the formulas used below to compute the average collision frequencies.

Note that in order for mass, momentum and energy to be conserved, Eqs. (2.6-2.8) must be self-consistent with the local molecular distribution being computed, f_{H_2}. Therefore, Eqs. (2.6-2.8) must be evaluated using f_{H_2}. However, the relaxation frequencies, which are only a function of x, can be evaluated from the 'seed' distribution, f_{H_2s} (which is iterated until f_{H_2s} converges to f_{H_2}).

$$\omega^{el}_{H_2:H^+}(x)=\frac{\int f_{H_2\,s}(\underline{v},x)\,\alpha^{mt}_{H_2:H^+}(\underline{v},x)\,\partial^3 v}{n_{H_2s}\left(U_{xH_{2_s}}-U_{xH^+}\right)}$$

$$\alpha^{mt}_{H_2:H^+}(\underline{v},x)\equiv\int f_i(\underline{v}',x)\left(v_x-v_x'\right)|\underline{v}-\underline{v}'|\,\sigma^{mt}_{H_2:H^+}(|\underline{v}-\underline{v}'|)\,\partial^3 v'$$

$$\omega^{el}_{H_2:H}(x)=\frac{\int f_{H_2\,s}(\underline{v},x)\,\alpha^{mt}_{H_2:H}(\underline{v},x)\,\partial^3 v}{n_{H_2s}\left(U_{xH_{2_s}}-U_{xH}\right)}$$

$$\alpha^{mt}_{H_2:H}(\underline{v},x)\equiv\int f_n(\underline{v}',x)\left(v_x-v_x'\right)|\underline{v}-\underline{v}'|\,\sigma^{mt}_{H_2:H}(|\underline{v}-\underline{v}'|)\,\partial^3 v' \qquad (2.9)$$

$$\omega^{el}_{H_2:H_2}(x) = \frac{\int f_{H_2\,s}(\underline{v},x)\,\alpha^{iso}_{H_2:H_2}(\underline{v},x)\,\partial^3 v}{\int f_{H_2 s}(\underline{v},x)\left[v_r^2 - 2\left(v_x - U_{xH_2 s}\right)^2\right]\partial^3 v}$$

$$\alpha^{iso}_{H_2:H_2}(\underline{v},x) \equiv$$

$$\int f_{H_2\,s}(\underline{v}',x)\left[v_r^2 + v_r'^2 - 2v_r v_r'\cos\theta' - 2\left(v_x - v_x'\right)^2\right]|\underline{v}-\underline{v}'|\frac{1}{8}\sigma^{vis}_{H_2:H_2}(|\underline{v}-\underline{v}'|)\,v_r'\partial\theta'\partial v_x'\partial v_r'$$

2.*2.4 Coefficients for the Mesh Equations*

It is useful to define the following quantities which can be evaluated directly for all (v_x, v_r, x) mesh locations using the inputted profiles:

Charge exchange collision frequency (option A - direct evaluation from $\sigma_{cx}(E_0)$)

$$\begin{aligned}\alpha_{cx}(v_x,v_r,x) &\equiv n_{H_2^+}\iint \hat{f}_{H_2^+}(v_x',v_r',x)\left[\int |\underline{v}-\underline{v}'|\,\sigma_{cx}(|\underline{v}-\underline{v}'|)\partial\theta'\right]v_r'\partial v_r'\partial v_x' \\ &\equiv n_{H_2^+}\iint \hat{f}_{H_2^+}(v_x',v_r',x)\Sigma_{cx}(v_x,v_r,v_x',v_r')\partial v_x'\partial v_r'\end{aligned} \tag{2.10a}$$

with

$$\Sigma_{cx}(v_x,v_r,v_x',v_r') \equiv v_r'\int |\underline{v}-\underline{v}'|\,\sigma_{cx}(|\underline{v}-\underline{v}'|)\,\partial\theta'. \tag{2.10a'}$$

Charge exchange collision frequency (option B - using $\langle\sigma v\rangle_{cx}$)

$$\alpha_{cx}(v_x,v_r,x) \equiv n_{H_2^+}\langle\sigma v\rangle_{cx}\left[\frac{T_{H_2^+}}{\mu}, \frac{1}{2}m_{H_2}\left(v_x^2+v_r^2\right)\right] \tag{2.10b}$$

Charge exchange source (option A)

$$\beta_{cx}(v_x,v_r,x) \equiv \hat{f}_{H_2^+} n_{H_2^+}\iint f_{H_2}(v_x',v_r',x)\Sigma_{cx}(v_x,v_r,v_x',v_r')\partial v_x'\partial v_r' \tag{2.11a}$$

Charge exchange source (option B)

$$\beta_{cx}(v_x,v_r,x) \equiv \hat{f}_{H_2^+} n_{H_2^+} \iiint f_{H_2}(v_x,v_r,x)\,|\underline{v}-\underline{v}'|\,\sigma_{cx}(|\underline{v}-\underline{v}'|)\,v_r\,\partial v_r\,\partial v_x\,\partial\theta$$
$$\approx 2\pi\,\hat{f}_{H_2^+} \iint f_{H_2}(v_x',v_r',x)\,\alpha_{cx}(v_x',v_r',x)\,v_r'\,\partial v_x'\,\partial v_r' \qquad (2.11b)$$

Elastic momentum transfer frequency for $H_2 : H^+$

$$\omega^{el}_{H_2:H^+}(x) = \frac{2\pi}{n_{H_2 s}\left(U_{xH_{2s}} - U_{xH^+}\right)} \iint f_{H_2 s}(v_x',v_r',x)\,\alpha^{mt}_{H_2:H^+}(v_x',v_r',x)\,v_r'\,\partial v_x'\,\partial v_r'$$
$$\alpha^{mt}_{H_2:H^+}(\underline{v},x) \equiv \iint f_n(v_x',v_r',x)\,\Sigma^{mt}_{H_2:H^+}(v_x,v_r,v_x',v_r')\,\partial v_r'\,\partial v_x'$$
$$\Sigma^{mt}_{H_2:H^+}(v_x,v_r,v_x',v_r') \equiv v_r'\left(v_x - v_x'\right)\int |\underline{v}-\underline{v}'|\,\sigma^{mt}_{H_2:H^+}(|\underline{v}-\underline{v}'|)\,\partial\theta' \qquad (2.12)$$

Elastic momentum transfer frequency for $H_2 : H$

$$\omega^{el}_{H_2:H}(x) = \frac{2\pi}{n_{H_2 s}\left(U_{xH_{2s}} - U_{xH}\right)} \iint f_{H_2 s}(v_x',v_r',x)\,\alpha^{mt}_{H_2:H}(v_x',v_r',x)\,v_r'\,\partial v_x'\,\partial v_r'$$
$$\alpha^{mt}_{H_2:H}(\underline{v},x) \equiv \iint f_n(v_x',v_r',x)\,\Sigma^{mt}_{H_2:H}(v_x,v_r,v_x',v_r')\,\partial v_r'\,\partial v_x'$$
$$\Sigma^{mt}_{H_2:H}(v_x,v_r,v_x',v_r') \equiv v_r'\left(v_x - v_x'\right)\int |\underline{v}-\underline{v}'|\,\sigma^{mt}_{H_2:H}(|\underline{v}-\underline{v}'|)\,\partial\theta' \qquad (2.13)$$

Elastic temperature isotropization frequency for $H_2 : H_2$

$$W_{\perp//}(x) \equiv 2\pi \iint f_{H_2 s}(v_x',v_r',x)\left[v_r'^2 - 2\left(v_x' - U_{xH_2 s}\right)^2\right] v_r'\,\partial v_x'\,\partial v_r'$$
$$\omega^{el}_{H_2:H_2}(x) = \frac{2\pi}{W_{\perp//}} \iint f_{H_2 s}(v_x',v_r',x)\,\alpha^{iso}_{H_2:H_2}(v_x',v_r',x)\,v_r'\,\partial v_x'\,\partial v_r'$$
$$\alpha^{iso}_{H_2:H_2}(\underline{v},x) \equiv \iint f_{H_2 s}(v_x',v_r',x)\,\Sigma^{iso}_{H_2:H_2}(v_x,v_r,v_x',v_r')\,\partial v_r'\,\partial v_x'$$
$$\Sigma^{iso}_{H_2:H_2}(v_x,v_r,v_x',v_r') \equiv$$
$$v_r'\,\frac{1}{8}\int\left[v_r^2 + v_r'^2 - 2v_r v_r'\cos\theta' - 2\left(v_x - v_x'\right)^2\right]|\underline{v}-\underline{v}'|\,\sigma^{vis}_{H_2:H_2}(|\underline{v}-\underline{v}'|)\,\partial\theta'$$
(2.14)

Total elastic scattering frequency

$$\omega_{el}(x) = \omega^{el}_{H_2:H^+}(x) + \omega^{el}_{H_2:H}(x) + \omega^{el}_{H_2:H_2}(x) \qquad (2.15)$$

Side-wall sink frequency

$$\gamma_{wall}(v_r, x) = \frac{2v_r}{D(x)} \qquad (2.15b)$$

Side-wall sourcedistribution

$$s_{wall}(v_r, v_x, x) = \hat{f}_w \iint \gamma_{wall}(v_r, x) f_{H_2} v_r \partial v_r \partial v_x \qquad (2.15c)$$

Total collision frequency

$$\alpha_c(v_x, v_r, x) \equiv \alpha_{cx}(v_x, v_r, x) + \alpha_{Loss}(x) + \omega_{el}(x) + \gamma_{wall}(v_r, x) \qquad (2.16)$$

Elastic scattering source distribution

$$M_{H_2}(v_x, v_r, x) = M_{H_2:H^+}(v_x, v_r, x) + M_{H_2:H}(v_x, v_r, x) + M_{H_2:H_2}(v_x, v_r, x) \qquad (2.17)$$

Now the Boltzmann equation becomes

$$v_x \frac{\partial f_{H_2}}{\partial x} = S_{H_2} \hat{f}_w + s_{wall} + \beta_{cx} - \alpha_c f_{H_2} + \omega_M, \qquad (2.18)$$

with

$$\omega_M \equiv \omega^{el}_{H_2:H^+} M_{H_2:H^+} + \omega^{el}_{H_2:H} M_{H_2:H} + \omega^{el}_{H_2:H_2} M_{H_2:H_2}.$$

2.2.5 Expanding f_{H_2} as a Series of collision 'Generations'

We now consider the neutral molecular distribution function to be composed of a sum of sub-distribution functions of neutrals which have survived j generations of collisions

$$\begin{aligned} f_{H_2}(v_x, v_r, x) &= \sum_j f_{H_2\, j}(v_x, v_r, x) \\ \beta_{cx}(v_x, v_r, x) &= \sum_j \beta_{cx\, j}(v_x, v_r, x) \\ \omega_M(v_x, v_r, x) &= \sum_j \omega_{M\, j}(v_x, v_r, x) \\ s_{wall}(v_x, v_r, x) &= \sum_j s_{wall\, j}(v_x, v_r, x) \end{aligned} \quad . \tag{2.19}$$

With the above definitions, Eq. (2.1) can be written as a series of separate Boltzmann equations, each representing the kinetic balance for that population of neutrals:

$$\begin{aligned} v_x \frac{\partial f_{H_2 0}}{\partial x} &= S_{H_2} \hat{f}_w && - \alpha_c f_{H_2 0} \\ v_x \frac{\partial f_{H_2 1}}{\partial x} &= && s_{wall\,0} + \beta_{cx0} - \alpha_c f_{H_2 1} + \omega_{M0} \\ v_x \frac{\partial f_{H_2 2}}{\partial x} &= && s_{wall\,1} + \beta_{cx1} - \alpha_c f_{H_2 2} + \omega_{M1} \\ &\cdots\cdots\cdots\cdots\cdots\cdots\cdots\cdots\cdots\cdots\cdots\cdots\cdots\cdots\cdots\cdots\cdots\cdots \\ v_x \frac{\partial f_{H_2 j}}{\partial x} &= && s_{wall\, j-1} + \beta_{cx\, j-1} - \alpha_c f_{H_2 j} + \omega_{M\, j-1} \end{aligned} \tag{2.20}$$

2.2.6 Numerical Grid & Scheme

The spatial and velocity grid coordinates are specified with arbitrary spacing:

$$\begin{aligned} v_x &= [-v_{x\max}, v_{x1}, ..., 0, ..., v_{xk}, v_{xk+1}, ..., v_{x\max}] \\ v_r &= [v_{r\min}, v_1, ..., v_{rl}, v_{xl+1}, ..., v_{r\max}] \\ x &= [x_a, x_1 ..., x_m, x_{m+1}, ..., x_b] \end{aligned}$$

We will be integrating Eqs. (2.20) along the x coordinate to obtain values for $f_{H_2\,j}$ at each grid location. Therefore we need to approximate the RHS of Eqs. (2.20) between grid points. For integration along the x coordinate between x_m and x_{m+1}, we will replace the integrand with the average of its values evaluated at x_m and x_{m+1}.

2.2.6.1 Mesh Equation - 0th Generation for $v_x \neq 0$

In this scheme, the mesh equation for the 0th generation (with $v_x > 0$) becomes

$$\frac{f_{H_2 0,m+1} - f_{H_2 0,m}}{x_{m+1} - x_m} = -\frac{1}{2v_x}(\alpha_{c,m+1} f_{H_2 0,m+1} + \alpha_{c,m} f_{H_2 0,m} - S_{H_2,m+1}\hat{f}_{w,m+1} - S_{H_2,m}\hat{f}_{w,m})$$

$$f_{H_2 0,m+1}(1 + \frac{x_{m+1} - x_m}{2v_x}\alpha_{c,m+1}) = f_{H_2 0,m}(1 - \frac{x_{m+1} - x_m}{2v_x}\alpha_{c,m}) + \frac{x_{m+1} - x_m}{2v_x}(S_{H_2,m+1}\hat{f}_{w,m+1} + S_{H_2,m}\hat{f}_{w,m}$$

$$f_{H_2 0,m+1} = f_{H_2 0,m}\frac{2v_x - (x_{m+1} - x_m)\alpha_{c,m}}{2v_x + (x_{m+1} - x_m)\alpha_{c,m+1}} + \frac{(x_{m+1} - x_m)(S_{H_2,m+1}\hat{f}_{w,m+1} + S_{H_2,m}\hat{f}_{w,m})}{2v_x + (x_{m+1} - x_m)\alpha_{c,m+1}}.$$

(2.21)

With the definitions,

$$A_m \equiv \frac{2v_x - (x_{m+1} - x_m)\alpha_{c,m}}{2v_x + (x_{m+1} - x_m)\alpha_{c,m+1}},$$

$$F_m \equiv \frac{(x_{m+1} - x_m)(S_{H_2,m+1}\hat{f}_{w,m+1} + S_{H_2,m}\hat{f}_{w,m})}{2v_x + (x_{m+1} - x_m)\alpha_{c,m+1}}, \qquad (2.22)$$

the mesh equation for the 0th generation ($v_x > 0$) becomes

$$f_{H_2 0,m+1} = f_{H_2 0,m}A_m + F_m. \qquad (2.23)$$

For the case of $v_x > 0$, the boundary condition $f_{H_2 0}(v_x > 0, v_r, x_a) = f_{H_2}(v_x > 0, v_r, x_a)$ -> specified is employed and a recursive use of Eq. (2.24) yields $f_{H_2 0}(v_x > 0, v_r, x_m)$ for all m.

A useful recursion formula for the case of $v_x < 0$ can be obtained from Eq. (2.21) by replacing $m+1$ with $m-1$,

$$f_{H_2 0,m-1} = f_{H_2 0,m} \frac{-2v_x - (x_m - x_{m-1})\alpha_{c,m}}{-2v_x + (x_m - x_{m-1})\alpha_{c,m-1}} + \frac{(x_m - x_{m-1})(S_{H_2,m}\hat{f}_{w,m} + S_{H_2,m-1}\hat{f}_{w,m-1})}{-2v_x + (x_m - x_{m-1})\alpha_{c,m-1}} \tag{2.24}$$

With the definitions,

$$C_m \equiv \frac{-2v_x - (x_m - x_{m-1})\alpha_{c,m}}{-2v_x + (x_m - x_{m-1})\alpha_{c,m-1}}$$

$$G_m \equiv \frac{(x_m - x_{m-1})(S_{H_2,m}\hat{f}_{w,m} + S_{H_2,m-1}\hat{f}_{w,m-1})}{-2v_x + (x_m - x_{m-1})\alpha_{c,m-1}} \tag{2.25}$$

the mesh equation for the 0th generation ($v_x < 0$) becomes

$$f_{H_2 0,m-1} = f_{H_2 0,m} C_m + G_m. \tag{2.26}$$

Now, applying the boundary condition $f_{H_2 0}(v_x < 0, v_r, x_b) = 0$, a recursive use of Eq. (2.26) yields $f_{H_2 0}(v_x < 0, v_r, x_m)$ for all m. Note that Eqs. (2.22) and (2.25) indicate that the x mesh spacing must be small enough to avoid nonsensical negative distribution functions. The mesh spacing must satisfy

$$(x_{m+1} - x_m) < \frac{2|v_x|}{\max[\alpha_{c,m}, \alpha_{c,m+1}]}. \tag{2.27}$$

Thus the maximum allowed x grid spacing is related to the magnitude of the smallest non-zero grid element in the v_x axis.

2.2.6.2 Mesh Equation - 0th Generation for $v_x = 0$

For $v_x = 0$, Eqs. (2.20) yield the direct relationship,

$$f_{H_2 0,m} = \frac{S_{H_2,m}\hat{f}_w}{\alpha_{c,m}}. \qquad (2.28)$$

2.2.6.3 Mesh Equation - jth Generation (j > 0) for $v_x \neq 0$

In this scheme, the mesh equation for the j^{th} generation (with $v_x \neq 0$) becomes

$$\begin{aligned}\frac{f_{H_2 j,m+1} - f_{H_2 j,m}}{x_{m+1} - x_m} &= \frac{1}{2v_x}(s_{wall\,j-1,m+1} + s_{wall\,j-1,m}) \\ &+ \frac{1}{2v_x}(\beta_{cx\,j-1,m+1} + \beta_{cx\,j-1,m}) \\ &- \frac{1}{2v_x}(\alpha_{c,m+1} f_{H_2 j,m+1} + \alpha_{c,m} f_{H_2 j,m}) \\ &+ \frac{1}{2v_x}(\omega_{el,m+1} M_{H_2 j-1,m+1} + \omega_{el,m} M_{H_2 j-1,m})\end{aligned}$$

$$\begin{aligned}f_{H_2 j,m+1}\left(1 + \frac{x_{m+1} - x_m}{2v_x}\alpha_{c,m+1}\right) &= f_{H_2 j,m}\left(1 - \frac{x_{m+1} - x_m}{2v_x}\alpha_{c,m}\right) \\ &+ \frac{x_{m+1} - x_m}{2v_x}(s_{wall\,j-1,m+1} + \beta_{cx\,j-1,m+1} + \omega_{el,m+1} M_{H_2 j-1,m+1} + s_{wall\,j-1,m} + \beta_{cx\,j-1,m} + \omega_{el,m} M_{H_2 j-1,m})\end{aligned}$$

$$\begin{aligned}f_{H_2 j,m+1} &= f_{H_2 j,m}\frac{2v_x - (x_{m+1} - x_m)\alpha_{c,m}}{2v_x + (x_{m+1} - x_m)\alpha_{c,m+1}} \\ &+ \frac{(x_{m+1} - x_m)\left(s_{wall\,j-1,m+1} + \beta_{cx\,j-1,m+1} + \omega_{el,m+1} M_{H_2 j-1,m+1} + s_{wall\,j-1,m} + \beta_{cx\,j-1,m} + \omega_{el,m} M_{H_2 j-1,m}\right)}{2v_x + (x_{m+1} - x_m)\alpha_{c,m+1}}\end{aligned}$$

. (2.29)

With the definition,

$$B_m = \frac{\left(x_{m+1} - x_m\right)}{2v_x + \left(x_{m+1} - x_m\right)\alpha_{c,m+1}} \tag{2.30}$$

the mesh equation for the j^{th} generation ($v_x > 0$) becomes

$$f_{H_2 j,m+1} = f_{H_2 j,m} A_m + B_m\left(s_{wall\, j-1,m+1} + \beta_{cx\, j-1,m+1} + \omega_{el,m+1} M_{H_2 j-1,m+1} + s_{wall\, j-1,m} + \beta_{cx\, j-1,m} + \omega_{el,m} M_{H_2 j-1,m}\right) \tag{2.31}$$

For the case of $v_x > 0$, the boundary condition $f_{H_2 j}(v_x > 0, v_r, x_a) = 0$ is employed and a recursive use of Eq. (2.31) yields $f_{H_2 j}(v_x > 0, v_r, x_m)$ for all m.

Again, a useful recursion formula for the case of $v_x < 0$ can be obtained from Eq. (2.29) by replacing $m+1$ with $m-1$,

$$f_{H_2 j,m-1} = f_{H_2 j,m} \frac{-2v_x - \left(x_m - x_{m-1}\right)\alpha_{c,m}}{-2v_x + \left(x_m - x_{m-1}\right)\alpha_{c,m-1}} + \frac{\left(x_m - x_{m-1}\right)\left(s_{wall\, j-1,m-1} + \beta_{cx\, j-1,m-1} + \omega_{el,m-1} M_{H_2 j-1,m-1} + s_{wall\, j-1,m} + \beta_{cx\, j-1,m} + \omega_{el,m} M_{H_2 j-1,m}\right)}{-2v_x + \left(x_m - x_{m-1}\right)\alpha_{c,m-1}} . \tag{2.32}$$

With the definition,

$$D_m = \frac{\left(x_m - x_{m-1}\right)}{-2v_x + \left(x_m - x_{m-1}\right)\alpha_{c,m-1}} \quad , \tag{2.33}$$

the mesh equation for the j^{th} generation ($v_x < 0$) becomes

$$f_{H_2 j,m-1} = f_{H_2 j,m} C_m + D_m\left(s_{wall\, j-1,m-1} + \beta_{cx\, j-1,m-1} + \omega_{el,m-1} M_{H_2 j-1,m-1} + s_{wall\, j-1,m} + \beta_{cx\, j-1,m} + \omega_{el,m} M_{H_2 j-1,m}\right) . \tag{2.34}$$

Now, applying the boundary condition $f_{H_2 j}(v_x < 0, v_r, x_b) = 0$, a recursive use of Eq. (2.34) yields $f_{H_2 j}(v_x < 0, v_r, x_m)$ for all m.

2.2.6.4 Mesh Equation - j^{th} Generation ($j > 0$) for $v_x = 0$

For $v_x = 0$, Eqs. (2.20) yield the direct relationships,

$$f_{H_2 j,m} = \frac{s_{wall\ j-1,m} + \beta_{cx\ j-1,m} + \omega_{el,m} M_{H_2 j-1,m}}{\alpha_{c,m}}. \qquad (2.35)$$

2.3 Numerical Procedure

The procedure for computing the neutral molecular distribution function can now be outlined as follows:

A. Compute $\alpha_{Loss}(x)$ from inputted T_e and n_e data using Eq. (2.2).

B. If charge exchange option 'A' is used, then compute $\Sigma_{cx}(v_x, v_r, v_x', v_r')$ from Eq. (2.10a').

C. Compute $\Sigma^{iso}_{H_2:H_2}(v_x, v_r, v_x', v_r')$ for computational grid using Eq. (2.14).

D. Compute $\Sigma^{mt}_{H_2:H}(v_x, v_r, v_x', v_r')$ and $\alpha^{mt}_{H_2:H}(v_x, v_r, x)$ for inputted f_n using Eq. (2.13).

E. Compute $\Sigma^{mt}_{H_2:H^+}(v_x, v_r, v_x', v_r')$ using Eq. (2.12).

------ *entry point for $f_{H_2 s}$ iteration* ------

F. Compute $\alpha_{cx}(v_x, v_r, x)$ from 'seed' $T_{H_2^+}$ and $n_{H_2^+}$ data using Eqs. (2.10 a/b).

G. Compute $\alpha^{mt}_{H_2:H^+}(v_x, v_r, x)$ from inputted T_i data and $n_i = n_e - n_{H_2^+}$ using Eq. (2.12).

H. Compute $\omega_{el}(x)$ from 'seed' $f_{H_2 s}$ using Eqs. (2.12)-(2.15).

I. Compute $\alpha_c(v_x, v_r, x)$ from Eq. (2.16).

J. Test x grid spacing using Eq. (2.27).

K. Compute A_m, F_m, C_m, G_m, B_m, and D_m from Eqs. (2.22), (2.25), (2.30) and (2.33).

L. Compute $f_{H_2 0}(v_x, v_r, x)$ from Eqs. (2.23), (2.26), and (2.28).

M. Compute β_{cx0} from $f_{H_2 0}(v_x, v_r, x)$ and $\alpha_{cx}(v_x, v_r, x)$ or $\Sigma_{cx}(v_x, v_r, v_x', v_r')$, Eq. (2.11 a/b).

N. Compute $M_{H_2 0}(v_x, v_r, x)$ from $f_{H_2 0}(v_x, v_r, x)$ using Eqs. (2.6)-(2.8) and (2.17).

------ *entry point for next generation loop* ------

O. Compute $f_{H_2\,j}(v_x, v_r, x)$ for next generation from Eqs. (2.31), (2.34) and (2.35).

P. Compute $\beta_{cx\,j}$ from $f_{H_2\,j}(v_x, v_r, x)$ and $\alpha_{cx}(v_x, v_r, x)$or $\Sigma_{cx}(v_x, v_r, v_x', v_r')$, Eq. (2.11 a/b).

Q. Compute $M_{H_2 j}(v_x, v_r, x)$ from $f_{H_2\,j}(v_x, v_r, x)$ using Eqs. (2.6)-(2.8) and (2.17).

R. Repeat steps O, P, and Q for succeeding generations until $\max(n_{H_2\,j}) / \max(n_{H_2\,0}) < \xi$ where ξ corresponds to the parameter , **`truncate`**.

S. Compute the total molecular neutral distribution function from the summation:

$$f_{H_2}(v_x, v_r, x) = \sum_j f_{H_2 j}(v_x, v_r, x).$$

T. Compute $n_{H_2^+}$ and $T_{H_2^+}$ from source rates, loss rates, and energy equilibration time.

U. Compare molecular densities with 'seed' values. If $\max(|n_{H_2\,s}) - n_{H_2}|) / \max(n_{H_2}) > \xi$ then set $f_{H_2} \rightarrow f_{H_2\,s}$ and return to step F.

V. Self-consistent computation of $f_{H_2}(v_x, v_r, x)$ is complete. Compute the velocity space source distribution of atomic hydrogren arising from the dissociation of neutral and ionized molecules using formulas outlined in section 2.1.3.E and velocity space model function described in 2.1.2.5.

W. Compute velocity space moments of $f_{H_2}(v_x, v_r, x)$ including, temperature, pressure, diagonal elements of the stress tensor, and heat fluxes.

2.4 IDL Program

The complete call to the IDL procedure, **`Kinetic_H2.pro`**, is listed below:

```
;+
; Kinetic_H2.pro
;
; This subroutine is part of the "KN1D" atomic and molecular neutal transport code.
;
;   This subroutine solves a 1-D spatial, 2-D velocity kinetic neutral transport
; problem for molecular hydrogen or deuterium (H2) by computing successive generations of
; charge exchange and elastic scattered neutrals. The routine handles electron-impact
; ionization and dissociation, molecular ion charge exchange, and elastic
; collisions with hydrogenic ions, neutral atoms, and molecules.
;
;   The positive vx half of the atomic neutral distribution function is inputted at x(0)
; (with arbitrary normalization). The desired flux on molecules entering the slab geometry at
; x(0) is specified. Background profiles of plasma ions, (e.g., Ti(x), Te(x), n(x), vxi(x),...)
; and atomic distribution function (fH) is inputted. (fH can be computed by procedure
; "Kinetic_H.pro".) Optionally, a molecular source profile (SH2(x)) is also inputted.
; The code returns the molecular hydrogen distribution function, fH2(vr,vx,x) for all
; vx, vr, and x of the specified vr,vx,x grid. The atomic (H) and ionic (P) hydrogen
; source profiles and the atomic source velocity distribution functions
; resulting from Franck-Condon reaction product energies of H are also returned.
;
;   Since the problem involves only the x spatial dimension, all distribution functions
; are assumed to have rotational symmetry about the vx axis. Consequently, the distributions
; only depend on x, vx and vr where vr =sqrt(vy^2+vz^2)
;
;  History:
;
;    B. LaBombard   First coding based on Kinetic_Neutrals.pro 22-Dec-2000
;
;    For more information, see write-up: "A 1-D Space, 2-D Velocity, Kinetic
;    Neutral Transport Algorithm for Hydrogen Molecules in an Ionizing Plasma", B. LaBombard
;
; Note: Variable names contain characters to help designate species -
;       atomic neutral (H), molecular neutral (H2), molecular ion (HP), proton (i) or (P)
;
;_____________________________________________________________________________
pro  Kinetic_H2,vx,vr,x,Tnorm,mu,Ti,Te,n,vxi,fH2BC,GammaxH2BC,NuLoss,PipeDia,fH,SH2,$
        fH2,nH2,GammaxH2,VxH2,pH2,TH2,qxH2,qxH2_total,Sloss,QH2,RxH2,QH2_total,AlbedoH2,WallH2,$
       truncate=truncate,$
       nHP,THP,fSH,SH,SP,SHP,NuE,NuDis,$
      Simple_CX=Simple_CX,Max_Gen=Max_Gen,Compute_H_Source=Compute_H_Source,$
      No_Sawada=No_Sawada,H2_H2_EL=H2_H2_EL,H2_P_EL=H2_P_EL,H2_H_EL=_H2_H_EL,H2_HP_CX=H2_HP_CX,$
      ni_correct=ni_correct,$
       ESH=ESH,Eaxis=Eaxis,error=error,compute_errors=compute_errors,$
       plot=plot,debug=debug,debrief=debrief,pause=pause

    common  Kinetic_H2_Output,piH2_xx,piH2_yy,piH2_zz,RxH2CX,RxH_H2,RxP_H2,RxW_H2,$
            EH2CX,EH_H2,EP_H2,EW_H2,Epara_PerpH2_H2

    common  Kinetic_H2_Errors,Max_dx,vbar_error,mesh_error,moment_error,C_Error,$
             CX_Error,Swall_Error,H2_H2_error,Source_Error,qxH2_total_error,QH2_total_error
;
;  Input:
;                  vx(*) - fltarr(nvx), normalized x velocity coordinate
;                          [negative values, positive values],
;                          monotonically increasing. Note: a nonuniform mesh can be used.
;                          Dimensional velocity (note: Vth is based on ATOM mass)
;                          is v = Vth * vx where Vth=sqrt(2 k Tnorm/(mH*mu))
;                          Note: nvx must be even and vx(*) symmetric about
;                          zero but not contain a zero element
;                  vr(*) - fltarr(nvr), normalized radial velocity coordinate
;                           [positive values], monotonically increasing. Note: a non-uniform mesh
;                          an be used.
;                           Dimensional velocity is v = Vth * vr where Vth=sqrt(2 k Tnorm/(mH*mu))
;                          Note: vr must not contain a zero element
;                   x(*) - fltarr(nx), spatial coordinate (meters),
;                           positive, monontonically increasing. Note: a non-uniform mesh can be
;                          used.
;                  Tnorm - Float, temperature corresponding to the thermal speed (see vx and vr
;                          above) (eV)
;                     mu - Float, 1=hydrogen, 2=deuterium
;                     Ti - fltarr(nx), Ion temperature profile (eV)
;                     Te - fltarr(nx), electron temperature profile (eV)
;                      n - fltarr(nx), electron density profile (m^-3)
;                    vxi - fltarr(nx), x-directed plasma ion and molecular ion flow profile
;                            (m s^1-)
```

```
;                fH2BC - fltarr(nvr,nvx), this is an input boundary condition
;                        specifying the shape of the neutral molecule velocity distribution
;                        function at location x(0). Normalization is arbitrary.
;                        Only values with positive vx, fH2BC(*,nvx/2:*) are used
;                       by the code.
;           GammaxH2BC - float, desired neutral molecule flux density in the +Vx
;                        direction at location x(0) (m^-2 s^-1)
;                        fH2BC is scaled to yield this flux density.
;              NuLoss - fltarr(nx), characteristic loss frequency for HP molecules (1/s)
;                        (for open field lines, this is ~Cs/L). If this variable is undefined,
;                       then NuLoss set set to zero.
;             PipeDia - fltarr(nx), effective pipe diameter (meters)
;                        This variable allows collisions with the 'side-walls' to be simulated.
;                        If this variable is undefined, then PipeDia set set to zero. Zero values
;                        of PipeDia are ignored (i.e., treated as an infinite diameter).
;                  fH - fltarr(nvr,nvx,nx), neutral atomic velocity distribution
;                        function. fH is normalized so that the atomic neutral density, nH(k), is
;                        defined as the velocity space integration:
;                          nH(k)=total(Vr2pidVr*(fH(*,*,k)#dVx))
;                        If this variable is undefined, then no molecule-atom collisions are
;                       included.
;                        NOTE: dVx is velocity space differential for Vx axis and
;                        Vr2pidVr = Vr*!pi*dVr with dVr being velocity space differential for Vr
;                         axis.
;                 SH2 - fltarr(nx), source profile of wall-temperature (room temperature) H2
;                         molecules (m^-3 s^-1)
;                        If this variable is undefined, it is set equal to zero.
;
; Input & Output:
;                 fH2 - fltarr(nvr,nvx,nx), neutral molecule velocity distribution
;                      function.
;                       'Seed' values for this may be specified on input. If this parameter
;                       is undefined, then a zero 'seed' value will be used.
;                       The algorithm outputs a self-consistent fH2.
;                       fH2 is normalized so that the neutral density, nH2(k), is defined as
;                       the velocity space integration:
;                           nH2(k)=total(Vr2pidVr*(fH2(*,*,k)#dVx))
;                 nHP - fltarr(nx), molecular ion density profile (m^-3)
;                          'Seed' values for this may be specified on input. If this parameter
;                          is undefined, then a zero 'seed' value will be used.
;                          The algorithm outputs a self-consistent profile for nHP.
;                 THP - fltarr(nx), molecular ion temperature profile (m^-3)
;                          'Seed' values for this may be specified on input. If this parameter
;                          is undefined, then a 'seed' value of 3 eV will be used.
;                          The algorithm outputs a self-consistent profile for THP.
;
; Output:
;                 fH2 - fltarr(nvr,nvx,nx), neutral molecule velocity distribution
;                        function. fH2 is normalized so that the neutral density, nH2(k), is
;                        defined as the velocity space integration:
;                            nH2(k)=total(Vr2pidVr*(fH2(*,*,k)#dVx))
;                 nH2 - fltarr(nx), neutral molecule density profile (m^-3)
;           GammaxH2 - fltarr(nx), neutral flux profile (# m^-2 s^-1)
;                           computed from GammaxH2(k)=Vth*total(Vr2pidVr*(fH2(*,*,k)#(Vx*dVx)))
;               VxH2 - fltarr(nx), neutral velocity profile (m s^-1)
;                           computed from GammaxH2/nH2
;
;                       To aid in computing the some of the quantities below, the procedure
;                      internally defines the quantities:
;                        vr2vx2_ran(i,j,k)=vr(i)^2+(vx(j)-VxH2(k))^2
;                                   which is the magnitude of 'random v^2' at each mesh point
;                        vr2vx2(i,j,k)=vr(i)^2+vx(j)^2
;                                   which is the magnitude of 'total v^2' at each mesh point
;                        q=1.602177D-19, mH=1.6726231D-27
;                        C(*,*,*) is the right hand side of the Boltzmann equation, evaluated
;                                 using the computed neutral distribution function
;
;                 pH2 - fltarr(nx), neutral pressure (eV m^-2)
;                 TH2 - fltarr(nx), neutral temperature profile (eV) computed from: TH2=pH2/nH2
;                qxH2 - fltarr(nx), neutral random heat flux profile (watts m^-2)
;          qxH2_total - fltarr(nx), total neutral heat flux profile (watts m^-2)
;                           This is the total heat flux transported by the neutrals
;               Sloss - fltarr(nx), H2 loss rate from ionization and dissociation (SH2)
;                         (m^-3 s^-1)
;                  QH2 - fltarr(nx), rate of net thermal energy transfer into neutral molecules
;                         (watts m^-3)
;                 RxH2 - fltarr(nx), rate of x momentum transfer to neutral molecules
;                         (=force, N m^-2).
;           QH2_total - fltarr(nx), net rate of total energy transfer into neutral molecules
;                         (watts m^-3)
;            AlbedoH2 - float, Ratio of molceular particle flux with Vx < 0 divided by particle
```

```
;                          flux with Vx > 0  at x=x(0)
;                         (Note: For SH2 non-zero, the flux with Vx < 0 will include
;                          contributions from molecular hydrogen sources within the 'slab'.
;                          In this case, this parameter does not return the true 'Albedo'.)
;                 WallH2 - fltarr(nx), molecular sink rate and source rate from interation with
;                           'side walls' (m^-3 s^-1)
;                          Note: There is no loss of molecules when they strike the side walls in
;                         this model. The molecules are just relaunched with a Maxwellian
;                         distribution at the wall temperature.
;
;                    nHP - fltarr(nx), molecular ion density profile (m^-3)
;                             'Seed' values for this may be specified on input.
;                    THP - fltarr(nx), molecular ion temperature profile (m^-3)
;                             'Seed' values for this may be specified on input.
;                    fSH - fltarr(nvr,nvx,nx), H source velocity distribution.
;                          fSH is normalized so that the total atomic neutral
;                          source, SH(k), is defined as the velocity space integration:
;                              SH(k)=total(Vr2pidVr*(fSH(*,*,k)#dVx))
;                     SH - fltarr(nx), atomic neutral source profile (m^-3 s^-1)
;                             computed from total(Vr2pidVr*(fSH(*,*,k)#dVx))
;                     SP - fltarr(nx), proton source profile (m^-3 s^-1)
;                    SHP - fltarr(nx), molecular ion source profile (m^-3 s^-1)
;                    NuE - fltarr(nx), energy equilibration frequency of molecular ion with bulk
;                           plasma (1/s)
;                  NuDis - fltarr(nx), molecular ion dissociation frequency (1/s)
;
; KEYWORDS:
;   Output:
;                     ESH - fltarr(nvr,nx) - returns normalized H source energy distribution
;                             derived from velocity-space distribution:
;                           ESH(*,*) = 0.5*mu*mH*Vr^2 FSH(*,vx=0,*)*4*pi*Vr/(mu*mH)
;                  Eaxis - fltarr(nvr) - returns energy coordinate for ESH (eV) = 0.5*mu*mH*Vr^2
;                  error - Returns error status: 0=no error, solution returned
;                                                1=error, no solution returned
;
; COMMON BLOCK KINETIC_H2_OUTPUT
;    Output:
;                 piH2_xx - fltarr(nx), xx element of stress tensor (eV m^-2)
;                 piH2_yy - fltarr(nx), yy element of stress tensor (eV m^-2)
;                 piH2_zz - fltarr(nx), zz element of stress tensor (eV m^-2) = piH2_yy
;                           Note: cylindrical system relates r^2 = y^2 + z^2. All other stress
;                           tensor elements are zero.
;
;            The following momentum and energy transfer rates are computed from charge-exchange
;            collsions between species:
;                 RxH2CX - fltarr(nx), rate of x momentum transfer from molecular ions to neutral
;                           molecules (=force/vol, N m^-3).
;                  EH2CX - fltarr(nx), rate of energy transfer from molecular ions to neutral
;                           molecules (watts m^-3).
;
;            The following momentum and energy transfer rates are computed from elastic collsions
;            between species:
;                 RxH_H2 - fltarr(nx), rate of x momentum transfer from neutral atoms to molecules
;                           (=force/vol, N m^-3).
;                 RxP_H2 - fltarr(nx), rate of x momentum transfer from hydrogen ions to neutral
;                           molecules (=force/vol, N m^-3).
;                  EH_H2 - fltarr(nx), rate of energy transfer from neutral atoms to molecules
;                           (watts m^-3).
;                  EP_H2 - fltarr(nx), rate of energy transfer from hydrogen ions to neutral
;                           molecules (watts m^-3).
;
;            The following momentum and energy transfer rates are computed from collisions with the
;           'side-walls'
;                 RxW_H2 - fltarr(nx), rate of x momentum transfer from wall to molecules
;                           (=force/vol, N m^-3).
;                  EW_H2 - fltarr(nx), rate of energy transfer from wall to neutral molecules
;                           (watts m^-3).
;
;            The following is the rate of parallel to perpendicular energy transfer computed from
;            elastic collisions
;
;          Epara_PerpH2_H2 - fltarr(nx), rate of parallel to perp energy transfer within molecular
;                            hydrogen species (watts m^-3).
;
; KEYWORDS:
;   Input:
;               truncate - float, stop computation when the maximum
;                          increment of neutral density normalized to
;                          inputed neutral density is less than this
;                          value in a subsequent generation. Default value is 1.0e-4
;
```

```
;             Simple_CX - if set, then use CX source option (B): Neutral molecules are born
;                         in velocity with a distribution proportional to the local
;                         molecular ion distribution function. Simple_CX=1 is default.
;
;                         if not set, then use CX source option (A): The CX source
;                         neutral molecule distribution function is computed by evaluating the
;                         the CX cross section for each combination of (vr,vx,vr',vx')
;                         and convolving it with the molecule neutral distribution function.
;                         This option requires more CPU time and memory.
;
;               Max_gen - integer, maximum number of collision generations to try including before
;                         giving up. Default is 50.
;
;      Compute_H_Source -  if set, then compute fSH, SH, SP, and SHP
;
;             No_Sawada - if set, then DO NOT correct reaction rates according to
;                           results from collisional-radiative model of Sawada
;                           [Sawada, K. and Fujimoto, T., Journal of Applied Physics 78 (1995)
;                           2913.]
;              H2_H2_EL - if set, then include H2 -> H2 elastic self collisions
;                           Note: if H2_H2_EL is set, then algorithm iterates fH2 until
;                           self consistent fH2 is achieved.
;              H2_HP_CX - if set, then include H2 -> H2(+) charge exchange collisions
;                           Note: if H2_HP_CX is set, then algorithm iterates until
;                           self consistent nHp is achieved.
;               H2_P_EL - if set, then include H2 -> H(+) elastic collisions (does not lead to an
;                         iteration loop)
;               H2_H_EL - if set, then include H2 -> H elastic collisions (does not lead to an
;                         iteration loop)
;            ni_correct - if set, then algorithm corrects hydrogen ion density
;                           according to quasineutrality: ni=ne-nHp
;                           This is done in an iteration loop.
;
;        Compute_Errors - if set, then return error estimates in common block KINETIC_H2_ERRORS
;                         below
;
;                  plot - 0= no plots, 1=summary plots, 2=detail plots, 3=very detailed plots
;                 debug - 0= do not execute debug code, 1=summary debug, 2=detail debug, 3=very
;                         detailed debug
;               debrief - 0= do not print, 1=print summary information, 2=print detailed
;                         information
;                 pause - if set, then pause between plots
;
; COMMON BLOCK KINETIC_H2_ERRORS
;
;       if COMPUTE_ERRORS keyword is set then the following is returned in common block
;       KINETIC_H2_ERRORS
;
;                 Max_dx - float(nx), Max_dx(k) for k=0:nx-2 returns maximum
;                          allowed x(k+1)-x(k) that avoids unphysical negative
;                          contributions to fH2
;           Vbar_error - float(nx), returns numerical error in computing
;                          the speed of neutrals averged over maxwellian distribution;
;                          over a temperature range spanning the Franck Condon energies
;                          of reactions R2, R3, R4, R5, R6, R7, R8, R10
;                          The average speed should be:
;                                  vbar_exact=2*Vth*sqrt(Ti(*)/Tnorm)/sqrt(!pi)
;                          Vbar_error returns: abs(vbar-vbar_exact)/vbar_exact
;                          where vbar is the numerically computed value.
;           mesh_error - fltarr(nvr,nvx,nx), normalized error of solution
;                          based on substitution into Boltzmann equation.
;         moment_error - fltarr(nx,m), normalized error of solution
;                          based on substitution into velocity space
;                          moments (v^m) of Boltzmann equation, m=[0,1,2,3,4]
;              C_error - fltarr(nx), normalized error in charge exchange and elastic scattering
;                          collision operator. This is a measure of how well the charge exchange
;                          and elastic scattering portions of the collision operator conserve
;                          particles.
;             CX_error - fltarr(nx), normalized particle conservation error in charge exchange
;                          collision operator.
;          H2_H2_error - fltarr(nx,[0,1,2]) return normalized errors associated with
;                          particle [0], x-momentum [1], and total energy [2] convervation of the
;                          elastic self-collision operator
;
;          Source_error - fltarr(nx), normalized error in mass continuity equation. This is a
;                          measure of how well atomic plus molecular mass continuity is satisfied.
;       qxH2_total_error - fltarr(nx), normalized error estimate in computation of qxH2_total
;        QH2_total_error - fltarr(nx), normalized error estimate in computation of QH2_total
;
;-------------------------------------------------------------------------
;-
```

2.5 Validation of Numerical Solution

The total neutral molecular distribution function, $f_{H_2}(v_x, v_r, x)$, computed from the numerical algorithm should satisfy the Boltzmann equation,

$$v_x \frac{\partial f_{H_2}}{\partial x} = S_{H_2}^{tot} \hat{f}_w + \beta_{cx} - \alpha_c f_{H_2} + \omega_M, \tag{2.36}$$

at every location on the mesh. According to the numerical scheme outlined in section 3, this equation can be written as the mesh equation,

$$\begin{aligned} 2v_x \frac{f_{H_2,m+1} - f_{H_2,m}}{x_{m+1} - x_m} = & (S_{H_2,m+1}^{tot} + S_{H_2,m}^{tot}) \hat{f}_w + (\beta_{cx,m+1} + \beta_{cx,m}) \\ & - (\alpha_{c,m+1} f_{H_2,m+1} + \alpha_{c,m} f_{H_2,m}) \\ & + (\omega_{M,m+1} + \omega_{M,m}) \end{aligned} \quad . \tag{2.37}$$

2.5.1 Mesh Point Error

By defining the five terms in Eq. (2.37) as

$$\begin{aligned} T1_m &= 2v_x \frac{f_{H_2,m+1} - f_{H_2,m}}{x_{m+1} - x_m}, \\ T2_m &= (S_{H_2,m+1}^{tot} + S_{H_2,m}^{tot}) \hat{f}_w, \\ T3_m &= \beta_{cx,m+1} + \beta_{cx,m}, \\ T4_m &= \alpha_{c,m+1} f_{n,m+1} + \alpha_{c,m} f_{n,m}, \\ T5_m &= \omega_{M,m+1} + \omega_{M,m}, \end{aligned} \tag{2.38}$$

a normalized error parameter can be defined for spatial mesh points with $x_a \le x < x_b$, and all velocity mesh points as

$$\varepsilon_{k,l,m} \equiv \frac{\left| T1_{k,l,m} - T2_{k,l,m} - T3_{k,l,m} + T4_{k,l,m} - T5_{k,l,m} \right|}{\max(\left|T1_{k,l,m}\right|, \left|T2_{k,l,m}\right|, \left|T3_{k,l,m}\right|, \left|T4_{k,l,m}\right|, \left|T5_{k,l,m}\right|)}. \tag{2.39}$$

Values of $\varepsilon_{k,l,m}$ are returned in parameter **`mesh_error`**.

2.5.2 Velocity Moment Error

$f_{H_2}(v_x, v_r, x)$ should also satisfy velocity moments (M) of the Boltzmann equation,

$$\iint \frac{\partial f_{H_2}}{\partial x} v_x^{M+1} \partial v_x v_r \partial v_r = \iint S_{H_2}^{tot} \hat{f}_w v_x^M \partial v_x v_r \partial v_r + \iint \beta_{cx} v_x^M \partial v_x v_r \partial v_r - \iint \alpha_c f_{H_2} v_x^M \partial v_x v_r \partial v_r + \iint \omega_M v_x^M \partial v_x v_r \partial v_r . \quad (2.40)$$

Making use of Eqs. (2.37) and (2.38), this can be expressed as

$$\iint T1_m v_x^M \partial v_x v_r \partial v_r = \iint T2_m v_x^M \partial v_x v_r \partial v_r + \iint T3_m v_x^M \partial v_x v_r \partial v_r - \iint T4_m v_x^M \partial v_x v_r \partial v_r + \iint T5_m v_x^M \partial v_x v_r \partial v_r .$$

Defining

$$\begin{aligned} T1_{M,m} &= \iint T1_m v_x^M \partial v_x v_r \partial v_r , \\ T2_{M,m} &= \iint T2_m v_x^M \partial v_x v_r \partial v_r , \\ T3_{M,m} &= \iint T3_m v_x^M \partial v_x v_r \partial v_r , \\ T4_{M,m} &= \iint T4_m v_x^M \partial v_x v_r \partial v_r , \\ T5_{M,m} &= \iint T5_m v_x^M \partial v_x v_r \partial v_r , \end{aligned} \quad (2.41)$$

a normalized 'velocity moment error' for spatial mesh points with $x_a \le x < x_b$, can be constructed as

$$\eta_{M,m} \equiv \frac{\left| T1_{M,m} - T2_{M,m} - T3_{M,m} + T4_{M,m} - T5_{M,m} \right|}{\max(\left|T1_{M,m}\right|, \left|T2_{M,m}\right|, \left|T3_{M,m}\right|, \left|T4_{M,m}\right|, \left|T5_{M,m}\right|)}. \quad (2.42)$$

Values of $\eta_{M,m}$ are returned in parameter **`moment_error`**.

2.5.3 Error Associated with Digital Representation of Distribution Functions

Discretization introduces errors in evaluating moments of the distribution functions. If the velocity space mesh is too coarse such that f varies strongly between mesh points or if the mesh does

not cover a sufficient range such that f is has a significant component *outside* the mesh, then numerically evaluated moments of f will not be accurate. As a test of the numerical accuracy in the digital representation of f, **`Kinetic_H2.pro`** computes the average speed of neutrals using a digital representation of a Maxwellian distribution for neutral temperatures spanning the Franck-Condon energy ranges of reactions 2.R2-2.R8 and 2.R10. This speed is compared to the exact theoretical value:

$$\bar{v}_{code} = 2\pi \iint \sqrt{v_r^2 + v_x^2}\, \hat{f}_{\max} \partial v_x v_r \partial v_r$$

$$\bar{v}_{exact} \equiv \int |\underline{v}|\, \hat{f}_{\max}\ \partial^3 v = 4\pi \int \hat{f}_{\max} v^3 \partial v\ = \frac{2v_{th}}{\sqrt{\pi}}$$

The parameter **`Vbar_error`** in **`Kinetic_H2.pro`** returns a normalized error defined as

$$\bar{v}_{error,m} \equiv \left| \bar{v}_{code,m} - \bar{v}_{exact,m} \right| / \bar{v}_{exact,m}\ .$$

Values of **`Vbar_error`** = 0.05 or less indicate that molecular distribution functions are reasonably well represented by their digital expressions and that the choice of velocity mesh size and spacing is appropriate. For the case when plasma conditions varies significantly across the mesh, a non-uniform velocity space mesh can be used to more evenly distribute **`Vbar_error`** over the mesh.

[Note: IDL procedure **`Create_Kinetic_H2_Mesh.pro`**, is used to generate a (v_x, v_r) mesh which is close to the optimum for specified plasma profiles.]

2.5.4 Molecule/Atom/Ion Particle Balance

If the algorithm properly conserves particles, then the molecular flux (Γ_{H_2}), the molecular, atomic and ionic source terms (S_{H_2}, S_H, S_{H^+}), and the molecular ion loss rate ($n_{H_2^+} \nu_{loss}^{H_2^+}$) should satisfy the relationship,

$$2\frac{\partial \Gamma_{H_2}}{\partial x} - 2S_{H_2} + S_H + S_{H^+} + 2n_{H_2^+} \nu_{loss}^{H_2^+} = 0.$$

The parameter **`Source_error`** returns the normalized particle balance error estimate:

$$S_{Error} = \frac{\left| 2\frac{\partial \Gamma_{H_2}}{\partial x} - 2S_{H_2} + S_H + S_{H^+} + 2n_{H_2^+} \nu_{loss}^{H_2^+} \right|}{\max\left[\left| 2\frac{\partial \Gamma_{H_2}}{\partial x} \right|, \left| -2S_{H_2} + S_H + S_{H^+} + 2n_{H_2^+} \nu_{loss}^{H_2^+} \right|, \left| S_H \right|, \left| 2S_{H_2} \right| \right]} .$$

Section 3 - Kinetic_H: A 1-D Kinetic Neutral Transport Algorithm for Atomic Hydrogen in an Ionizing Plasma

The numerical algorithm embodied in **`Kinetic_H`** is summarized in the following graphic:

Kinetic_H
1-D Atomic Neutral Transport Code

Solve: $$v_x \frac{\partial f_H}{\partial x} = \left[\frac{\partial f_H}{\partial t}\right]_c + S_H$$

by method of successive collision generations (e.g. [a])

Electron-impact reactions included:

Ionization

$$e^- + H(1s) \rightarrow e^- + H^+ + e^- \quad \text{(R1)}$$

Radiative Recombination

$$e^- + H^+ \rightarrow H(1s) + h\nu \quad \text{(R2)}$$

Multistep corrections to reaction rates based on CR model of Johnson-Hinnov [d] are applied

Elastic collisions included using a BGK model [c]:

$$H + H^+ \rightarrow H + H^+ \quad \text{(R3)}$$

$$H_2 + H \rightarrow H_2 + H \quad \text{(R4)}$$

$$H + H \rightarrow H + H \quad \text{(R5)}$$

Collision frequencies set by:

Momentum transfer rate for mixed binary collisions
Temperature isotropization rate for self collisions

Charge exchange

$$H + H^+ \rightarrow H^+ + H \quad \text{(R6)}$$

[a] PFC Report: www.psfc.mit.edu/library/00rr/00RR009

[d] L. C. Johnson and E. Hinnov, J. Quant. Spectrosc. Radiat. Transfer **13**, 333 (1973).

[c] Bhatnagar, P.L., Gross, E.P., and Krook, M., Phys. Rev. **94** (1954) 511.

Fig. 3.1 - Overview of Atomic Neutral Transport Algorithm

3.0 Overview

The IDL procedure **`Kinetic_H`** computes the hydrogen or deuterium atomic neutral distribution function, f_n, in a slab geometry for inputted plasma profiles (density, ion and electron temperature). The distribution function is described in terms of two velocity components (making use of the rotational symmetry in velocity space about the *x*-axis) and one spatial component (*x*). The atomic neutral flux density entering the edge of the slab and its velocity distribution (positive *x* velocities) are prescribed boundary conditions. Velocity space source distributions of atomic neutrals (as a function of *x*) may be inputted. The algorithm constructs f_n by summing up successive generations of neutrals which have experienced a charge-exchange or elastic scattering event. Rates for charge exchange and elastic scattering of hydrogen or deuterium are computed using data compiled by Janev [3, 7]. Rates for electron impact ionization and radiative recombination are computed using the results from the collisional radiative model of Johnson and Hinnov[2]. The output of the computation is $f_n(v_x, v_r, x)$ and velocity moments of f_n including atomic neutral density, fluid velocity, temperature, pressure, diagonal elements of the stress tensor, and heat fluxes. In addition, the spatial profiles of the net rate of energy and *x*-directed momentum transfer between unlike species and to the 'side walls' are outputted. A number of numerical consistency checks are performed in the code involving mesh size limitations and errors associated with discrete representation of ion and neutral distribution functions. The accuracy of the numerical solution of f_n is optionally checked by direct substitution into the Boltzmann equation and reported at each point on the computational mesh.

3.1 Method

3.1.1 Computational Domain, Inputted Conditions

The parameter to be computed is the atomic neutral distribution function, f_n, over spatial region $[x_a, x_b]$. It is assumed that all distribution functions have rotational symmetry about the v_x axis so that they can be described in terms of two velocity coordinates and one spatial coordinate, e.g., $f_n = f_n(v_x, v_r, x)$, with $v_r^2 = v_y^2 + v_z^2$.

The computational domain is specified by input parameters as

$$-v_{x,\max} \le v_x \le v_{x,\max}, \quad v_{r,\min} \le v_r \le v_{r,\max}, \quad x_a \le x \le x_b.$$

The boundary conditions and constraints on the atomic neutral distribution function are:

$f_n(v_x > 0, v_r, x_a)$- specified (input)

$f_n(v_x < 0, v_r, x_b) = 0$

$\frac{\partial f_n}{\partial x}(v_x = 0, v_r, x)$ - finite

Background plasma conditions are inputted over spatial region $[x_a, x_b]$:

$n(x)$ - electron density profile

$T_e(x)$ - electron temperature profile

$T_i(x)$ - hydrogen ion temperature profile

$v_{xi}(x)$ - plasma ion fluid velocity profile in x-direction ($-x$ is towards the 'wall')

$n_{H_2^+}(x)$ - molecular ion density profile

A velocity space source function, S_{H^0}, of neutral hydrogen (or deuterium) atoms may also be specified over the spatial region $[x_a, x_b]$:

$S_{H^0}(v_x, v_r, x)$- atomic hydrogen velocity space source (optional)

An effective 'pipe diameter', may also be specified to simulate the effect of atoms colliding with 'side walls'and evolving as room temperature molecules.

$D(x)$ - effective pipe diameter (optional)

Background molecular hydrogen distribution function may be inputted over $[x_a, x_b]$:

$f_{H_2}(v_x, v_r, x)$- molecular hydrogen distribution function (optional)

3.1.2 Atomic Physics

The following 6 reactions are included in the computation:

Electron-Impact Ionization

$$e^- + H(1s) \rightarrow e^- + H^+ + e^- \qquad (3.R1)$$

Radiative Recombination

$$e^- + H^+ \rightarrow H(1s) + h\nu \qquad (3.R2)$$

Charge Exchange

$$H^+ + H(1s) \rightarrow H(1s) + H^+ \qquad (3.R3)$$

Elastic Collisions

$$H + H^+ \rightarrow H + H^+ \qquad \text{(3.R4)}$$

$$H + H_2 \rightarrow H + H_2 \qquad \text{(3.R5)}$$

$$H + H \rightarrow H + H \qquad \text{(3.R6)}$$

All reactions are assumed to occur with hydrogen atoms and molecules in the ground state, with the exception of reactions 3.R1 and 3.R3 which can normally includes multistep corrections (discussed in section 3.1.2.1).

Figure 3.2 shows the maxwellian-averaged reaction rate for 3.R1, $\langle \sigma v \rangle_{ion}$, reported by Janev [3] for a range of electron temperatures (not including multistep corrections).

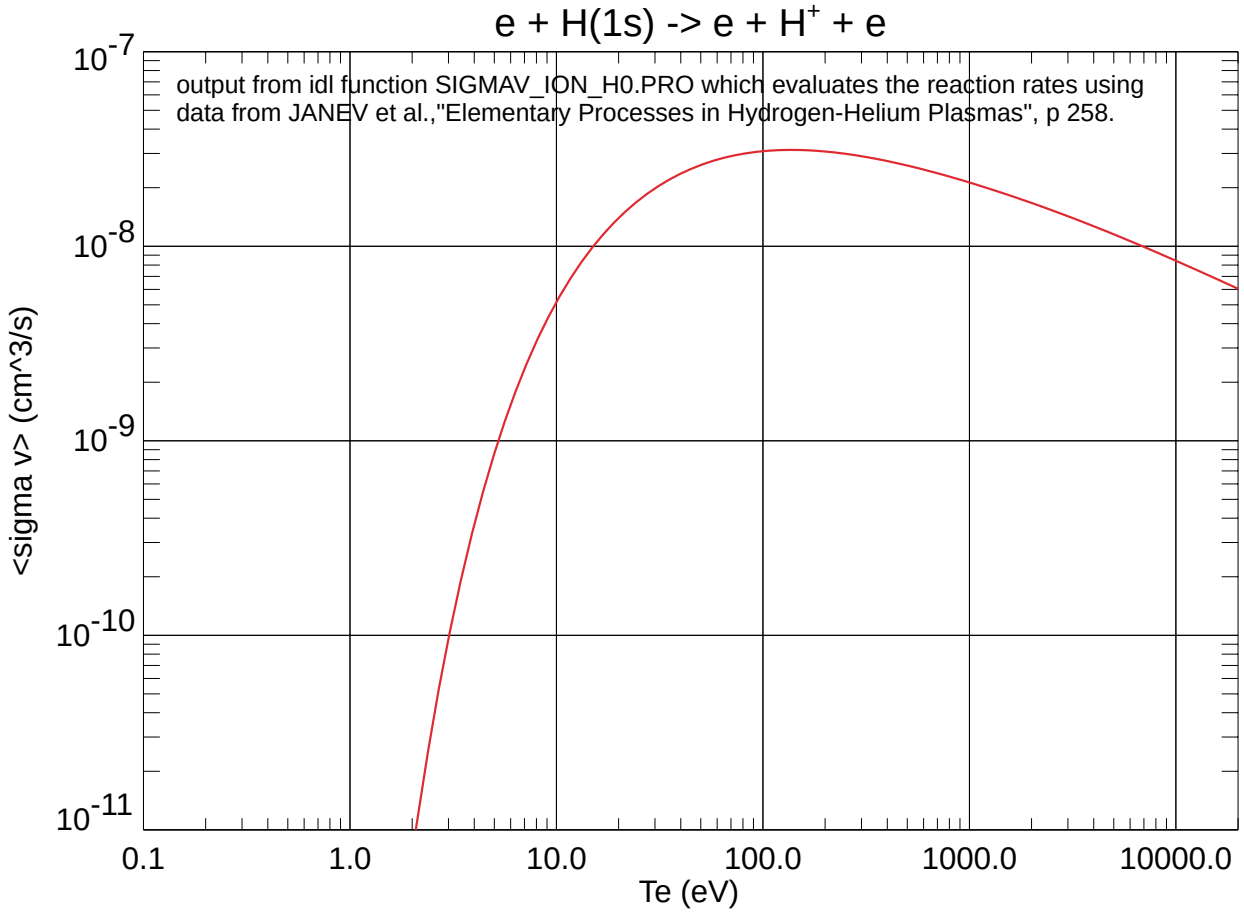

Fig. 3.2 - $\langle \sigma v \rangle_{ion}$ *as a function of Te.*

Figure 3.3 shows the maxwellian-averaged reaction rate for 3.R2, $\langle \sigma v \rangle_{rec}[T_e]$, tabulated by Janev [3] (multistep processes not included).

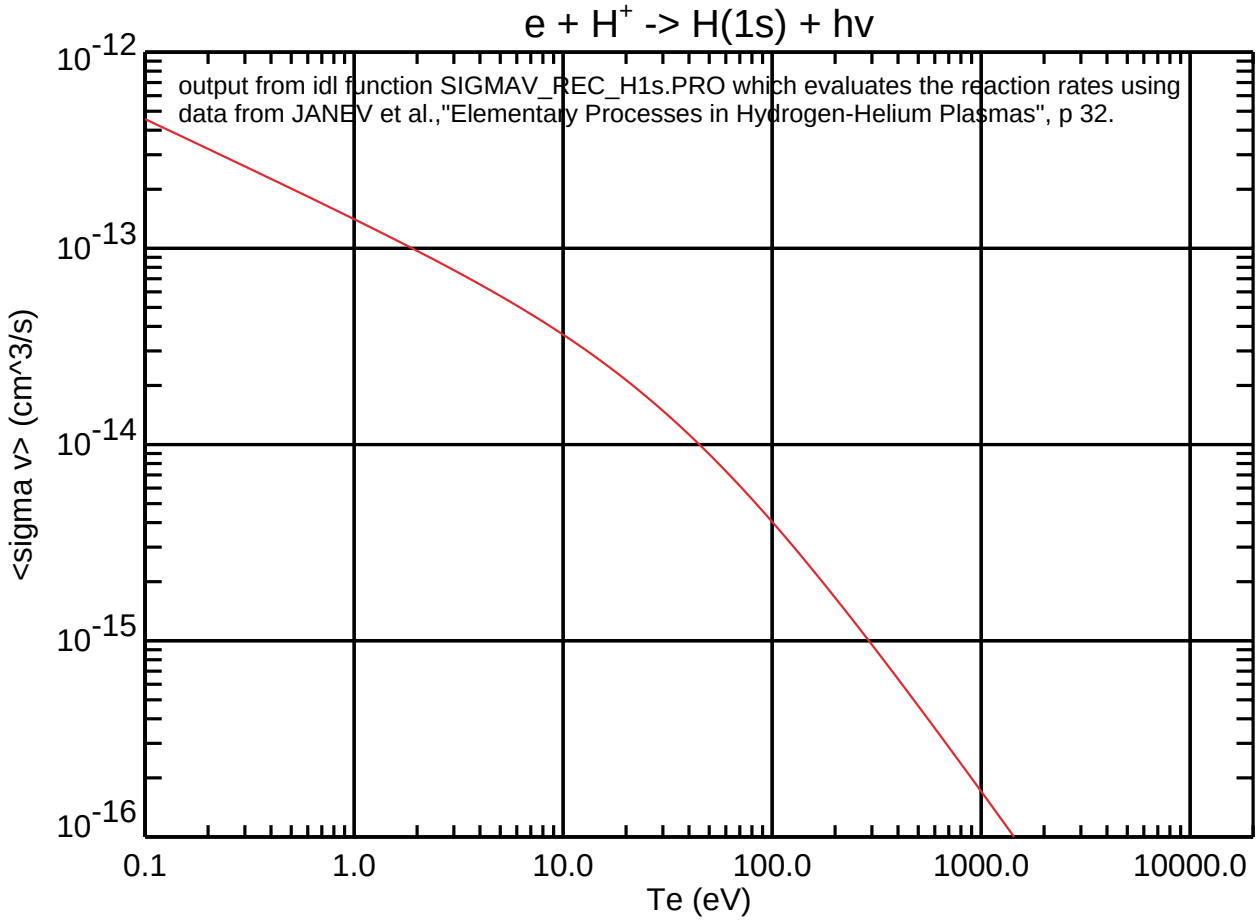

Fig. 3.3 – Radiative recombination rate as a function of electron temperature.

Figure 3.4 shows maxwellian-averaged reaction rates for 3.R3, $\langle \sigma v \rangle_{cx}[T_i, E_0]$, and Fig. 3.5 shows the cross-section for reaction 3.R3, $\sigma_{cx}[E_0]$, tabulated by Janev [3].

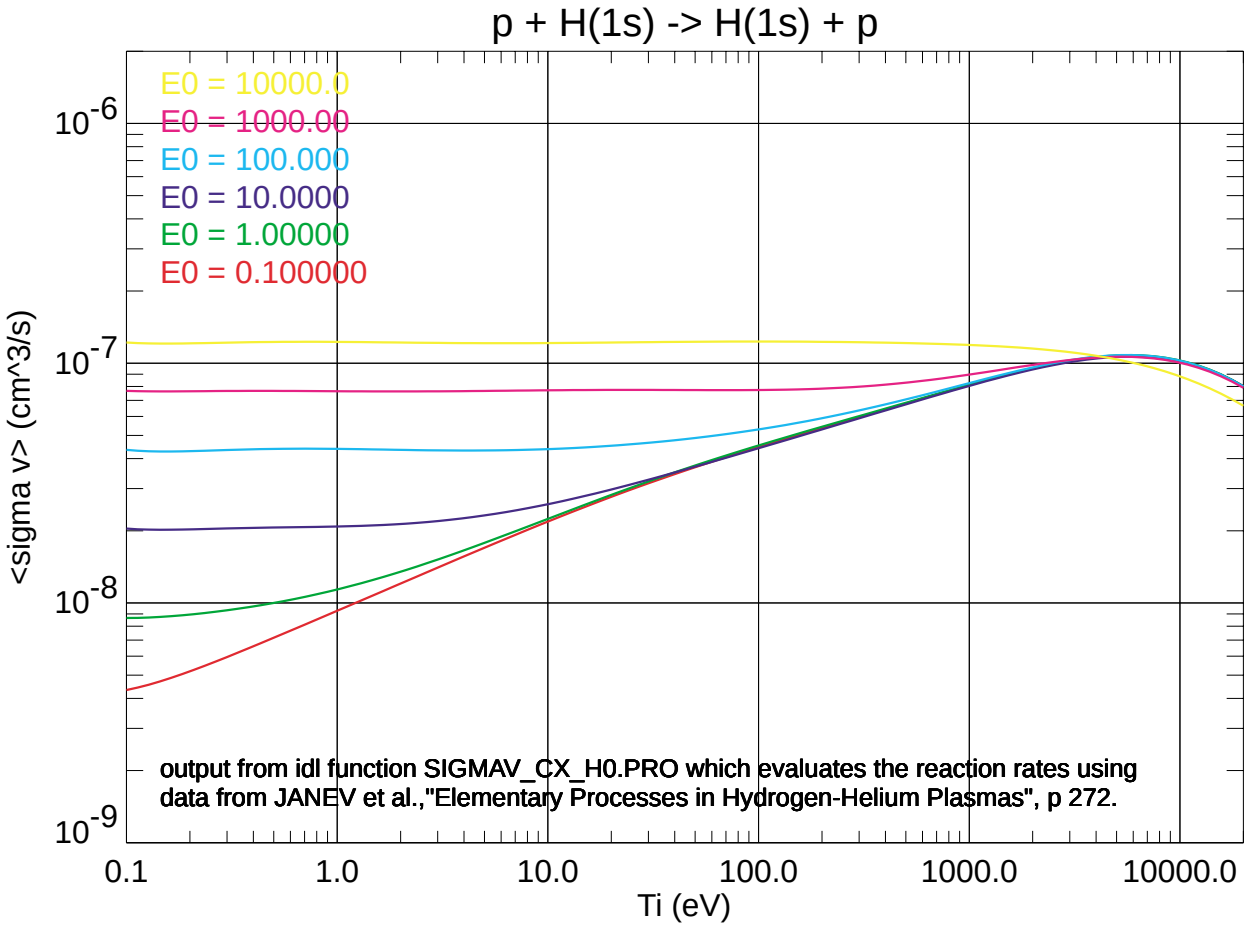

Fig. 3.4 – Proton charge exchange rate as a function of ion temperature and neutral energy.

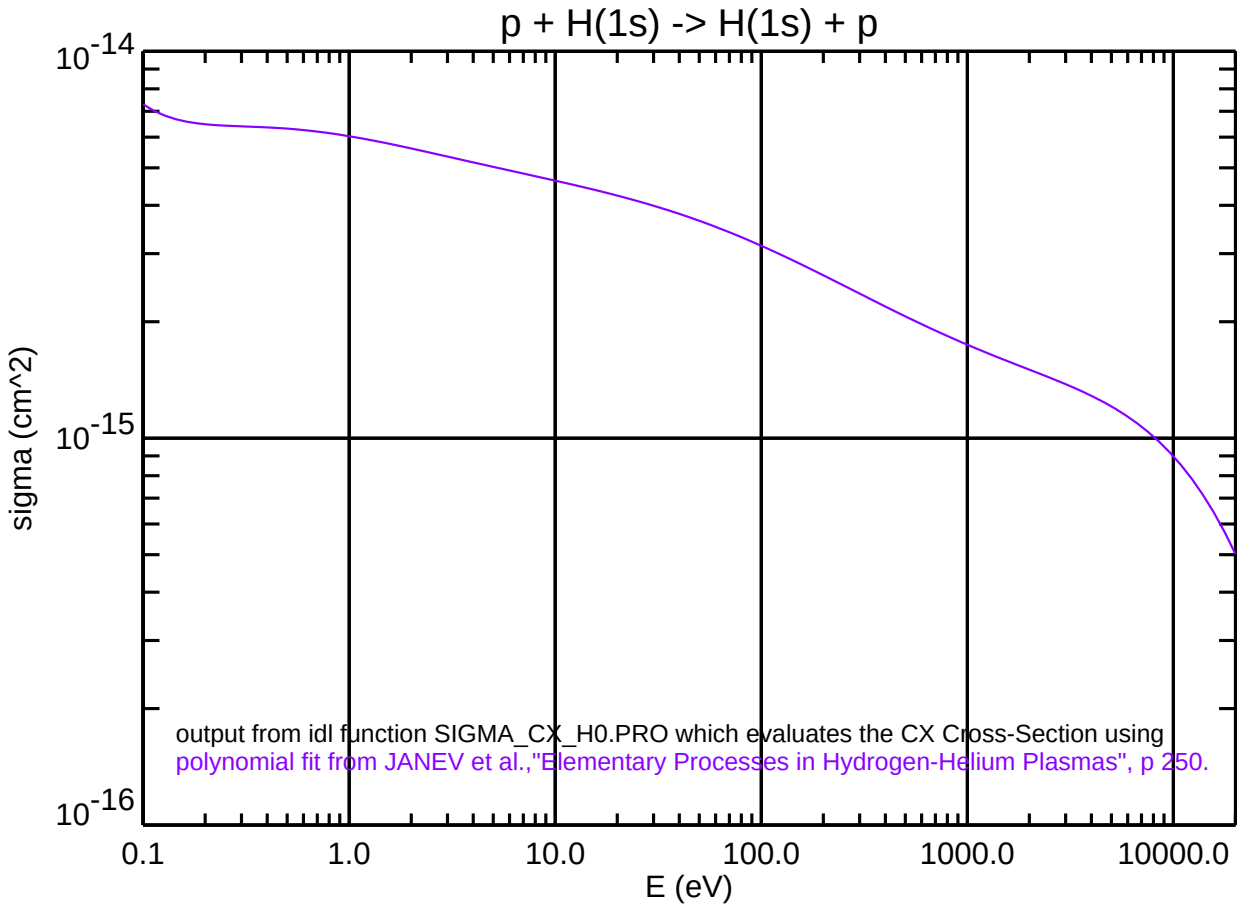

Fig. 3.5 – Proton charge exchange cross section as a function of neutral energy (evaluated using relative proton and neutral velocities).

We are interested in using the data from Figs. 3.4 and 3.5 to compute the charge exchange rate both for hydrogen neutrals in a hydrogen plasma and deuterium neutrals in a deuterium plasma. The charge exchange cross-sections, σ_{cx}, are virtually identical for hydrogen and deuterium and depend only on the relative velocities of the interacting ions and atoms. The Maxwellian-averaged deuterium cross sections can therefore be related to the hydrogen case by accounting for the mass of the deuterium nuclei relative to the mass of hydrogen,

$$\langle \sigma v \rangle_{cx}[T_i, E_0] \rightarrow \langle \sigma v \rangle_{cx}[\frac{T_i}{\mu}, \frac{1}{2} m_H \left(v_x^2 + v_r^2 \right)] \quad .$$

Here T_i is still the temperature of the ion species and $\left(v_x, v_r \right)$ the neutral velocities but the factor, μ, (=1 for hydrogen and 2 for deuterium) appropriately scales the ion velocities. Similarly, for direct evaluation of $\sigma_{cx}[E_0]$ using tabulated hydrogen data, the relative energy is evaluated using the proton mass for both hydrogen and deuterium cases.

The momentum transfer (mt) and viscosity (vis) cross-sections for elastic scattering reactions 3.R4 and 3.R6 are shown in Fig. 3.6 (data taken from Janev [7]). The cross section for reaction 3.R.5 can be obtained from Fig. 2.4 using the energy that corresponds to the relative velocity between particles. Note that these cross-sections apply for deuterium using the scaling relationships: $\sigma^{mt}_{el,D}[E_D] \leftrightarrow \sigma^{mt}_{el,H}[E_D/2]$ and $\sigma^{vis}_{el,D}[E_D] \leftrightarrow \sigma^{vis}_{el,H}[E_D]$ [7]. It is also useful to tabulate the proton-hydrogen elastic scattering reaction rate (3.R4) as a function of proton temperature (Maxwellian) and hydrogen neutral energy. The resultant curves are shown in Fig. 3.7.

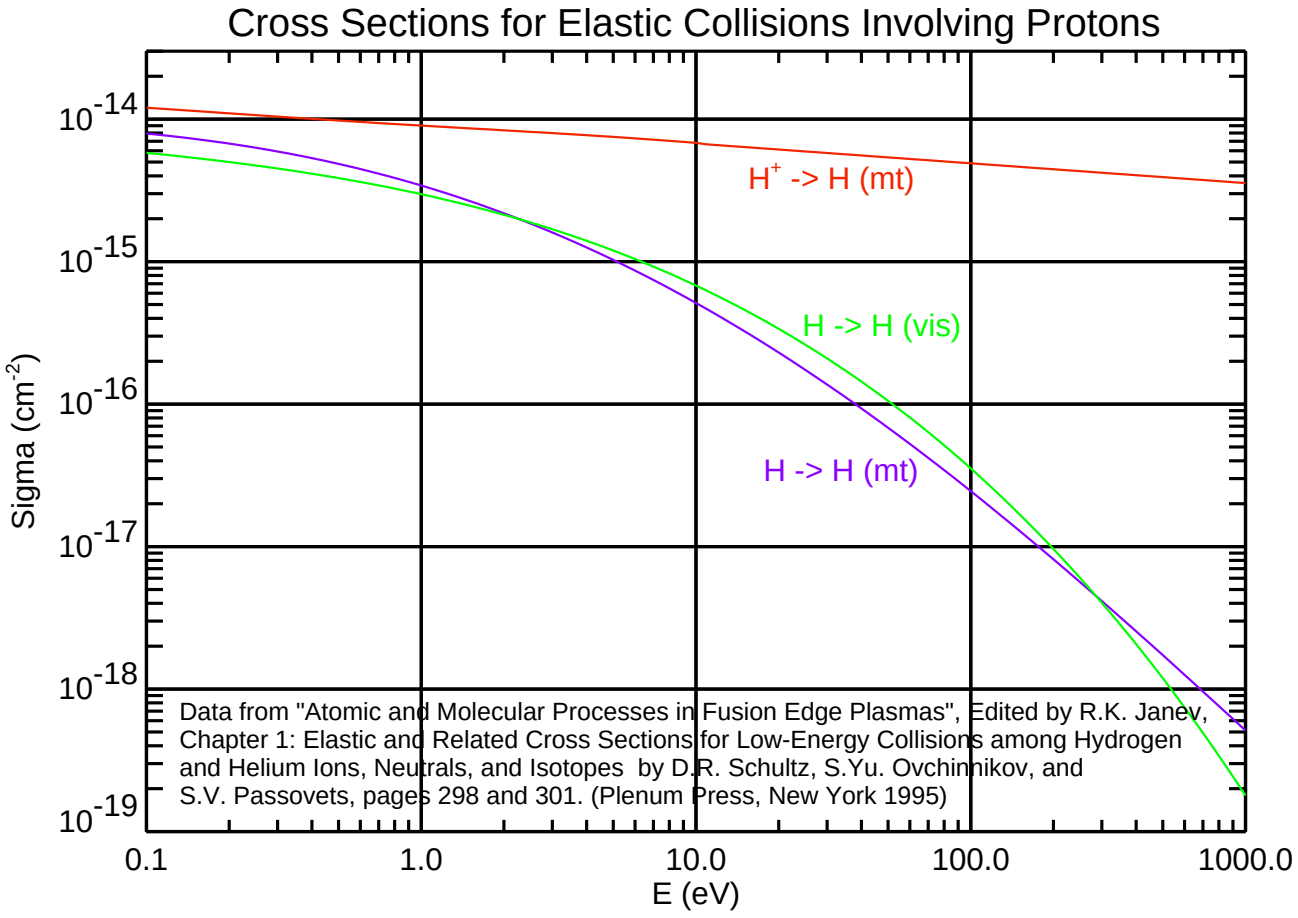

Fig. 3.6 - Elastic scattering cross-sections for collisions 3.R4 and 3.R6

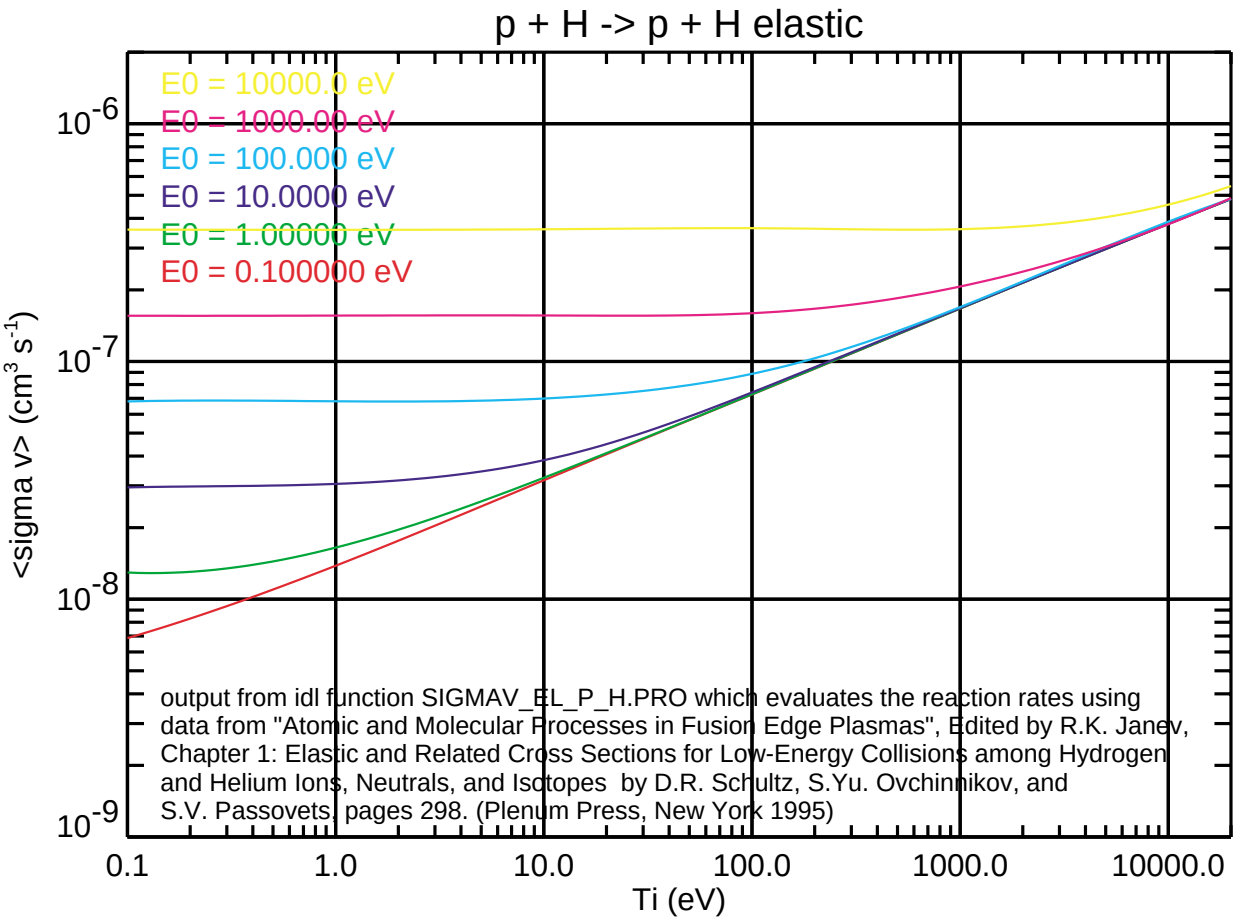

Fig. 3.7 - Proton-hydrogen momentum transfer reaction rate for reaction 3.R4 as a function of proton temperature (T_i) and hydrogen neutral energy (E_0)

3.1.2.1 Multistep Corrections to Electron-Impact Ionization and Recombination

The algorithm normally uses the ionization and recombination rate coefficients compiled from the collisional-radiative model of Johnson and Hinnov [2] for reactions 3.R1 and 3.R2. This model accounts for multistep processes which can affect the ionization and recombination rates in the high density plasmas of interest. If the parameter **`No_Johnson_Hinnov`** is set to 1, then the rates shown in Figs. 3.2 and 3.3 are used. Figures 3.8 and 3.9 show the ionization and recombination rates for a range of electron temperatures and plasma densities.

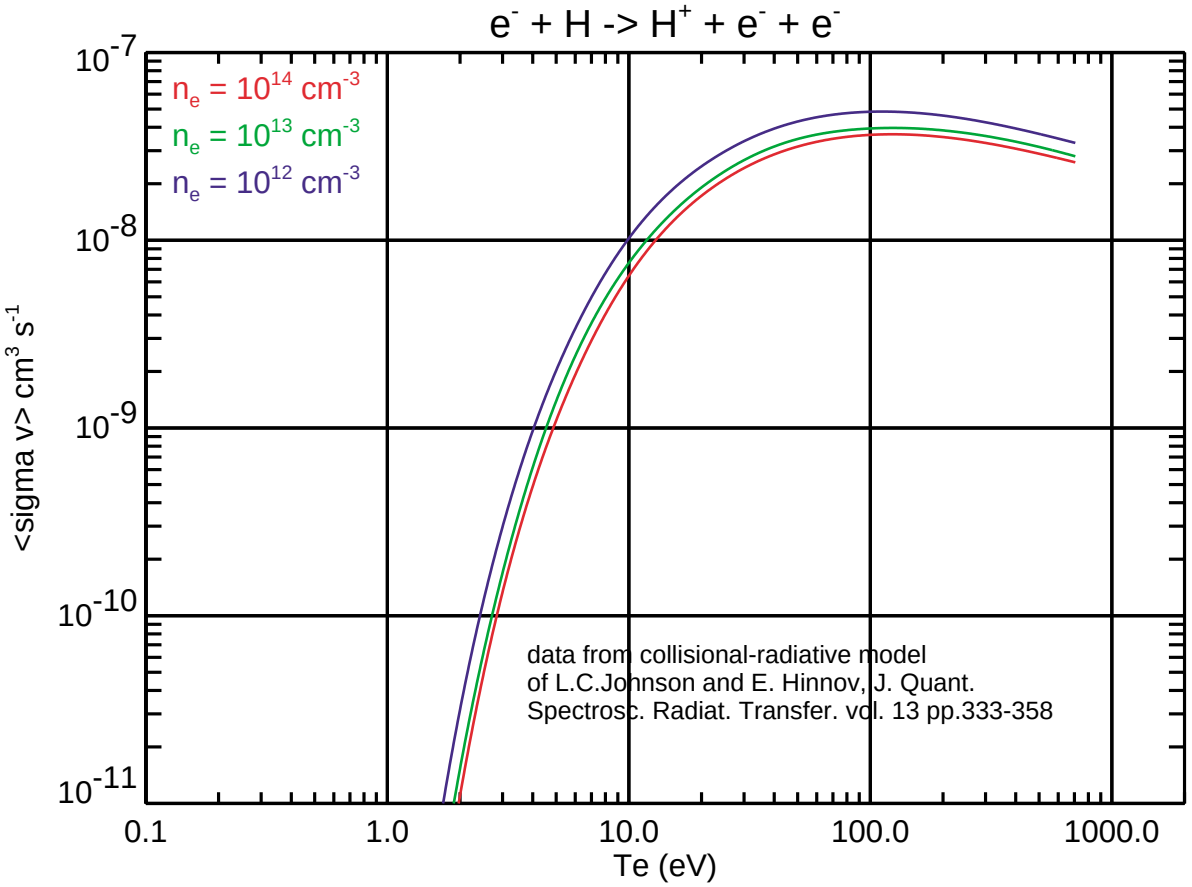

Fig. 3.8 - Ionization rate versus T_e for various plasma densities (from Johnson-Hinnov [2] *)*

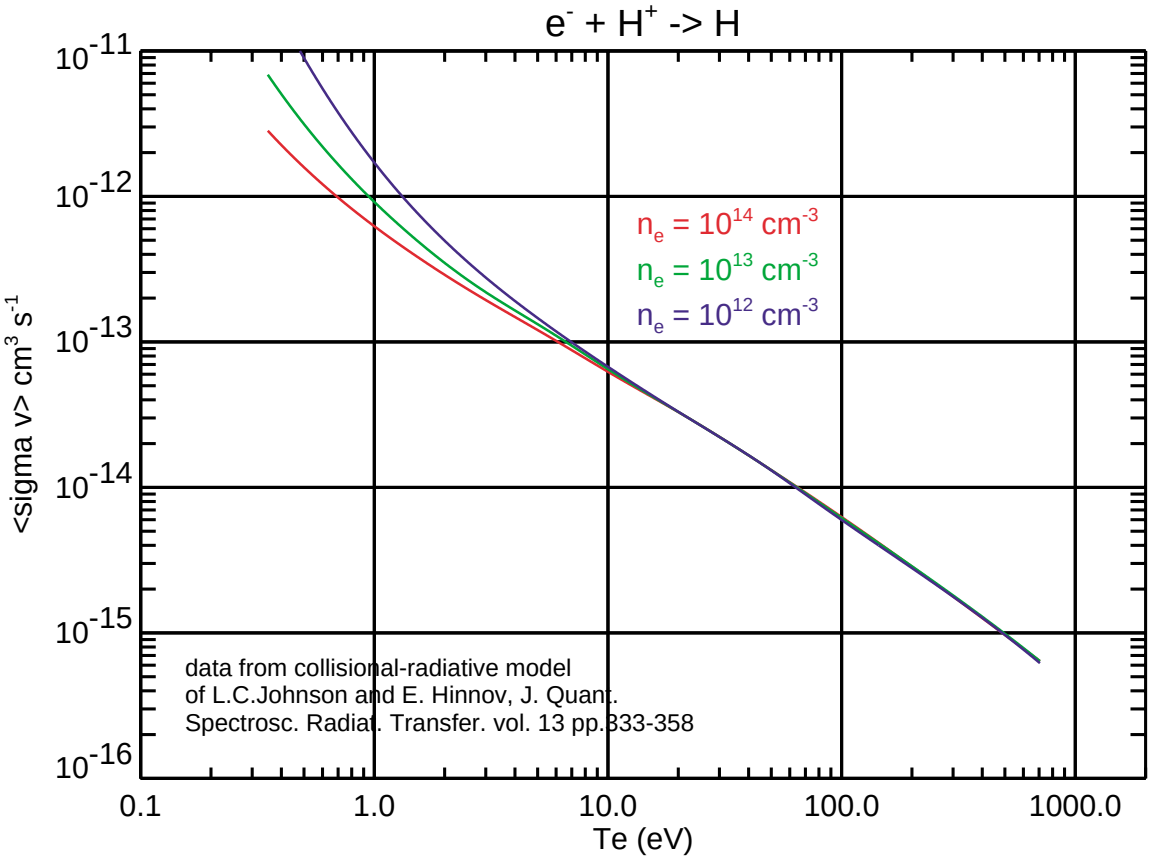

Fig. 3.9 - Recombination rate versus T_e for various plasma densities (from Johnson-Hinnov [2] *))*

3.1.2.2 Other Reactions

It should be noted that collisions of neutral hydrogen with molecular ions are not included in the present algorithm.

3.1.3 Overview of Computation

The background plasma profiles of density, electron temperature and ion temperature are specified. The molecular hydrogen (or deuterium) distribution function and a velocity space source function of neutral hydrogen (or deuterium) atoms are also optionally specified. If self-collisions of the atoms are to be included, then a first guess or 'seed' atomic distribution function, $f_{ns}(v_x, v_r, x)$, may also be inputted. (If this input is zero, the result is an increased number of iterations outlined below).The incident distribution function of atomic neutrals, $f_n(v_x > 0, v_r, x_a)$, attacking plasma is also specified:

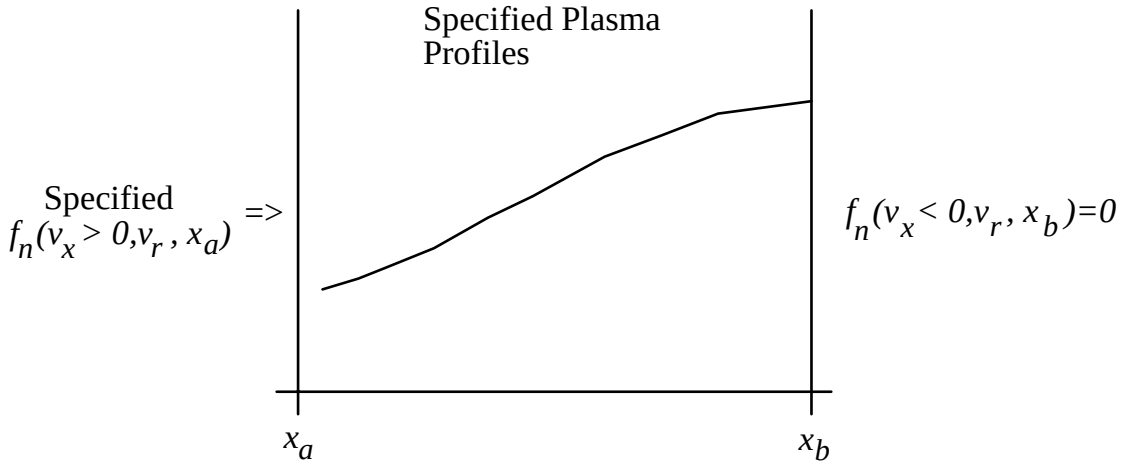

First, the portion of the neutral distribution function which transports through the plasma without ionization, charge exchange, or elastic scattering is computed. This population is designated as $f_{n0}(v_x, v_r, x)$, or the '0th generation'.

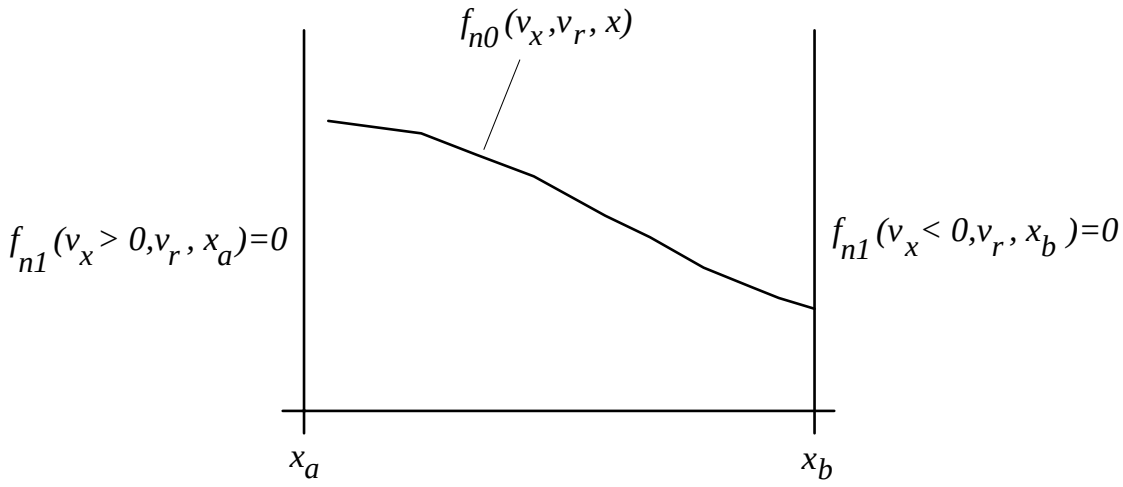

Then the neutral distribution function arising from '1st generation' of charge exchange and elastic scattering, $f_{n1}(v_x, v_r, x)$, is computed by considering the three cases of (A) $v_x > 0$, (B) $v_x < 0$ and (C) $v_x = 0$.

I. $f_{n1}(v_x, v_r, x)$ for $v_x > 0$ is determined by integrating the Boltzmann equation over $[x_a, x]$ and applying the boundary condition of $f_{n1}(v_x > 0, v_r, x_a) = 0$. Here the charge exchange and elastic scattering 'source' term only includes the contribution from the previous generation (0^{th} generation).

J. $f_{n1}(v_x, v_r, x)$ for $v_x < 0$ is determined by integrating the Boltzmann equation over $[x, x_b]$ and applying the boundary condition of $f_{n1}(v_x < 0, v_r, x_b) = 0$. Again the charge exchange and elastic scattering 'source' term only includes the contribution from the previous generation (0^{th} generation).

K. $f_{n1}(v_x, v_r, x)$ for $v_x = 0$ is computed from the Boltzmann equation for the special case of $v_x = 0$, making use of the 'regularity condition' $\frac{\partial f_n}{\partial x}(v_x = 0, v_r, x)$ - finite

The above calculations are repeated for subsequent charge exchange generations, $f_{n2}(v_x, v_r, x)$, $f_{n3}(v_x, v_r, x)$, …The total neutral distribution function in the plasma is then computed by summing over a finite number of charge-exchange generations:

$$f_n(v_x, v_r, x) = \sum_j f_{nj}(v_x, v_r, x)$$

This distribution function is then compared to $f_{ns}(v_x, v_r, x)$. If the difference between $f_n(v_x, v_r, x)$ and $f_{ns}(v_x, v_r, x)$ is found to exceed an inputted tolerance range, then $f_{ns}(v_x, v_r, x)$ is set equal to $f_n(v_x, v_r, x)$ and the computation for $f_n(v_x, v_r, x)$ is repeated again until the tolerance is met. (Note: now $f_n(v_x < 0, v_r, x_a)$ and $f_n(v_x > 0, v_r, x_b)$ is also known. For the case when $S_{H^0} = 0$, this allows the 'albedo' of the plasma to be determined.)

3.2. Formulation

3.2.1 Boltzmann Equation

The atomic neutral distribution function satisfies the Boltzmann equation,

$$
\begin{aligned}
v_x \frac{\partial f_n}{\partial x} = & - f_n \alpha_{ion} + \hat{f}_i n_e n_i \langle \sigma v \rangle_{rec} + S_{H^0} \\
& - f_n n_i \int \hat{f}_i(\underline{v}', x) |\underline{v} - \underline{v}'| \sigma_{cx}(|\underline{v} - \underline{v}'|) \partial^3 v' \\
& + \hat{f}_i n_i \int f_n(\underline{v}', x) |\underline{v} - \underline{v}'| \sigma_{cx}(|\underline{v} - \underline{v}'|) \partial^3 v' \\
& + n_i \int\int [f_n'' \hat{f}_i''' - f_n \hat{f}_i'] |\underline{v} - \underline{v}'| \frac{\delta \sigma^{el}_{H:H^+}(|\underline{v} - \underline{v}'|)}{\delta \Omega} \delta\Omega \partial^3 v' \quad . \qquad (3.1) \\
& + \int\int [f_n'' f_{H_2}''' - f_n f_{H_2}'] |\underline{v} - \underline{v}'| \frac{\delta \sigma^{el}_{H:H_2}(|\underline{v} - \underline{v}'|)}{\delta \Omega} \delta\Omega \partial^3 v' \\
& + \int\int [f_n'' f_n''' - f_n f_n'] |\underline{v} - \underline{v}'| \frac{\delta \sigma^{el}_{H:H}(|\underline{v} - \underline{v}'|)}{\delta \Omega} \delta\Omega \partial^3 v'
\end{aligned}
$$

Spatial symmetries in all distribution functions, $\frac{\partial f}{\partial y} = 0$ and $\frac{\partial f}{\partial z} = 0$ are assumed. $\int \partial^3 v'$ denotes integration over all velocity space and solid angle integration, $\int \partial\Omega$, denotes integration over all scattering angles $\int_0^{2\pi} \int_0^{\pi} \sin\theta \partial\theta \partial\phi$. $\hat{f}_i(\underline{v}, x)$ is normalized so that $\int \hat{f}(\underline{v}', x)\, \partial^3 v' = 1$. The shorthand notation, $f' = f(\underline{v}', x)$, $f'' = f(\underline{v}'', x)$ and $f''' = f(\underline{v}''', x)$, has been used. It is implicit that the velocity pairs $(\underline{v}, \underline{v}')$ and $(\underline{v}'', \underline{v}''')$ are related to each other through the scattering angles.

Since the neutrals are nearly stationary relative to the electrons, $|v_n| << |v_e|$, Maxwellian-averaged ionization, $\alpha_{ion}(x) \equiv n_e \langle \sigma v \rangle_{ion}$, and recombination, $n_e \langle \sigma v \rangle_{rec}$, reaction rates are used for these collision integrals. An externally specified velocity space source function, S_{H^0}, of neutral atoms is included in Eq. (3.1). This source can arise from molecular dissociation and is computed in routine **`Kinetic_H2`**.

3.2.2 Charge Exchange Collision Operator

The first integral on the right hand side of Eq. (3.1) depends on the ion temperature and the energy of the neutral species and can be written in the form

$$\int \hat{f}_i(\underline{v}', x)|\underline{v} - \underline{v}'|\sigma_{cx}(|\underline{v} - \underline{v}'|)\,\partial^3 v' = \langle \sigma v \rangle_{cx}[T_i, E_0], \tag{3.2}$$

where $\langle \sigma v \rangle_{cx}[T_i, E_0]$ is the hydrogen charge exchange cross-section averaged over a Maxwellian hydrogen ion distribution (temperature, T_i), accounting for the energy of the hydrogen neutral species, E_0, which for a specified neutral velocity, $\left(v_x, v_r\right)$, is $E_0 = \frac{1}{2} m_H \left(v_x^2 + v_r^2\right)$. This reaction rate is evaluated using the data compiled in Fig. 3.4. To evaluate this reaction rate for deuterium, the substitution,

$$\langle \sigma v \rangle_{cx}[T_{H_2/D_2}, E_0] \rightarrow \langle \sigma v \rangle_{cx}[\frac{T_{H_2}}{\mu}, \frac{1}{2} m_{H_2} \left(v_x^2 + v_r^2\right)], \tag{3.3}$$

is made ($\mu = 2$ for deuterium, $\mu = 1$ for hydrogen). This assumes that the reaction rates for deuterium are identical to hydrogen when the relative velocities between colliding nuclei are the same. Similarly, for direct evaluation of $\sigma_{cx}[E_0]$ using tabulated hydrogen data, the relative energy is evaluated using the atomic hydrogen mass for both hydrogen and deuterium cases.

The second integral on the right hand side of Eq. (3.1) is not so readily evaluated in terms of tabulated values. It requires a velocity-space integral to be performed over (v_x', v_r') for each combination of (v_x, v_r), weighted by $f_n(v_x', v_r', x)$. This integral computes the charge exchange frequency for a specified combination of (v_x, v_r). For large velocity space meshes, this computation can take some time. Therefore two options for computing this integral are included in this algorithm: (A) an 'exact' integration (using the cross section shown in Fig.3.4) and (B) an approximation of the integral. For option (B) the approximation,

$$\begin{aligned} &\hat{f}_i n_i \int f_n(\underline{v}', x)|\underline{v} - \underline{v}'|\sigma_{cx}(|\underline{v} - \underline{v}'|)\,\partial^3 v' \approx \\ &\quad \hat{f}_i n_i \iint \hat{f}_i f_n(\underline{v}', x)|\underline{v}'' - \underline{v}'|\sigma_{cx}(|\underline{v}'' - \underline{v}'|)\,\partial^3 v'\,\partial^3 v'' = \\ &\quad\quad \hat{f}_i n_i \int f_n(\underline{v}', x)\langle \sigma v \rangle_{cx}[T_i, E_0']\,\partial^3 v' \end{aligned} \quad , \tag{3.4}$$

is made, replacing the charge exchange frequency for a specified combination of (v_x, v_r) with the velocity-spaced average charge exchange frequency [which is independent of (v_x, v_r)]. In effect, this option assumes that all charge exchange neutrals are 'born' with a distribution that is the same as the ion

distribution function. As a result, distortions in this source distribution function due to the charge exchange rate being different at different values of relative ion-neutral velocities are not taken into account.

3.2.3 Elastic Collision Operator

The last three collision integrals in Eq. (3.1) compute the change in the atomic neutral distribution function due to elastic scattering reactions, R4-R6. The explicit numerical evaluation of these integrals is not practical, even if the differential scattering cross-sections where known. Owing to the 5-dimensional integration space, the computation would require about two orders of magnitude more computer memory and CPU time than that used to solve Eq. (3.1) without these three terms. This problem of evaluating collision integrals routinely arises in kinetic analysis. A reasonable approach, which is very often adopted, is to replace the collision integrals with a simpler kinetic model, such as the BKG [10] model. Reiter [8] recently outlined the algorithm used in the EIRENE Monte-Carlo which approximates elastic collision integrals with a BKG model. A similar method is used here,

$$\left[\frac{\partial f_n}{\partial t}\right]_{elastic} = \omega^{el}_{H:H^+}(M_{H:H^+} - f_n) + \omega^{el}_{H:H_2}(M_{H:H_2} - f_n) + \omega^{el}_{H:H}(M_{H:H} - f_n) \quad , \tag{3.5}$$

where $\left[\frac{\partial f_n}{\partial t}\right]_{elastic}$ represents the sum of the three elastic collision integrals on the RHS of Eq. (3.1). The M terms correspond to local drifting Maxwellians and ω^{el} terms correspond to mean elastic scattering collision frequencies. It is possible to choose M such that the kinetic model represented by Eq. (3.5) conserves mass, momentum, and energy of the total species mixture and conserves mass of each species. In addition, M distributions can be chosen so as to yield identical momentum and energy relaxation times as that obtained from the full collision integrals for the case when the distribution functions of the species are Maxwellians [11, 12]. This choice for the M distributions is:

$$\begin{aligned} M_{H:H^+} &= n_n \hat{f}_M[m_H, T_{H:H^+}, \underline{U}_{H:H^+}] \\ M_{H:H_2} &= n_n \hat{f}_M[m_H, T_{H:H_2}, \underline{U}_{H:H_2}] \\ M_H &= n_n \hat{f}_M[m_H, T_H, \underline{U}_H] \end{aligned} \tag{3.6}$$

with $\hat{f}_M[m,T,\underline{U}]$ being a normalized Maxwellian velocity distribution for particles with mass m at temperature T, drifting with velocity $\underline{U}$. The hybrid drift velocities are 'center of mass' velocities given by

$$\underline{U}_{H:H^+} = (m_H \underline{U}_H + m_{H^+} \underline{U}_{H^+})/(m_H + m_{H^+})$$
$$\underline{U}_{H:H_2} = (m_H \underline{U}_H + m_{H_2} \underline{U}_{H_2})/(m_H + m_{H_2}) \qquad (3.7)$$

and the hybrid temperatures are given by

$$T_{H:H^+} = T_H + \frac{2m_H m_{H^+}}{(m_H + m_{H^+})^2}\left[(T_{H^+} - T_H) + \frac{m_{H^+}}{6k}(\underline{U}_{H^+} - \underline{U}_H)^2\right]$$
$$T_{H:H_2} = T_H + \frac{2m_H m_{H_2}}{(m_H + m_{H2})^2}\left[(T_{H_2} - T_H) + \frac{m_{H_2}}{6k}(\underline{U}_{H_2} - \underline{U}_H)^2\right] \qquad (3.8)$$

while $\{T_{H^+}, T_H, T_{H_2}\}$ and $\{\underline{U}_{H^+}, \underline{U}_H, \underline{U}_{H_2}\}$ are the respective kinetic temperatures and drift velocities evaluated from $\{f_i\ , f_n\ , f_{H_2}\}$.

Having chosen the model M distributions, the next task is to determine values for the average collision frequencies (ω^{el}) which yield momentum and/or energy relaxation rates which are consistent with those obtained from the full collision integrals and which best describe the transport physics being studied. One should note that except for the special cases of when (1) the distribution functions of all species are Maxwellians and/or (2) the collision rates are independent of particle velocity [$|\underline{v} - \underline{v}'|\sigma^{el}(|\underline{v} - \underline{v}'|)$~ constant] it is not possible to choose ω^{el} such that the BKG collision model yields the same relaxation rates for *all* moments as that obtained from the full collision integral. A reasonable approach for determining ω^{el} is to require that the relaxation rates for the lowest order moments of the BKG collision model yield the same results as the full collision integral. All higher order moments will be only approximately satisfied.

The following procedure is used here: For mixed collisions, the x-directed momentum transfer rate is used to compute a consistent value for ω^{el}. The x-directed momentum transfer rate can be computed from the full collision integral using tabulated values of the momentum transfer cross-sections. For self-collisions, the temperature isotropization rate is used. The temperature isotropization rate can also be computed from the full collision integral using tabulated values of the viscosity cross-sections. Appendix B discusses the basis for the formulas used below to compute the average collision frequencies.

Note that in order for mass, momentum and energy to be conserved, Eqs. (3.6-3.8) must be self-consistent with the local atomic neutral distribution being computed, f_n. Therefore, Eqs. (3.6-3.8) must be evaluated using f_n. However, the mean collision frequencies, which are only a function of x, can be evaluated from the 'seed' distribution, f_{ns} (which is iterated until f_{ns} converges to f_n).

$$\omega^{el}_{H:H^+}(x) = \frac{\int f_{ns}(\underline{v},x)\,\alpha^{mt}_{H:H^+}(\underline{v},x)\,\partial^3 v}{n_{Hs}\left(U_{xH_s} - U_{xH^+}\right)}$$

$$\alpha^{mt}_{H:H^+}(\underline{v},x) \equiv \int f_i(\underline{v}',x)\left(v_x - v_x'\right)|\underline{v} - \underline{v}'|\,\sigma^{mt}_{H:H^+}(|\underline{v} - \underline{v}'|)\,\partial^3 v'$$

$$\omega^{el}_{H:H_2}(x) = \frac{\int f_{ns}(\underline{v},x)\,\alpha^{mt}_{H:H_2}(\underline{v},x)\,\partial^3 v}{n_{Hs}\left(U_{xH_s} - U_{xH_2}\right)}$$

$$\alpha^{mt}_{H:H_2}(\underline{v},x) \equiv \int f_{H_2}(\underline{v}',x)\left(v_x - v_x'\right)|\underline{v} - \underline{v}'|\,\sigma^{mt}_{H:H_2}(|\underline{v} - \underline{v}'|)\,\partial^3 v' \qquad (3.9)$$

$$\omega^{el}_{H:H}(x) = \frac{\int f_{ns}(\underline{v},x)\,\alpha^{iso}_{H:H}(\underline{v},x)\,\partial^3 v}{\int f_{ns}(\underline{v},x)\left[v_r^2 - 2\left(v_x - U_{xHs}\right)^2\right]\partial^3 v}$$

$$\alpha^{iso}_{H:H}(\underline{v},x) \equiv \int f_{ns}(\underline{v}',x)\left[v_r^2 + v_r'^2 - 2\left(v_x - v_x'\right)^2\right]|\underline{v} - \underline{v}'|\,\frac{1}{8}\,\sigma^{vis}_{H:H}(|\underline{v} - \underline{v}'|)\,\partial^3 v'$$

3.2.4 *Coefficients for the Mesh Equations*

It is useful to define the following quantities which can be evaluated directly for all (v_x, v_r, x) mesh locations using the inputted plasma density and temperature profiles with $n = n_i = n_e$:

Charge exchange sink frequency (option A - direct evaluation from $\sigma_{cx}(E_0)$)

$$\alpha_{cx}(v_x,v_r,x) \equiv n_i \iint \hat{f}_i(v_x',v_r',x)\left[\int |\underline{v} - \underline{v}'|\,\sigma_{cx}(|\underline{v} - \underline{v}'|)\partial\theta'\right] v_r'\,\partial v_r'\,\partial v_x' \equiv n_i \iint \hat{f}_i(v_x',v_r',x)\,\Sigma_{cx}(v_x,v_r,v_x',v_r')\,\partial v_x'\,\partial v_r' \qquad (3.10a)$$

with

$$\Sigma_{cx}(v_x,v_r,v_x',v_r') \equiv v_r' \int |\underline{v} - \underline{v}'|\,\sigma_{cx}(|\underline{v} - \underline{v}'|)\,\partial\theta'. \qquad (3.10a')$$

Charge exchange sink frequency (option B - using $\langle \sigma v \rangle_{cx}$)

$$\alpha_{cx}(v_x, v_r, x) \equiv n_i \langle \sigma v \rangle_{cx} [\frac{T_i}{\mu}, \frac{1}{2} m_H \left(v_x^2 + v_r^2 \right)] \tag{3.10b}$$

Charge exchange source rate (option A)

$$\beta_{cx}(v_x, v_r, x) \equiv \hat{f}_i n_i \iint f_n(v_x', v_r', x) \Sigma_{cx}(v_x, v_r, v_x', v_r') \partial v_x' \partial v_r' \tag{3.11a}$$

Charge exchange source rate (option B)

$$\begin{aligned} \beta_{cx}(v_x, v_r, x) &\equiv \hat{f}_i n_i \iiint f_n(v_x, v_r, x) |\underline{v} - \underline{v}'| \sigma_{cx}(|\underline{v} - \underline{v}'|) v_r \partial v_r \partial v_x \partial \theta \\ &\approx 2\pi \hat{f}_i \iint f_n(v_x', v_r', x) \alpha_{cx}(v_x', v_r', x) v_r' \partial v_x' \partial v_r' \end{aligned} \tag{3.11b}$$

Elastic momentum transfer frequency for $H : H^+$

$$\begin{aligned} \omega_{H:H^+}^{el}(x) &= \frac{2\pi}{n_{Hs}\left(U_{xH_s} - U_{xH^+} \right)} \iint f_{ns}(v_x', v_r', x) \alpha_{H:H^+}^{mt}(v_x', v_r', x) v_r' \partial v_x' \partial v_r' \\ \alpha_{H:H^+}^{mt}(\underline{v}, x) &\equiv n_i \iint \hat{f}_i(v_x', v_r', x) \Sigma_{H:H^+}^{mt}(v_x, v_r, v_x', v_r') \partial v_r' \partial v_x' \\ \Sigma_{H:H^+}^{mt}(v_x, v_r, v_x', v_r') &\equiv v_r' \left(v_x - v_x' \right) \int |\underline{v} - \underline{v}'| \sigma_{H:H^+}^{mt}(|\underline{v} - \underline{v}'|) \partial \theta' \end{aligned} \tag{3.12}$$

Elastic momentum transfer frequency for $H : H_2$

$$\begin{aligned} \omega_{H:H_2}^{el}(x) &= \frac{2\pi}{n_{Hs}\left(U_{xH_s} - U_{xH_2} \right)} \iint f_{ns}(v_x', v_r', x) \alpha_{H:H_2}^{mt}(v_x', v_r', x) v_r' \partial v_x' \partial v_r' \\ \alpha_{H:H_2}^{mt}(\underline{v}, x) &\equiv \iint f_{H_2}(v_x', v_r', x) \Sigma_{H:H_2}^{mt}(v_x, v_r, v_x', v_r') \partial v_r' \partial v_x' \\ \Sigma_{H:H_2}^{mt}(v_x, v_r, v_x', v_r') &\equiv v_r' \left(v_x - v_x' \right) \int |\underline{v} - \underline{v}'| \sigma_{H:H_2}^{mt}(|\underline{v} - \underline{v}'|) \partial \theta' \end{aligned} \tag{3.13}$$

Elastic temperature isotropization frequency for $H : H$

$$W_{\perp //}(x) \equiv 2\pi \iint f_{ns}(v_x', v_r', x) \left[v_r'^2 - 2\left(v_x' - U_{xHs} \right)^2 \right] v_r' \partial v_x' \partial v_r'$$

$$\omega^{el}_{H:H}(x) = \frac{2\pi}{W_{\perp//}} \iint f_{ns}(v'_x, v'_r, x)\, \alpha^{iso}_{H:H}(v'_x, v'_r, x) v'_r \partial v'_x \partial v'_r$$

$$\alpha^{iso}_{H:H}(\underline{v}, x) \equiv \iint f_{ns}(v'_x, v'_r, x) \Sigma^{iso}_{H:H}(v_x, v_r, v'_x, v'_r) \partial v'_r \partial v'_x$$

$$\Sigma^{iso}_{H:H}(v_x, v_r, v'_x, v'_r) \equiv$$

$$v'_r \left[v_r^2 + v_r'^2 - 2(v_x - v'_x)^2 \right] \frac{1}{8} \int |\underline{v} - \underline{v'}| \sigma^{vis}_{H:H}(|\underline{v} - \underline{v'}|)\, \partial\theta' \qquad (3.14)$$

Total elastic scattering frequency

$$\omega_{el}(x) = \omega^{el}_{H:H^+}(x) + \omega^{el}_{H:H_2}(x) + \omega^{el}_{H:H}(x) \qquad (3.15)$$

Total collision frequency

$$\alpha_c(v_x, v_r, x) \equiv \alpha_{cx}(v_x, v_r, x) + \alpha_{ion}(x) + \omega_{el}(x) \qquad (3.16)$$

Elastic scattering source distribution

$$M_H(v_x, v_r, x) = M_{H:H^+}(v_x, v_r, x) + M_{H:H_2}(v_x, v_r, x) + M_{H:H}(v_x, v_r, x) \qquad (3.17)$$

Atomic hydrogen source rate

$$S_n(v_x, v_r, x) \equiv \hat{f}_i n_e n_i \langle \sigma v \rangle_{rec}[T_e] + S_{H^0} \qquad (3.18)$$

Now the Boltzmann equation becomes

$$v_x \frac{\partial f_n}{\partial x} = S_n + \beta_{cx} - \alpha_c f_n + \omega_{el} M_H. \qquad (3.19)$$

3.2.5 Expanding f_n as a Series of Collision 'Generations'

We now consider the neutral distribution function to be composed of a sum of sub-distribution functions of neutrals which have survived j generations of collisions

$$f_n(v_x, v_r, x) = \sum_j f_{n\,j}(v_x, v_r, x)$$
$$\beta_{cx}(v_x, v_r, x) = \sum_j \beta_{cx\,j}(v_x, v_r, x) \quad .$$
$$M_H(v_x, v_r, x) = \sum_j M_{H\,j}(v_x, v_r, x)$$

With the above definitions, Eq. (3.1) can be written as a series of separate Boltzmann equations, each representing the kinetic balance for that charge-exchange population of neutrals:

$$\begin{aligned}
v_x \frac{\partial f_{n0}}{\partial x} &= S_n \qquad\qquad - \alpha_c f_{n0} \\
v_x \frac{\partial f_{n1}}{\partial x} &= \qquad \beta_{cx0} - \alpha_c f_{n1} + \omega_{el} M_{H\,0} \\
v_x \frac{\partial f_{n2}}{\partial x} &= \qquad \beta_{cx1} - \alpha_c f_{n2} + \omega_{el} M_{H\,1} \\
&\cdots\cdots\cdots\cdots\cdots\cdots\cdots\cdots\cdots\cdots\cdots\cdots\cdots\cdots\cdots\cdots \\
v_x \frac{\partial f_{nj}}{\partial x} &= \qquad \beta_{cxj-1} - \alpha_c f_{nj} + \omega_{el} M_{H\,2}
\end{aligned} \qquad (3.20)$$

3.2.6 Numerical Grid & Scheme

The spatial and velocity grid coordinates are specified with arbitrary spacing:

$$\begin{aligned}
v_x &= [-v_{x\max}, v_{x1}, ..., 0, ..., v_{xk}, v_{xk+1}, ..., v_{x\max}] \\
v_r &= [v_{r\min}, v_1, ..., v_{rl}, v_{xl+1}, ..., v_{r\max}] \\
x &= [x_a, x_1 ..., x_m, x_{m+1}, ..., x_b]
\end{aligned}$$

We will be integrating Eqs. (3.20) along the x coordinate to obtain values for f_{nj} at each grid location. Therefore we need to approximate the RHS of Eqs. (3.20) between grid points. For integration along the

x coordinate between x_m and x_{m+1}, we will replace the integrand with the average of its values evaluated at x_m and x_{m+1}.

3.2.6.1 Mesh Equation - 0th Generation for $v_x \neq 0$

In this scheme, the mesh equation for the 0th generation (with $v_x > 0$) becomes

$$\frac{f_{n0,m+1} - f_{n0,m}}{x_{m+1} - x_m} = -\frac{1}{2v_x}(\alpha_{c,m+1} f_{n0,m+1} + \alpha_{c,m} f_{n0,m} - S_{n,m+1} - S_{n,m})$$

$$f_{n0,m+1}(1 + \frac{x_{m+1} - x_m}{2v_x}\alpha_{c,m+1}) = f_{n0,m}(1 - \frac{x_{m+1} - x_m}{2v_x}\alpha_{c,m}) + \frac{x_{m+1} - x_m}{2v_x}(S_{n,m+1} + S_{n,m})$$

$$f_{n0,m+1} = f_{n0,m}\frac{2v_x - (x_{m+1} - x_m)\alpha_{c,m}}{2v_x + (x_{m+1} - x_m)\alpha_{c,m+1}} + \frac{(x_{m+1} - x_m)(S_{n,m+1} + S_{n,m})}{2v_x + (x_{m+1} - x_m)\alpha_{c,m+1}}. \qquad (3.21)$$

With the definitions,

$$A_m \equiv \frac{2v_x - (x_{m+1} - x_m)\alpha_{c,m}}{2v_x + (x_{m+1} - x_m)\alpha_{c,m+1}},$$

$$F_m \equiv \frac{(x_{m+1} - x_m)(S_{n,m+1} + S_{n,m})}{2v_x + (x_{m+1} - x_m)\alpha_{c,m+1}}, \qquad (3.22)$$

the mesh equation for the 0th generation ($v_x > 0$) becomes

$$f_{n0,m+1} = f_{n0,m}A_m + F_m. \qquad (3.23)$$

For the case of $v_x > 0$, the boundary condition $f_{n0}(v_x > 0, v_r, x_a) = f_n(v_x > 0, v_r, x_a)$ -> specified is employed and a recursive use of Eq. (3.23) yields $f_{n0}(v_x > 0, v_r, x_m)$ for all m.

A useful recursion formula for the case of $v_x < 0$ can be obtained from Eq. (21) by replacing $m+1$ with $m-1$,

$$f_{n0,m-1} = f_{n0,m}\frac{-2v_x - (x_m - x_{m-1})\alpha_{c,m}}{-2v_x + (x_m - x_{m-1})\alpha_{c,m-1}} + \frac{(x_m - x_{m-1})(S_{n,m} + S_{n,m-1})}{-2v_x + (x_m - x_{m-1})\alpha_{c,m-1}} \quad (3.24)$$

With the definitions,

$$C_m \equiv \frac{-2v_x - (x_m - x_{m-1})\alpha_{c,m}}{-2v_x + (x_m - x_{m-1})\alpha_{c,m-1}}$$

$$G_m \equiv \frac{(x_m - x_{m-1})(S_{n,m} + S_{n,m-1})}{-2v_x + (x_m - x_{m-1})\alpha_{c,m-1}} \quad (3.25)$$

the mesh equation for the 0th generation ($v_x < 0$) becomes

$$f_{n0,m-1} = f_{n0,m}C_m + G_m. \quad (3.26)$$

Now, applying the boundary condition $f_{n0}(v_x < 0, v_r, x_b) = 0$, a recursive use of Eq. (3.26) yields $f_{n0}(v_x < 0, v_r, x_m)$ for all m. Note that Eqs. (3.22) and (3.25) indicate that the x mesh spacing must be small enough to avoid nonsensical negative distribution functions. The mesh spacing must satisfy

$$(x_{m+1} - x_m) < \frac{2|v_x|}{\max[\alpha_{c,m}, \alpha_{c,m+1}]}. \quad (3.27)$$

Thus the maximum allowed x grid spacing is related to the magnitude of the smallest non-zero grid element in the v_x axis.

3.2.6.2 Mesh Equation - 0th Generation for $v_x = 0$

For $v_x = 0$, Eqs. (3.20) yield the direct relationship,

$$f_{n0,m} = \frac{S_{n,m}}{\alpha_{c,m}}. \quad (3.28)$$

3.2.6.3 Mesh Equation - j^{th} Generation ($j > 0$) for $v_x \neq 0$

In this scheme, the mesh equation for the j^{th} generation (with $v_x \neq 0$) becomes

$$\frac{f_{nj,m+1} - f_{nj,m}}{x_{m+1} - x_m} = \frac{1}{2v_x}(\beta_{cx\,j-1,m+1} + \beta_{cx\,j-1,m}) - \frac{1}{2v_x}(\alpha_{c,m+1} f_{n\,j,m+1} + \alpha_{c,m} f_{n\,j,m}) + \frac{1}{2v_x}(\omega_{el,m+1} M_{H\,j-1,m+1} + \omega_{el,m} M_{H\,j-1,m})$$

$$f_{n\,j,m+1}(1 + \frac{x_{m+1} - x_m}{2v_x}\alpha_{c,m+1}) = f_{n\,j,m}(1 - \frac{x_{m+1} - x_m}{2v_x}\alpha_{c,m}) + \frac{x_{m+1} - x_m}{2v_x}(\beta_{cx\,j-1,m+1} + \omega_{el,m+1} M_{H\,j-1,m+1} + \beta_{cx\,j-1,m} + \omega_{el,m} M_{H\,j-1,m})$$

$$f_{n\,j,m+1} = f_{n\,j,m}\frac{2v_x - (x_{m+1} - x_m)\alpha_{c,m}}{2v_x + (x_{m+1} - x_m)\alpha_{c,m+1}} + \frac{(x_{m+1} - x_m)(\beta_{cx\,j-1,m+1} + \omega_{el,m+1} M_{H\,j-1,m+1} + \beta_{cx\,j-1,m} + \omega_{el,m} M_{H\,j-1,m})}{2v_x + (x_{m+1} - x_m)\alpha_{c,m+1}} \quad . \quad (3.29)$$

With the definition,

$$B_m = \frac{(x_{m+1} - x_m)}{2v_x + (x_{m+1} - x_m)\alpha_{c,m+1}} \quad (3.30)$$

the mesh equation for the j^{th} generation ($v_x > 0$) becomes

$$f_{n\,j,m+1} = f_{n\,j,m} A_m + B_m(\beta_{cx\,j-1,m+1} + \omega_{el,m+1} M_{H\,j-1,m+1} + \beta_{cx\,j-1,m} + \omega_{el,m} M_{H\,j-1,m}) \quad (3.31)$$

For the case of $v_x > 0$, the boundary condition $f_{nj}(v_x > 0, v_r, x_a) = 0$ is employed and a recursive use of Eq. (3.31) yields $f_{nj}(v_x > 0, v_r, x_m)$ for all m.

Again, a useful recursion formula for the case of $v_x < 0$ can be obtained from Eq. (29) by replacing $m+1$ with $m-1$,

$$f_{n\,j,m-1} = f_{n\,j,m}\frac{-2v_x - (x_m - x_{m-1})\alpha_{c,m}}{-2v_x + (x_m - x_{m-1})\alpha_{c,m-1}} + \frac{(x_m - x_{m-1})\left(\beta_{cx\,j-1,m-1} + \omega_{el,m-1}M_{H\,j-1,m-1} + \beta_{cx\,j-1,m} + \omega_{el,m}M_{H\,j-1,m}\right)}{-2v_x + (x_m - x_{m-1})\alpha_{c,m-1}} \quad . \quad (3.32)$$

With the definition,

$$D_m = \frac{(x_m - x_{m-1})}{-2v_x + (x_m - x_{m-1})\alpha_{c,m-1}} \quad , \quad (3.33)$$

the mesh equation for the j^{th} generation ($v_x < 0$) becomes

$$f_{n\,j,m-1} = f_{n\,j,m}C_m + D_m\left(\beta_{cx\,j-1,m-1} + \omega_{el,m-1}M_{H\,j-1,m-1} + \beta_{cx\,j-1,m} + \omega_{el,m}M_{H\,j-1,m}\right). \quad (3.34)$$

Now, applying the boundary condition $f_{nj}(v_x < 0, v_r, x_b) = 0$, a recursive use of Eq. (3.34) yields $f_{nj}(v_x < 0, v_r, x_m)$ for all m.

3.2.6.4 Mesh Equation - j^{th} Generation (j > 0) for $v_x = 0$

For $v_x = 0$, Eqs. (3.20) yield the direct relationships,

$$f_{n\,j,m} = \frac{\beta_{cx\,j-1,m} + \omega_{el,m}M_{H\,j-1,m}}{\alpha_{c,m}}. \quad (3.35)$$

3.3 Numerical Procedure

The procedure for computing the neutral distribution function can now be outlined as follows:

A. If charge exchange option 'A' is used, then compute $\Sigma_{cx}(v_x, v_r, v_x', v_r')$ from Eq. (3.10a')

B. Compute $\alpha_{cx}(v_x, v_r, x)$ from $n_i = n_e - n_{H_2^+}$ using Eqs. (3.10 a/b).

C. Compute $\Sigma_{H:H}^{iso}(v_x, v_r, v_x', v_r')$ for computational grid using Eq. (3.14).

D. Compute $\Sigma_{H:H_2}^{mt}(v_x, v_r, v_x', v_r')$ and $\alpha_{H:H_2}^{mt}(v_x, v_r, x)$ for inputted f_{H_2} using Eq. (3.13).

E. Compute $\Sigma_{H:H^+}^{mt}(v_x, v_r, v_x', v_r')$ and $\alpha_{H:H^+}^{mt}(v_x, v_r, x)$ from inputted T_i data and $n_i = n_e - n_{H_2^+}$ using Eq. (3.12).

------ *entry point for* f_{ns} *iteration* ------

F. Compute $\omega_{el}(x)$ from 'seed' f_{ns} using Eqs. (3.12)-(3.15).

G. Compute $\alpha_c(v_x, v_r, x)$ from Eq. (3.16).

H. Test x grid spacing using Eq. (3.27).

I. Compute A_m, F_m, C_m, G_m, B_m, and D_m from Eqs. (3.22), (3.25), (3.30) and (3.33)

J. Compute $f_{n0}(v_x, v_r, x)$ from Eqs. (3.23), (3.26), and (3.28)

K. Compute β_{cx0} from $f_{n0}(v_x, v_r, x)$ and $\alpha_{cx}(v_x, v_r, x)$ or $\Sigma_{cx}(v_x, v_r, v_x', v_r')$, Eq. (3.11 a/b)

L. Compute $M_{H0}(v_x, v_r, x)$ from $f_{n0}(v_x, v_r, x)$ using Eqs. (3.6)-(3.8) and (3.17).

------ *entry point for next generation loop* ------

M. Compute $f_{nj}(v_x, v_r, x)$ for next generation from Eqs. (3.31), (3.34) and (3.35).

N. Compute β_{cxj} from $f_{nj}(v_x, v_r, x)$ and $\alpha_{cx}(v_x, v_r, x)$ or $\Sigma_{cx}(v_x, v_r, v_x', v_r')$, Eq. (3.11 a/b)

O. Compute $M_{Hj}(v_x, v_r, x)$ from $f_{nj}(v_x, v_r, x)$ using Eqs. (3.6)-(3.8) and (3.17).

P. Repeat steps M, N, and O for succeeding generations until $\max(n_{Hj}) / \max(n_{H0}) < \xi$ where ξ corresponds to the parameter , **`truncate`**.

Q. Compute the total atomic neutral distribution function from the summation:

$$f_n(v_x, v_r, x) = \sum_j f_{nj}(v_x, v_r, x).$$

R. Compare atomic densities with 'seed' values. If $\max(|n_{Hs}) - n_H|) / \max(n_H) > \xi$ then return to step F.

S. Self-consistent computation of $f_n(v_x, v_r, x)$ is complete. Compute velocity space moments of $f_n(v_x, v_r, x)$ including, temperature, pressure, diagonal elements of the stress tensor, and heat fluxes.

3.4 IDL Program

The complete call to the IDL procedure, **`Kinetic_H.pro`**, is listed below:

```
;+
; Kinetic_H.pro
;
; This subroutine is part of the "KN1D" atomic and molecular neutral transport code.
;
;   This subroutine solves a 1-D spatial, 2-D velocity kinetic neutral transport
; problem for atomic hydrogen (H) or deuterium by computing successive generations of
; charge exchange and elastic scattered neutrals. The routine handles electron-impact
; ionization, proton-atom charge exchange, radiative recombination, and elastic
; collisions with hydrogenic ions, neutral atoms, and molecules.
;
;   The positive vx half of the atomic neutral distribution function is inputted at x(0)
; (with arbitrary normalization) and the desired flux of hydrogen atoms entering the slab,
; at x(0) is specified. Background profiles of plasma ions, (e.g., Ti(x), Te(x), n(x), vxi(x),...)
; molecular ions, (nHP(x), THP(x)), and molecular distribution function (fH) are inputted.
;
; Optionally, the hydrogen source velocity distribution function is also inputted.
; (The H source and fH2 distribution functions can be computed using procedure
; "Kinetic_H2.pro".) The code returns the atomic hydrogen distribution function, fH(vr,vx,x)
; for all vx, vr, and x of the specified vr,vx,x grid.
;
;   Since the problem involves only the x spatial dimension, all distribution functions
; are assumed to have rotational symmetry about the vx axis. Consequently, the distributions
; only depend on x, vx and vr where vr =sqrt(vy^2+vz^2)
;
;  History:
;
;    B. LaBombard   First coding based on Kinetic_Neutrals.pro          22-Dec-2000
;
;    For more information, see write-up: "A 1-D Space, 2-D Velocity, Kinetic
;    Neutral Transport Algorithm for Hydrogen Atoms in an Ionizing Plasma", B. LaBombard
;
; Note: Variable names contain characters to help designate species -
;       atomic neutral (H), molecular neutral (H2), molecular ion (HP), proton (i) or (P)
;
;_____________________________________________________________________________
pro  Kinetic_H,vx,vr,x,Tnorm,mu,Ti,Te,n,vxi,fHBC,GammaxHBC,PipeDia,fH2,fSH,nHP,THP,$
        fH,nH,GammaxH,VxH,pH,TH,qxH,qxH_total,NetHSource,Sion,QH,RxH,QH_total,AlbedoH,WallH,$
        truncate=truncate,Simple_CX=Simple_CX,Max_Gen=Max_Gen,$
        No_Johnson_Hinnov=No_Johnson_Hinnov,No_Recomb=No_Recomb,$
        H_H_EL=H_H_EL,H_P_EL=H_P_EL,H_H2_EL=_H_H2_EL,H_P_CX=H_P_CX,ni_correct=ni_correct,$
        error=error,compute_errors=compute_errors,$
        plot=plot,debug=debug,debrief=debrief,pause=pause

    common  Kinetic_H_Output,piH_xx,piH_yy,piH_zz,RxHCX,RxH2_H,RxP_H,RxW_H,EHCX,EH2_H,EP_H,$
           EW_H,Epara_PerpH_H,SourceH,SRecomb

    common  Kinetic_H_Errors,Max_dx,vbar_error,mesh_error,moment_error,C_Error,CX_Error,H_H_error,$
                             qxH_total_error,QH_total_error
;
;  Input:
;                  vx(*) - fltarr(nvx), normalized x velocity coordinate
;                          [negative values, positive values],
;                          monotonically increasing. Note: a nonuniform mesh can be used.
;                          Dimensional velocity (note: Vth is based on ATOM mass)
;                          is v = Vth * vx where Vth=sqrt(2 k Tnorm/(mH*mu))
;                          Note: nvx must be even and vx(*) symmetric about
;                          zero but not contain a zero element
;                  vr(*) - fltarr(nvr), normalized radial velocity coordinate
;                           [positive values], monotonically increasing. Note: a non-uniform mesh
;                         can be used.
;                           Dimensional velocity is v = Vth * vr where Vth=sqrt(2 k Tnorm/(mH*mu))
;                          Note: vr must not contain a zero element
;                   x(*) - fltarr(nx), spatial coordinate (meters),
;                           positive, monontonically increasing. Note: a non-uniform mesh can be
;                          used.
;                  Tnorm - Float, temperature corresponding to the thermal speed (see vx and vr
;                          above) (eV)
;                     mu - Float, 1=hydrogen, 2=deuterium
;                     Ti - fltarr(nx), Ion temperature profile (eV)
;                     Te - fltarr(nx), electron temperature profile (eV)
;                      n - fltarr(nx), electron density profile (m^-3)
;                    vxi - fltarr(nx),x-directed plasma ion and molecular ion flow profile (m s^-1)
;                   fHBC - fltarr(nvr,nvx), this is an input boundary condition
;                          specifying the shape of the neutral atom velocity distribution
;                          function at location x(0). Normalization is arbitrary.
;
```

```
;                         Only values with positive vx, fHBC(*,nvx/2:*) are used
;                        by the code.
;             GammaxHBC - float, desired neutral atom flux density in the +Vx
;                         direction at location x(0) (m^-2 s^-1)
;                         fHBC is scaled to yield this flux density.
;               PipeDia - fltarr(nx), effective pipe diameter (meters)
;                         This variable allows collisions with the 'side-walls' to be simulated.
;                         If this variable is undefined, then PipeDia set set to zero. Zero values
;                         of PipeDia are ignored (i.e., treated as an infinite diameter).
;                   fH2 - fltarr(nvr,nvx,nx), neutral molecule velocity distribution
;                         function. fH2 is normalized so that the molecular neutral density,
;                        nH2(k), is
;                         defined as the velocity space integration:
;                            nH2(k)=total(Vr2pidVr*(fH2(*,*,k)#dVx))
;                         If this variable is undefined, then it is set equal to zero and
;                         no molecule-atom collisions are included.
;                         NOTE: dVx is velocity space differential for Vx axis and Vr2pidVr =
;                              Vr*!pi*dVr with dVr being velocity space differential for Vr axis.
;                   fSH - fltarr(nvr,nvx,nx), atomic hydrogen source velocity distribution.
;                         fSH must be normalized so that the total atomic neutral
;                         source, SourceH(k), is defined as the velocity space integration:
;                             SourceH(k)=total(Vr2pidVr*(fSH(*,*,k)#dVx))
;                         fSH can be computed from IDL procedure Kinetic_H2.pro
;                         If this variable is undefined, then it is set equal to zero.
;                  nHP - fltarr(nx), molecular ion density profile (m^-3)
;                         If this parameter is undefined, then it is set equal to zero.
;                         nHP can be computed from IDL procedure Kinetic_H2.pro
;                  THP - fltarr(nx), molecular ion temperature profile (m^-3)
;                         If this parameter is undefined, then it is set equal to 3 eV at each
;                         grid point. THP can be computed from IDL procedure Kinetic_H2.pro
;
; Input & Output:
;                    fH - fltarr(nvr,nvx,nx), neutral atom velocity distribution
;                         function. 'Seed' values for this may be specified on input.
;                         If this parameter is undefined on input, then a zero 'seed' value will
;                         be used. The algorithm outputs a self-consistent fH.
;                         fH is normalized so that the neutral density, nH(k), is defined as
;                          the velocity space integration: nH(k)=total(Vr2pidVr*(fH(*,*,k)#dVx))
;
; Output:
;                    nH - fltarr(nx), neutral atom density profile (m^-3)
;             GammaxH - fltarr(nx), neutral atom flux profile (# m^-2 s^-1)
;                          computed from GammaxH(k)=Vth*total(Vr2pidVr*(fH(*,*,k)#(Vx*dVx)))
;                 VxH - fltarr(nx), neutral atom velocity profile (m s^-1)
;                           computed from GammaxH/nH
;
;                       To aid in computing the some of the quantities below, the procedure
;                       internally defines the quantities:
;                       vr2vx2_ran(i,j,k)=vr(i)^2+(vx(j)-VxH(k))^2
;                                  which is the magnitude of 'random v^2' at each mesh point
;                       vr2vx2(i,j,k)=vr(i)^2+vx(j)^2
;                                  which is the magnitude of 'total v^2' at each mesh point
;                       q=1.602177D-19, mH=1.6726231D-27
;                       C(*,*,*) is the right hand side of the Boltzmann equation, evaluated
;                                using the computed neutral distribution function
;
;                    pH - fltarr(nx), neutral atom pressure (eV m^-2)
;                    TH - fltarr(nx), neutral atom temperature profile (eV)
;                                    computed from: TH=pH/nH
;                  qxH - fltarr(nx), neutral atom random heat flux profile (watts m^-2)
;             qxH_total - fltarr(nx), total neutral atom heat flux profile (watts m^-2)
;                           This is the total heat flux transported by the neutrals.
;            NetHSource - fltarr(nx), net H0 source [H0 source - ionization sink - wall sink]
;                         (m^-3 s^-1)
;                 Sion - fltarr(nx), H ionization rate (m^-3 s^-1)
;                   QH - fltarr(nx), rate of net thermal energy transfer into neutral atoms
;                         (watts m^-3)
;                  RxH - fltarr(nx), rate of x momentum transfer to neutral atoms
;                         (=force, N m^-2).
;                QH_total - fltarr(nx), net rate of total energy transfer into neutral atoms
;                           = QH + RxH*VxH - 0.5*(mu*mH)*(Sloss-SourceH)*VxH*VxH (watts m^-3)
;                 AlbedoH - float, Ratio of atomic neutral particle flux with Vx < 0 divided by
;                           particle flux with Vx > 0  at x=x(0)
;                           (Note: For fSH non-zero, the flux with Vx < 0 will include
;                           contributions from molecular hydrogen sources within the 'slab'.
;                           In this case, this parameter does not return the true 'Albedo'.)
;                    WallH - fltarr(nx), atomic neutral sink rate arising from hitting the 'side
;                           walls' (m^-3 s^-1). Unlike the molecules in Kinetic_H2, wall collisions
;                         result in the destruction of atoms.
;                           This parameter can be used to specify a resulting source of molecular
;                           neutrals in Kinetic_H2. (molecular source = 2 times WallH)
```

```
;
; KEYWORDS:
;   Output:
;                 error - Returns error status: 0=no error, solution returned
;                                               1=error, no solution returned
;
; COMMON BLOCK Kinetic_H_OUTPUT
;    Output:
;                piH_xx - fltarr(nx), xx element of stress tensor (eV m^-2)
;                piH_yy - fltarr(nx), yy element of stress tensor (eV m^-2)
;                piH_zz - fltarr(nx), zz element of stress tensor (eV m^-2) = piH_yy
;                           Note: cylindrical system relates r^2 = y^2 + z^2. All other stress
;                            tensor elements are zero.
;
;            The following momentum and energy transfer rates are computed from charge-exchange
;           collsions between species:
;                  RxHCX - fltarr(nx), rate of x momentum transfer from hydrogren ions to atoms
;                          (=force/vol, N m^-3).
;                   EHCX - fltarr(nx), rate of energy transfer from hydrogren ions to atoms
;                           (watts m^-3).
;
;            The following momentum and energy transfer rates are computed from elastic collsions
;           between species:
;                 RxH2_H - fltarr(nx), rate of x momentum transfer from neutral molecules to atoms
;                          (=force/vol, N m^-3).
;                  RxP_H - fltarr(nx), rate of x momentum transfer from hydrogen ions to neutral
;                            atoms (=force/vol, N m^-3).
;                  EH2_H - fltarr(nx), rate of energy transfer from neutral molecules to atoms
;                            (watts m^-3).
;                   EP_H - fltarr(nx), rate of energy transfer from hydrogen ions to neutral atoms
;                            (watts m^-3).
;
;            The following momentum and energy transfer rates are computed from collisions with the
;           'side-walls'
;                  RxW_H - fltarr(nx), rate of x momentum transfer from wall to neutral atoms
;                            (=force/vol, N m^-3).
;                   EW_H - fltarr(nx), rate of energy transfer from wall to neutral atoms
;                            (watts m^-3).
;
;            The following is the rate of parallel to perpendicular energy transfer computed from
;           elastic collisions
;
;          Epara_PerpH_H - fltarr(nx), rate of parallel to perp energy transfer within atomic
;                            hydrogen species (watts m^-3).
;
;            Source/Sink info:
;                 SourceH - fltarr(nx), source rate of neutral atoms from H2 dissociation (from
;                            integral of inputted fSH) (m^-3 s^-1).
;                  SRecom - fltarr(nx), source rate of neutral atoms from recombination (m^-3 s^-1).
;
; KEYWORDS:
;   Input:
;               truncate - float, stop computation when the maximum
;                          increment of neutral density normalized to
;                          inputed neutral density is less than this
;                          value in a subsequent generation. Default value is 1.0e-4
;
;              Simple_CX - if set, then use CX source option (B): Neutrals are born
;                          in velocity with a distribution proportional to the local
;                          ion distribution function. Simple_CX=1 is default.
;
;                          if not set, then use CX source option (A): The CX source
;                          neutral atom distribution function is computed by evaluating the
;                          the CX cross section for each combination of (vr,vx,vr',vx')
;                          and convolving it with the neutral atom distribution function.
;                          This option requires more CPU time and memory.
;
;                 Max_gen - integer, maximum number of collision generations to try including before
;                            giving up. Default is 50.
;
;       No_Johnson_Hinnov - if set, then compute ionization and recombination rates
;                           directly from reaction rates published by Janev* for
;                          ground state hydrogen
;
;                              Ionization:    e + H(1s) -> p + e
;                              Recombination: e + p -> H(1s) + hv
;
;                           *Janev, R.K., et al, "Elementary processes in hydrogen-helium plasmas",
;                           (Springer-Verlag, Berlin ; New York, 1987)
;
;                           Otherwise, compute ionization and recombination rates using
```

```
;                          results from the collisional-radiative model published by Johnson
;                          and Hinnov [L.C.Johnson and E. Hinnov, J. Quant. Spectrosc. Radiat.
;                          Transfer. vol. 13 pp.333-358]. This is the default.
;                          Note: charge exchange is always computed using the ground state reaction
;                         rates published by Janev:
;
;                              Charge Exchange: p + H(1s) -> H(1s) + p
;
;              No_Recomb - if set, then DO NOT include recombination as a source of atomic neutrals
;                          in the algorithm
;
;                 H_H_EL - if set, then include H -> H elastic self collisions
;                             Note: if H_H_EL is set, then algorithm iterates fH until
;                             self consistent fH is achieved.
;                 H_P_CX - if set, then include H -> H(+) charge exchange collisions
;                 H_P_EL - if set, then include H -> H(+) elastic collisions
;               H_H2_EL - if set, then include H -> H2 elastic collisions
;             ni_correct - if set, then algorithm corrects hydrogen ion density
;                              according to quasineutrality: ni=ne-nHP. Otherwise, nHP is assumed to
;                            be small.
;
;          Compute_Errors - if set, then return error estimates in common block Kinetic_H_ERRORS
;                            below
;
;                    plot - 0= no plots, 1=summary plots, 2=detail plots, 3=very detailed plots
;                   debug - 0= do not execute debug code, 1=summary debug, 2=detail debug, 3=very
;                             detailed debug
;                 debrief - 0= do not print, 1=print summary information, 2=print detailed
;                             information
;                   pause - if set, then pause between plots
;
; COMMON BLOCK Kinetic_H_ERRORS
;
;        if COMPUTE_ERRORS keyword is set then the following is returned in common block
;        Kinetic_H_ERRORS
;
;                  Max_dx - float(nx), Max_dx(k) for k=0:nx-2 returns maximum
;                           allowed x(k+1)-x(k) that avoids unphysical negative
;                          contributions to fH
;              Vbar_error - float(nx), returns numerical error in computing
;                           the speed of ions averged over maxwellian distribution.
;                           The average speed should be:
;                                  vbar_exact=2*Vth*sqrt(Ti(*)/Tnorm)/sqrt(!pi)
;                            Vbar_error returns: abs(vbar-vbar_exact)/vbar_exact
;                           where vbar is the numerically computed value.
;              mesh_error - fltarr(nvr,nvx,nx), normalized error of solution
;                           based on substitution into Boltzmann equation.
;           moment_error - fltarr(nx,m), normalized error of solution
;                           based on substitution into velocity space
;                           moments (v^m) of Boltzmann equation, m=[0,1,2,3,4]
;                 C_error - fltarr(nx), normalized error in charge exchange and elastic scattering
;                          collision operator. This is a measure of how well the charge exchange and
;                          elastic scattering portions of the collision operator
;                           conserve particles.
;                CX_error - fltarr(nx), normalized particle conservation error in charge exchange
;                           collision operator.
;                H_H_error - fltarr(nx,[0,1,2]) return normalized errors associated with
;                           particle [0], x-momentum [1], and total energy [2] convervation of the
;                           elastic self-collision operator
;
;        qxH_total_error - fltarr(nx), normalized error estimate in computation of qxH_total
;         QH_total_error - fltarr(nx), normalized error estimate in computation of QH_total
;
; History:
;        22-Dec-2000 - B. LaBombard - first coding.
;        11-Feb-2001 - B. LaBombard - added elastic collisions
;
;_____________________________________________________________________________
;-
```

3.5 Validation of Numerics

The total neutral distribution function, $f_n(v_x, v_r, x)$, computed from the numerical algorithm should satisfy the Boltzmann equation,

$$v_x \frac{\partial f_n}{\partial x} = S_n + \beta_{cx} - \alpha_c f_n + \omega_{el} M_H, \tag{3.36}$$

at every location on the mesh. According to the numerical scheme outlined in section 3, this equation can be written as the mesh equation,

$$\begin{aligned} 2v_x \frac{f_{n,m+1} - f_{n,m}}{x_{m+1} - x_m} = &(S_{n,m+1} + S_{n,m}) + (\beta_{cx,m+1} + \beta_{cx,m}) \\ &- (\alpha_{c,m+1} f_{n,m+1} + \alpha_{c,m} f_{n,m}) \\ &+ (\omega_{el,m+1} M_{H,m+1} + \omega_{el,m} M_{H,m}) \end{aligned} \quad . \tag{3.37}$$

3.5.1 Mesh Point Error

By defining the three terms in Eq. (3.23) as

$$\begin{aligned} T1_m &= 2v_x \frac{f_{n,m+1} - f_{n,m}}{x_{m+1} - x_m}, \\ T2_m &= S_{n,m+1} + S_{n,m} \\ T3_m &= \beta_{cx,m+1} + \beta_{cx,m}, \\ T4_m &= \alpha_{c,m+1} f_{n,m+1} + \alpha_{c,m} f_{n,m} \\ T5_m &= \omega_{el,m+1} M_{H,m+1} + \omega_{el,m} M_{H,m} \end{aligned} \tag{3.38}$$

a normalized error parameter can be defined for spatial mesh points with $x_a \le x < x_b$, and all velocity mesh points as

$$\varepsilon_{k,l,m} \equiv \frac{\left| T1_{k,l,m} - T2_{k,l,m} - T3_{k,l,m} + T4_{k,l,m} - T5_{k,l,m} \right|}{\max(\left|T1_{k,l,m}\right|, \left|T2_{k,l,m}\right|, \left|T3_{k,l,m}\right|, \left|T4_{k,l,m}\right|, \left|T5_{k,l,m}\right|)}. \tag{3.39}$$

Values of $\varepsilon_{k,l,m}$ are returned in parameter **`mesh_error`**.

3.5.2 Velocity Moment Error

$f_n(v_x, v_r, x)$ should also satisfy velocity moments (M) of the Boltzmann equation,

$$\iint \frac{\partial f_n}{\partial x} v_x^{M+1} \partial v_x v_r \partial v_r = \iint S_n v_x^M \partial v_x v_r \partial v_r + \iint \beta_{cx} v_x^M \partial v_x v_r \partial v_r - \iint \alpha_c f_n v_x^M \partial v_x v_r \partial v_r + \iint \omega_{el} M_H v_x^M \partial v_x v_r \partial v_r \quad . \tag{3.40}$$

Making use of Eqs. (3.37) and (3.38), this can be expressed as

$$\iint T1_m v_x^M \partial v_x v_r \partial v_r = \iint T2_m v_x^M \partial v_x v_r \partial v_r + \iint T3_m v_x^M \partial v_x v_r \partial v_r - \iint T4_m v_x^M \partial v_x v_r \partial v_r + \iint T5_m v_x^M \partial v_x v_r \partial v_r \quad .$$

Defining

$$\begin{aligned} T1_{M,m} &= \iint T1_m v_x^M \partial v_x v_r \partial v_r \,, \\ T2_{M,m} &= \iint T2_m v_x^M \partial v_x v_r \partial v_r \,, \\ T3_{M,m} &= \iint T3_m v_x^M \partial v_x v_r \partial v_r \,, \\ T4_{M,m} &= \iint T4_m v_x^M \partial v_x v_r \partial v_r \,, \\ T5_{M,m} &= \iint T5_m v_x^M \partial v_x v_r \partial v_r \,, \end{aligned} \tag{3.41}$$

a normalized 'velocity moment error' for spatial mesh points with $x_a \le x < x_b$, can be constructed as

$$\eta_{M,m} \equiv \frac{\left| T1_{M,m} - T2_{M,m} - T3_{M,m} + T4_{M,m} - T5_{M,m} \right|}{\max(\left|T1_{M,m}\right|, \left|T2_{M,m}\right|, \left|T3_{M,m}\right|, \left|T4_{M,m}\right|, \left|T5_{M,m}\right|)}. \tag{3.42}$$

Values of $\eta_{M,m}$ are returned in parameter **`moment_error`**.

3.5.3 Error Associated with Digital Representation of Distribution Functions

Discretization introduces errors in evaluating moments of the distribution functions. If the velocity space mesh is too coarse such that f varies strongly between mesh points or if the mesh does not cover a sufficient range such that f is has a significant component *outside* the mesh, then numerically evaluated moments of f will not be accurate. As a test of the numerical accuracy in the digital representation of f, **`Kinetic_H.pro`** computes the average speed of the Maxwellian plasma ions ($\hat{f}_i$) at each x_m location and compares it to the theoretical value:

$$\bar{v}_{code} = 2\pi \iint \sqrt{v_r^2 + v_x^2}\, \hat{f}_i \partial v_x v_r \partial v_r$$

$$\bar{v}_{exact} \equiv \int |\underline{v}| \hat{f}_i \;\; \partial^3 v = 4\pi \int \hat{f}_i v^3 \partial v \;\; = \frac{2v_{th}}{\sqrt{\pi}}$$

The parameter **`Vbar_error`** in **`Kinetic_H.pro`** returns a normalized error defined as

$$\bar{v}_{error,m} \equiv \left| \bar{v}_{code,m} - \bar{v}_{exact,m} \right| / \bar{v}_{exact,m} \; .$$

Values of **`Vbar_error`** = 0.01 or less indicate that $\hat{f}_i$ (and by inference, f_n) are reasonably well represented by their digital expressions and that the choice of velocity mesh size and spacing is appropriate. For the case when $T_i(x)$ varies significantly across the mesh, a non-uniform velocity space mesh can be used to more evenly distribute **`Vbar_error`** over the mesh.

[Note: IDL procedure **`Create_Kinetic_H_Mesh.pro`**, is used to generate a (v_x, v_r) mesh which is close to the optimum for a specified $T_i(x)$ profile.]

Appendix A: Kinematics of Elastic Collisions

A.1 Magnitudes of Initial and Final Velocity Components

Consider an elastic collision between particle a (initial velocity $\underline{v}$ in lab frame, final velocity $\underline{v'}$ in lab frame, mass m_a) and particle b (initial velocity $\underline{w}$ in lab frame, mass M_b).

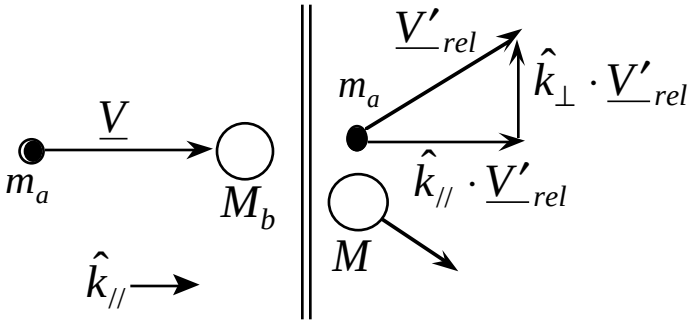

Fig. A.1 - Elastic scattering event as seen in a coordinate system with particle b initially at rest.

The following quantities can be defined:

$$\underline{V}_{rel} = \underline{v} - \underline{w} \;\; ; \;\; \hat{k}_{//} = \frac{\underline{v} - \underline{w}}{|\underline{v} - \underline{w}|} \;\; ; \;\; \hat{k}_{\perp} \cdot \hat{k}_{//} = 0 \;\; ; \;\; \mu = \frac{m_a M_b}{m_a + M_b} \;\; ; \;\; s = \frac{\mu}{m_a}. \quad \text{(A.1)}$$

From conservation of mass and momentum , the resultant velocity of particle a after collision relative to the initial velocity of particle b ($\underline{V'}_{rel} = \underline{v'} - \underline{w}$) has the following magnitudes in the directions parallel ($\hat{k}_{//}$) and perpendicular ($\hat{k}_{\perp}$) to the direction of initial relative velocity,

$$\hat{k}_{//} \cdot \underline{V'}_{rel} = V_{rel} \left[1 - s(1 - \cos\theta)\right] \quad \text{(A.2)}$$

$$\hat{k}_{\perp} \cdot \underline{V'}_{rel} = V_{rel} \; s \sin\theta \quad \text{(A.3)}$$

where θ is scattering angle in the center-of-mass reference frame.

A.2 Definitions of Elastic, Momentum Transfer, and Viscosity Cross-Sections

The *elastic scattering* cross-section (in units of area) is defined as an integral over all solid angles of the differential elastic scattering cross-section,

$$\sigma^{el} \equiv 2\pi \int_0^{\pi} \frac{\delta\sigma^{el}}{\delta\Omega} \sin\theta \, \partial\theta . \qquad \text{(A.4)}$$

The *momentum transfe*r cross-section is similarly defined, but with a $(1-\cos\theta)$ weighting factor,

$$\sigma^{mt} \equiv 2\pi \int_0^{\pi} (1-\cos\theta) \frac{\delta\sigma^{el}}{\delta\Omega} \sin\theta \, \partial\theta , \qquad \text{(A.5)}$$

and the definition of *viscosity* cross-section includes a $\sin^2\theta$ weighting factor,

$$\sigma^{vis} \equiv 2\pi \int_0^{\pi} \sin^2\theta \frac{\delta\sigma^{el}}{\delta\Omega} \sin\theta \, \partial\theta . \qquad \text{(A.6)}$$

A.3 Vector Relationships Between Initial and Final Velocities

Using the following geometry and nomenclature to describe the elastic collision, a vector relationship between the final velocity of particle a in the lab frame $\underline{v'}$ in terms of the initial velocities $\underline{v}$ and $\underline{w}$ can be constructed.

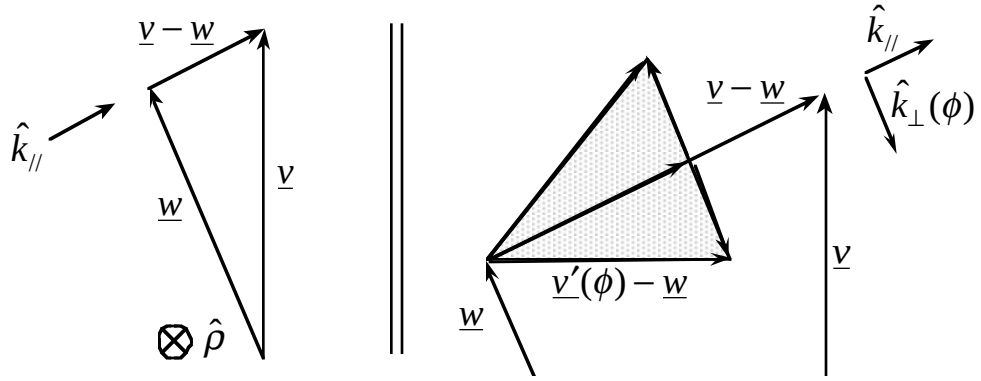

Fig. A.2 - Initial and final velocity vector relationships. Vector $\underline{v}'(\phi)-\underline{w}$ sweeps out a cone as the azimuthal scattering angle ϕ is varied for a fixed value of θ.

The following definitions apply:

$$\hat{\rho} = \frac{\underline{w}\times\underline{v}}{|\underline{w}\times\underline{v}|} \; ; \; \hat{x} = \frac{\underline{v}}{|\underline{v}|} \; ; \; \hat{k}_{\perp}(\phi) = \sin\phi \, \hat{k}_{//} \times \hat{\rho} + \cos\phi \, \hat{\rho} . \qquad \text{(A.7)}$$

The angle ϕ is the azimuthal angle ($\hat{\phi} = \hat{k}_{//} \times \hat{k}_{\perp}(\phi)$). It is the angle that $\hat{k}_{\perp}(\phi)$ has following the scattering event. By symmetry, all scattering events result in ϕ populating the range 0 to 2π with equal

probability. From (A.2), (A.3), and the relationships above, the final velocity of particle a can be written in terms of the initial velocities and the scattering angles,

$$\begin{aligned}\underline{v}' - \underline{w} &= |\underline{v} - \underline{w}|\,[1 - s(1-\cos\theta)]\,\hat{k}_{//} \\ &\quad + |\underline{v} - \underline{w}|\, s \sin\theta \left(\sin\phi\ \hat{k}_{//} \times \hat{\rho} + \cos\phi\ \hat{\rho}\right)\end{aligned} \quad . \qquad \text{(A.8)}$$

A.4 Average Final Velocity of Particle a, $\langle \underline{v}' \rangle$

Averaging (A.8) over all scattering angles, $\langle u \rangle \equiv \frac{1}{4\pi} \int_0^{2\pi} \int_0^{\pi} u \sin\theta\, \partial\theta\, \partial\phi$, leads to the result,

$$\begin{aligned}\langle \underline{v}' \rangle &= \underline{w} + (\underline{v} - \underline{w}) \left(1 - s \frac{\sigma^{mt}}{\sigma^{el}}\right), \\ \langle \underline{v}' \rangle &= \underline{v} - (\underline{v} - \underline{w}) s \frac{\sigma^{mt}}{\sigma^{el}}\end{aligned} \qquad \text{(A.9)}$$

where the definitions (A.4) and (A.5) have been used.

A.5 Average Square of Final Velocity, $\langle \underline{v}'^2 \rangle$

Computing $(\underline{v}' - \underline{w}) \cdot (\underline{v}' - \underline{w})$ from (A.8),

$$(\underline{v}' - \underline{w}) \cdot (\underline{v}' - \underline{w}) = |\underline{v} - \underline{w}|^2\, [1 - s(1-\cos\theta)]^2 + |\underline{v} - \underline{w}|^2 s^2 \sin^2\theta \ . \qquad \text{(A.10)}$$

Note the relationships,

$$\begin{aligned} G \equiv [1 - s(1-\cos\theta)]^2 &= 1 - 2s(1-\cos\theta) + s^2(1-\cos\theta)^2 \\ &= 1 - 2s(1-\cos\theta) + s^2(1 - 2\cos\theta + \cos^2\theta) \\ &= 1 - 2s(1-\cos\theta) + s^2(2 - 2\cos\theta - \sin^2\theta) \\ &= 1 - 2s + 2s\cos\theta + 2s^2 - 2s^2\cos\theta - s^2\sin^2\theta \\ &= 1 - 2s(1-s)(1-\cos\theta) - s^2\sin^2\theta \end{aligned} \quad , \qquad \text{(A.11)}$$

so that (A.10) becomes

$$\underline{v'}^2 - 2\underline{v'}\cdot\underline{w} + \underline{w^2} = |\underline{v} - \underline{w}|^2 \left[1 - 2s(1-s)(1-\cos\theta)\right]. \qquad \text{(A.12)}$$

Averaging (A.12) over all scattering angles leads to

$$\left\langle \underline{v'}^2 \right\rangle = 2\langle \underline{v'} \rangle \cdot \underline{w} - w^2 + |\underline{v} - \underline{w}|^2 \left[1 - 2s(1-s)\frac{\sigma^{mt}}{\sigma^{el}}\right]. \qquad \text{(A.13)}$$

From (A.9),

$$2\langle \underline{v'} \rangle \cdot \underline{w} = 2w^2 + 2\left(\underline{v}\cdot\underline{w} - w^2\right)\left(1 - s\frac{\sigma^{mt}}{\sigma^{el}}\right), \qquad \text{(A.14)}$$

so that,

$$\left\langle \underline{v'}^2 \right\rangle = w^2 + 2\left(\underline{v}\cdot\underline{w} - w^2\right)\left(1 - s\frac{\sigma^{mt}}{\sigma^{el}}\right) + |\underline{v} - \underline{w}|^2 \left[1 - 2s(1-s)\frac{\sigma^{mt}}{\sigma^{el}}\right]. \qquad \text{(A.15)}$$

This can be rewritten as

$$\left\langle \underline{v'}^2 \right\rangle = w^2 + \left(2\underline{v}\cdot\underline{w} - 2w^2\right)\left(1 - s\frac{\sigma^{mt}}{\sigma^{el}}\right) + \left(v^2 - 2\underline{v}\cdot\underline{w} + w^2\right)\left[1 - 2s(1-s)\frac{\sigma^{mt}}{\sigma^{el}}\right]$$

$$= v^2 - \left(2\underline{v}\cdot\underline{w} - 2w^2\right)s\frac{\sigma^{mt}}{\sigma^{el}} - \left(v^2 - 2\underline{v}\cdot\underline{w} + w^2\right)2s(1-s)\frac{\sigma^{mt}}{\sigma^{el}}$$

$$= v^2 - \left(\underline{v}\cdot\underline{w} - w^2\right)2s\frac{\sigma^{mt}}{\sigma^{el}} - \left(v^2 - 2\underline{v}\cdot\underline{w} + w^2\right)2s\frac{\sigma^{mt}}{\sigma^{el}}$$

$$+ \left(v^2 - 2\underline{v}\cdot\underline{w} + w^2\right)2s^2\frac{\sigma^{mt}}{\sigma^{el}}$$

$$= v^2 - \left(v^2 - \underline{v}\cdot\underline{w}\right)2s\frac{\sigma^{mt}}{\sigma^{el}} + \left(v^2 - 2\underline{v}\cdot\underline{w} + w^2\right)2s^2\frac{\sigma^{mt}}{\sigma^{el}}$$

Leading to the final result,

$$\left\langle \underline{v'}^2 \right\rangle = v^2 + \left[w^2 s + \underline{v}\cdot\underline{w}(1-2s) - v^2(1-s)\right]2s\frac{\sigma^{mt}}{\sigma^{el}}. \qquad \text{(A.16)}$$

A.5.1 Special case: Particle b stationary in lab frame, $\underline{w} = 0$

When $\underline{w} = 0$, (A.12) becomes

$$\underline{v'}^2 = v^2 \left[1 - 2s(1-s) + 2s(1-s)\cos\theta)\right]. \qquad \text{(A.17)}$$

From the relationship $2s(1-s) = \dfrac{2m_a M_b}{\left(m_a + M_b\right)^2}$, (A.17) can be written explicitly in terms of particle masses,

$$\underline{v'}^2 = v^2 \left[\frac{{m_a}^2 + {M_b}^2 + 2m_a M_b \cos\theta}{\left(m_a + M_b\right)^2} \right]. \qquad \text{(A.18)}$$

This formula arises in nuclear reactor physics [13] where the relationship between the final energy of a scattered neutron (particle a) and its initial energy is of interest. From Henry [13], page 55, Eq. (2.5.14),

$$E' = E \left[\frac{A^2 + 1 + 2A\cos\theta}{(1+A)^2} \right] \quad ; \quad A \equiv \frac{M_b}{m_a} \qquad \text{(A.19)}$$

Performing the substitution leads to

$$E' = E \left[\frac{\dfrac{{M_b}^2}{{m_a}^2} + 1 + 2\dfrac{M_b}{m_a}\cos\theta}{\left(1 + \dfrac{M_b}{m_a}\right)^2} \right] \qquad \text{(A.20)}$$

$$= E \left[\frac{{M_b}^2 + {m_a}^2 + 2m_a M_b \cos\theta}{\left(m_a + M_b\right)^2} \right]$$

which is identical to (A.18).

A.5.2 Special case: $m_a = M_b$

For the special case when particle a has the same mass as particle b ($s = \dfrac{1}{2}$), (A.16) becomes

$$\left\langle \underline{v'}^2 \right\rangle = v^2 + \left[\frac{1}{2} w^2 - \frac{1}{2} v^2 \right] \frac{\sigma^{mt}}{\sigma^{el}} \qquad \text{(A.21)}$$

For isotropic scattering in the center-of-mass frame, $\sigma^{mt} = \sigma^{el}$, (A.21) yields the expected result that the average energy of particle a after collision is simply the average of the sum of particle a and b energies before collision.

A.5.3 Conservation of Energy

The energy of particle b after collision can be found from (A.16), interchanging velocites $\underline{v} \leftrightarrow \underline{w}$ and replacing $s \rightarrow s\frac{m_a}{M_b} = 1 - s$. The total particle energy after collision is therefore

$$\begin{aligned}
&\frac{1}{2}m_a\left\langle \underline{v}'^2 \right\rangle + \frac{1}{2}M_b\left\langle \underline{w}'^2 \right\rangle = \frac{1}{2}m_a v^2 + \frac{1}{2}M_b w^2 \\
&\quad + m_a\left[w^2 s + \underline{v}\cdot\underline{w}(1-2s) - v^2(1-s)\right]s\frac{\sigma^{mt}}{\sigma^{el}} \\
&\quad + M_b\left[v^2(1-s) - \underline{v}\cdot\underline{w}(1-2s) - w^2 s\right](1-s)\frac{\sigma^{mt}}{\sigma^{el}}
\end{aligned} \qquad \text{(A.22)}$$

Noting that $m_a s = M_b(1-s)$results in

$$\frac{1}{2}m_a\left\langle \underline{v}'^2 \right\rangle + \frac{1}{2}M_b\left\langle \underline{w}'^2 \right\rangle = \frac{1}{2}m_a v^2 + \frac{1}{2}M_b w^2 \quad , \qquad \text{(A.23)}$$

as required for elastic collisions.

A.6 Average Square of Final Velocity in the Direction of Initial Velocity, $\left\langle \left(\underline{v}' \cdot \frac{\underline{v}}{|\underline{v}|} \right)^2 \right\rangle$

Note the following relationships,

$$\frac{\underline{v}}{|\underline{v}|}\cdot\hat{k}_{//} = \frac{v^2 - \underline{v}\cdot\underline{w}}{|\underline{v}|\,|\underline{v}-\underline{w}|} \qquad ; \qquad \frac{\underline{v}}{|\underline{v}|}\cdot\hat{\rho} = \frac{\underline{v}\cdot\underline{w}\times\underline{v}}{|\underline{v}||\underline{w}\times\underline{v}|} = 0 \quad ;$$

$$\frac{\underline{v}}{|\underline{v}|}\cdot\left(\hat{k}_{//}\times\hat{\rho}\right)=\frac{\underline{v}}{|\underline{v}|}\cdot\frac{\underline{v}-\underline{w}}{|\underline{v}-\underline{w}|}\times\frac{\underline{w}\times\underline{v}}{|\underline{w}\times\underline{v}|}$$

$$=\frac{\underline{v}}{|\underline{v}|}\cdot\frac{v^2\underline{w}-(\underline{v}\cdot\underline{w})\underline{v}+w^2\underline{v}-(\underline{v}\cdot\underline{w})\underline{w}}{|\underline{v}-\underline{w}|\,|\underline{w}\times\underline{v}|}$$

$$=\frac{v^2(\underline{v}\cdot\underline{w})-(\underline{v}\cdot\underline{w})v^2+w^2v^2-(\underline{v}\cdot\underline{w})^2}{|\underline{v}|\,|\underline{v}-\underline{w}|\,|\underline{w}\times\underline{v}|}\quad . \qquad \text{(A.24)}$$

$$\frac{\underline{v}}{|\underline{v}|}\cdot\left(\hat{k}_{//}\times\hat{\rho}\right)=\frac{w^2v^2-(\underline{v}\cdot\underline{w})^2}{|\underline{v}|\,|\underline{v}-\underline{w}|\,|\underline{w}\times\underline{v}|}$$

From these relationships and (A.8),

$$\frac{\underline{v}}{|\underline{v}|}\cdot\underline{v'}=\frac{\underline{v}\cdot\underline{w}}{|\underline{v}|}+\frac{v^2-\underline{v}\cdot\underline{w}}{|\underline{v}|}\left[1-s(1-\cos\theta)\right]$$

$$+\frac{w^2v^2-(\underline{v}\cdot\underline{w})^2}{|\underline{v}|\,|\underline{w}\times\underline{v}|}\,s\sin\theta\sin\phi \quad . \qquad \text{(A.25)}$$

With the definitions,

$$A\equiv\frac{\underline{v}\cdot\underline{w}}{|\underline{v}|}\;;\;\; B\equiv\frac{v^2-\underline{v}\cdot\underline{w}}{|\underline{v}|}\;;\;\; C\equiv\frac{w^2v^2-(\underline{v}\cdot\underline{w})^2}{|\underline{v}|\,|\underline{w}\times\underline{v}|} \qquad \text{(A.26)}$$

$$G\equiv\left[1-s(1-\cos\theta)\right];\; F\equiv s\sin\theta\sin\phi$$

(A.25) becomes $\frac{\underline{v}}{|\underline{v}|}\cdot\underline{v'}=A+B\,G+C\,F$ so that

$$\left(\frac{\underline{v}}{|\underline{v}|}\cdot\underline{v'}\right)^2=A^2+ABG+ACF$$

$$+BGA+B^2G^2+BGCF \quad . \qquad \text{(A.27)}$$

$$+CFA+CFBG+C^2F^2$$

[The term G^2 has already been written out explicitly in (A.11).] Note that averaging over azimuthal angle, ϕ, results in

$$\langle F \rangle_\phi = 0 \; ; \; \langle F^2 \rangle_\phi = \frac{s^2}{2} \sin^2\theta \tag{A.28}$$

so that (A.27) becomes

$$\left\langle \left(\frac{\underline{v}}{|\underline{v}|} \cdot \underline{v}' \right)^2 \right\rangle_\phi = \frac{(\underline{v}\cdot\underline{w})^2}{|\underline{v}|} + 2\frac{(\underline{v}\cdot\underline{w})}{|\underline{v}|}\frac{\left(v^2 - \underline{v}\cdot\underline{w}\right)}{|\underline{v}|}[1 - s(1-\cos\theta)]$$
$$+ \left[\frac{v^2 - \underline{v}\cdot\underline{w}}{|\underline{v}|}\right]^2 \left[1 - 2s(1-s)(1-\cos\theta) - s^2\sin^2\theta\right] \tag{A.29}$$
$$+ \left[\frac{w^2v^2 - (\underline{v}\cdot\underline{w})^2}{|\underline{v}|\,|\underline{w}\times\underline{v}|}\right]^2 \frac{s^2}{2}\sin^2\theta$$

Now consider (A.29) when $\underline{v} \equiv v_x\hat{x}$ and $\underline{w} = w_x\hat{x} + w_y\hat{y} + w_z\hat{z}$ with $w_r^2 \equiv w_y^2 + w_z^2$ and noting that $|\underline{w}\times\underline{v}_x| = v_x\sqrt{w_y^2 + w_z^2} = v_x w_r$,

$$\langle v_x'^2 \rangle_\phi = w_x^2 + 2w_x(v_x - w_x)[1 - s(1-\cos\theta)]$$
$$+ (v_x - w_x)^2\left[1 - 2s(1-s)(1-\cos\theta) - s^2\sin^2\theta\right] \tag{A.30}$$
$$+ w_r^2\frac{s^2}{2}\sin^2\theta$$

Averaging over scattering angle in the center-of-mass reference frame and making use of the cross-sections defined in (A.4)-(A.6) yields,

$$\langle v_x'^2 \rangle = w_x^2 + 2w_x(v_x - w_x)\left[1 - s\frac{\sigma^{mt}}{\sigma^{el}}\right] + w_r^2\frac{s^2}{2}\frac{\sigma^{vis}}{\sigma^{el}}$$
$$+ (v_x - w_x)^2\left[1 - 2s(1-s)\frac{\sigma^{mt}}{\sigma^{el}} - s^2\frac{\sigma^{vis}}{\sigma^{el}}\right] \tag{A.31}$$

A.7 Average Square of Final Velocity in the Arbitrary Direction, $\left\langle \underline{v}'^{2}_{x} \right\rangle$

In order to compute the temperature isotropization time of a particle velocity distribution function, the square of final velocity of particle a in the $\hat{x}$ direction, $\left\langle \underline{v}'^{2}_{x} \right\rangle$, for arbitrary initial velocites $\underline{v}$ and $\underline{w}$ is of particular interest. The following relationships apply to this calculation,

$$\underline{R} \equiv \underline{v} - \underline{w} \quad ; \quad \underline{X} = \underline{w} \times \underline{v} \quad ; \quad \underline{R} \cdot \underline{X} = 0 \ ;$$

$$\hat{x} \cdot \hat{k}_{//} = \frac{v_x - w_x}{|\underline{v} - \underline{w}|} \quad ; \quad \hat{x} \cdot \hat{\rho} = \hat{x} \cdot \frac{\underline{w} \times \underline{v}}{|\underline{w} \times \underline{v}|} = \frac{X_x}{|\underline{X}|} \ ;$$

$$\hat{x} \cdot \left(\hat{k}_{//} \times \hat{\rho} \right) = \hat{x} \cdot \frac{\underline{R}}{|\underline{R}|} \times \frac{\underline{X}}{|\underline{X}|} = \frac{R_y X_z - R_z X_y}{|\underline{R}|\,|\underline{X}|} \ . \tag{A.32}$$

From these relationships and (A.8),

$$v'_x = w_x + (v_x - w_x)[1 - s(1 - \cos\theta)] + \frac{R_y X_z - R_z X_y}{|\underline{X}|}\, s \sin\theta \sin\phi + \frac{X_x}{|\underline{X}|} |\underline{R}|\, s \sin\theta \cos\phi \ . \tag{A.33}$$

With the definitions,

$$A \equiv w_x \ ; \ B \equiv v_x - w_x \ , \ C \equiv \frac{R_y X_z - R_z X_y}{|\underline{X}|} \ ,$$

$$D \equiv \frac{X_x}{|\underline{X}|} |\underline{R}| \quad , \ E \equiv s \sin\theta \cos\phi \quad , \tag{A.34}$$

$$F \equiv s \sin\theta \sin\phi \quad , \quad G \equiv [1 - s(1 - \cos\theta)]$$

(A.33) becomes $v'_x = A + B\,G + C\,F + D\,E$ so that

$$\begin{aligned} v'^{2}_{x} = {} & A^2 + ABG + ACF + ADE \\ & + BGA + B^2 G^2 + BGCF + BGDE \\ & + CFA + CFBG + C^2 F^2 + CFDE \\ & + DEA + DEBG + DECF + D^2 E^2 \end{aligned} \ . \tag{A.35}$$

Note that averaging over azimuthal angle, ϕ , results in

$$\langle F\rangle_\phi = 0 \; ; \left\langle F^2\right\rangle_\phi = \frac{s^2}{2}\sin^2\theta \; ; \langle E\rangle_\phi = 0 \; ;$$

$$\left\langle E^2\right\rangle_\phi = \frac{s^2}{2}\sin^2\theta \; ; \langle FE\rangle_\phi = 0 \qquad \text{(A.36)}$$

so that (A.35) reduces to

$$\left\langle v_x'^2\right\rangle_\phi = A^2 + 2ABG + B^2G^2 + C^2\left\langle F^2\right\rangle_\phi + D^2\left\langle E^2\right\rangle_\phi . \qquad \text{(A.37)}$$

Using the expression for G^2 in (A.11) and the definitions in (A.34),

$$\begin{aligned}\left\langle v_x'^2\right\rangle_\phi &= w_x^2 + 2w_x\left(v_x - w_x\right)[1 - s(1-\cos\theta)] \\ &+ \left(v_x - w_x\right)^2\left[1 - 2s(1-s)(1-\cos\theta) - s^2\sin^2\theta\right] \\ &+ \left[\frac{\left(R_yX_z - R_zX_y\right)^2 + X_x^2R^2}{X^2}\right]\frac{s^2}{2}\sin^2\theta\end{aligned} \qquad \text{(A.38)}$$

Averaging over scattering angle in the center-of-mass reference frame and making use of the cross-sections defined in (A.4)-(A.6) yields,

$$\begin{aligned}\left\langle v_x'^2\right\rangle &= w_x^2 + 2w_x\left(v_x - w_x\right)\left[1 - s\frac{\sigma^{mt}}{\sigma^{el}}\right] \\ &+ \left(v_x - w_x\right)^2\left[1 - 2s(1-s)\frac{\sigma^{mt}}{\sigma^{el}} - s^2\frac{\sigma^{vis}}{\sigma^{el}}\right] \\ &+ \left[\frac{\left(R_yX_z - R_zX_y\right)^2 + X_x^2R^2}{X^2}\right]\frac{s^2}{2}\frac{\sigma^{vis}}{\sigma^{el}}\end{aligned} \qquad \text{(A.39)}$$

The bracketed term in (A.39) can be written as

$$\frac{\left(R_y X_z - R_z X_y\right)^2 + X_x^2 R^2}{X^2}$$

$$= \frac{R_y^2 X_z^2 - 2R_y X_z R_z X_y + R_z^2 X_y^2 + X_x^2 R^2}{X^2}$$

$$= \frac{R_y^2 X_z^2 - 2R_y X_z R_z X_y + R_z^2 X_y^2 + X_x^2 (R_x^2 + R_y^2 + R_z^2)}{X_x^2 + X_y^2 + X_z^2}$$

$$= \frac{(R_y^2 + R_z^2)X_z^2 - R_z^2 X_z^2 - 2R_y X_z R_z X_y + (R_y^2 + R_z^2)X_y^2 - R_y^2 X_y^2 + (R_y^2 + R_z^2)X_x^2 + R_x^2 X_x^2}{X_x^2 + X_y^2 + X_z^2}$$

$$= (R_y^2 + R_z^2) + \frac{-R_z^2 X_z^2 - 2R_y X_z R_z X_y - R_y^2 X_y^2 + R_x^2 X_x^2}{X_x^2 + X_y^2 + X_z^2}$$

$$= (R_y^2 + R_z^2) + \frac{R_x^2 X_x^2 - \left(R_z X_z + R_y X_y\right)^2}{X_x^2 + X_y^2 + X_z^2} \tag{A.40}$$

Noting that

$$\begin{aligned} \underline{R} \cdot \underline{X} = 0 &= R_x X_x + R_y X_y + R_z X_z \\ R_y X_y + R_z X_z &= -R_x X_x \end{aligned}, \tag{A.41}$$

(A.40) becomes

$$\frac{\left(R_y X_z - R_z X_y\right)^2 + X_x^2 R^2}{X^2} = R_y^2 + R_z^2 = \left(v_y - w_y\right)^2 + \left(v_z - w_z\right)^2 \tag{A.42}$$

Collecting terms, (A.39) reduces to,

$$\begin{aligned} \left\langle v_x'^2 \right\rangle = w_x^2 + 2w_x\left(v_x - w_x\right)\left[1 - s\frac{\sigma^{mt}}{\sigma^{el}}\right] + \left(v_x - w_x\right)^2\left[1 - 2s(1-s)\frac{\sigma^{mt}}{\sigma^{el}}\right] \\ + \left[\left(v_y - w_y\right)^2 + \left(v_z - w_z\right)^2 - 2\left(v_x - w_x\right)^2\right]\frac{s^2}{2}\frac{\sigma^{vis}}{\sigma^{el}} \end{aligned} \tag{A.43}$$

This result is seen to be a consistent generalization of (A.31). It is useful to manipulate this equation into a different form,

$$\left\langle v_x'^2 \right\rangle = w_x^2 + 2w_x\left(v_x - w_x\right)\left[1 - s\frac{\sigma^{mt}}{\sigma^{el}}\right] + \left(v_x - w_x\right)^2\left[1 - 2s(1-s)\frac{\sigma^{mt}}{\sigma^{el}}\right]$$
$$+\left[\left(v_y - w_y\right)^2 + \left(v_z - w_z\right)^2 - 2\left(v_x - w_x\right)^2\right]\frac{s^2}{2}\frac{\sigma^{vis}}{\sigma^{el}}$$

$$\left\langle v_x'^2 \right\rangle = w_x^2 + 2w_x\left(v_x - w_x\right) - 2w_x\left(v_x - w_x\right)s\frac{\sigma^{mt}}{\sigma^{el}}$$
$$+\left(v_x - w_x\right)^2 - \left(v_x - w_x\right)^2\left[2s(1-s)\frac{\sigma^{mt}}{\sigma^{el}}\right]$$
$$+\left[\left(v_y - w_y\right)^2 + \left(v_z - w_z\right)^2 - 2\left(v_x - w_x\right)^2\right]\frac{s^2}{2}\frac{\sigma^{vis}}{\sigma^{el}}$$

$$\left\langle v_x'^2 \right\rangle = w_x^2 + 2w_xv_x - 2w_x^2 - 2w_x\left(v_x - w_x\right)s\frac{\sigma^{mt}}{\sigma^{el}}$$
$$+v_x^2 - 2w_xv_x + w_x^2 - \left(v_x - w_x\right)^2\left[2s(1-s)\frac{\sigma^{mt}}{\sigma^{el}}\right]$$
$$+\left[\left(v_y - w_y\right)^2 + \left(v_z - w_z\right)^2 - 2\left(v_x - w_x\right)^2\right]\frac{s^2}{2}\frac{\sigma^{vis}}{\sigma^{el}}$$

$$\left\langle v_x'^2 \right\rangle = v_x^2 - 2w_x\left(v_x - w_x\right)s\frac{\sigma^{mt}}{\sigma^{el}} - \left(v_x - w_x\right)^2\left[2s(1-s)\frac{\sigma^{mt}}{\sigma^{el}}\right]$$
$$+\left[\left(v_y - w_y\right)^2 + \left(v_z - w_z\right)^2 - 2\left(v_x - w_x\right)^2\right]\frac{s^2}{2}\frac{\sigma^{vis}}{\sigma^{el}}$$

$$\left\langle v_x'^2 \right\rangle = v_x^2 - 2\left(v_x - w_x\right)\left[w_x + \left(v_x - w_x\right)(1-s)\right]s\frac{\sigma^{mt}}{\sigma^{el}}$$
$$+\left[\left(v_y - w_y\right)^2 + \left(v_z - w_z\right)^2 - 2\left(v_x - w_x\right)^2\right]\frac{s^2}{2}\frac{\sigma^{vis}}{\sigma^{el}}$$

$$\left\langle v_x'^2 \right\rangle = v_x^2 - 2\left(v_x - w_x\right)\left[w_x + \left(v_x - w_x\right) - s\left(v_x - w_x\right)\right]s\frac{\sigma^{mt}}{\sigma^{el}}$$
$$+\left[\left(v_y - w_y\right)^2 + \left(v_z - w_z\right)^2 - 2\left(v_x - w_x\right)^2\right]\frac{s^2}{2}\frac{\sigma^{vis}}{\sigma^{el}}$$

leading to the final result,

$$\left\langle v_x'^2 \right\rangle = v_x^2 - 2\left(v_x - w_x\right)\left[v_x - s\left(v_x - w_x\right)\right]s\frac{\sigma^{mt}}{\sigma^{el}}$$
$$+\left[\left(v_y - w_y\right)^2 + \left(v_z - w_z\right)^2 - 2\left(v_x - w_x\right)^2\right]\frac{s^2}{2}\frac{\sigma^{vis}}{\sigma^{el}} \qquad \text{(A.44)}$$

A.7.1 Special case: $m_a = M_b$

For the special case when particle a has the same mass as particle b ($s = \frac{1}{2}$), (A.44) becomes

$$\left\langle v_x'^2 \right\rangle = v_x^2 - \left(v_x - w_x\right)\left[v_x - \frac{1}{2}\left(v_x - w_x\right)\right]\frac{\sigma^{mt}}{\sigma^{el}} + \left[\left(v_y - w_y\right)^2 + \left(v_z - w_z\right)^2 - 2\left(v_x - w_x\right)^2\right]\frac{1}{8}\frac{\sigma^{vis}}{\sigma^{el}}$$

$$\left\langle v_x'^2 \right\rangle = v_x^2 - \left(v_x - w_x\right)\left(v_x + w_x\right)\frac{1}{2}\frac{\sigma^{mt}}{\sigma^{el}} + \left[\left(v_y - w_y\right)^2 + \left(v_z - w_z\right)^2 - 2\left(v_x - w_x\right)^2\right]\frac{1}{8}\frac{\sigma^{vis}}{\sigma^{el}}$$

Leading to the useful result,

$$\left\langle v_x'^2 \right\rangle = v_x^2 + \left(w_x^2 - v_x^2\right)\frac{1}{2}\frac{\sigma^{mt}}{\sigma^{el}} + \left[\left(v_y - w_y\right)^2 + \left(v_z - w_z\right)^2 - 2\left(v_x - w_x\right)^2\right]\frac{1}{8}\frac{\sigma^{vis}}{\sigma^{el}} \qquad \text{(A.45)}$$

Appendix B: Relaxation Rates for BKG Elastic Collision Model

B.1 ω^{el} for Mixed Collisions: Inferred from Momentum Transfer Rate

From (A.9), the average change in x-directed momentum for particle a (initial velocity $\underline{v}$ in lab frame, final velocity $\underline{v'}$ in lab frame, mass m_a) colliding on particle b (initial velocity $\underline{w}$ in lab frame, mass M_b) is

$$m_a\left(\langle v_x' \rangle - v_x\right) = -\left(v_x - w_x\right)\frac{m_a M_b}{m_a + M_b}\frac{\sigma^{mt}}{\sigma^{el}} \qquad . \qquad \text{(B.1)}$$

For velocity distributions f_a and f_b, the rate of x-directed momentum transfer from the b to a species is

$$R^{mt}_{b\to a} = -\frac{m_a M_b}{m_a + M_b}\int\int f_a(\underline{v})\, f_b(\underline{w})(v_x - w_x)\sigma^{mt}_{a:b}|\underline{v} - \underline{w}|\partial^3 w \partial^3 v. \qquad \text{(B.2)}$$

As an aside, it is noted that this result can also be obtained directly (but somewhat less intuitively) from the collision integral. $R^{mt}_{b\to a}$ corresponds to the v_x moment of the collision integral,

$$R^{mt}_{b\to a} = m_a \int\int\int [\, f_a(\underline{v'})\, f_b(\underline{w'}) - f_a(\underline{v})\, f_b(\underline{w})]\; v_x\; |\underline{v} - \underline{w}|\frac{\delta\sigma^{el}_{a:b}(|\underline{v} - \underline{w}|)}{\delta\Omega}\delta\Omega\partial^3 w \partial^3 v\,,$$

which can also be written as

$$\begin{aligned} R^{mt}_{b\to a} &= m_a \int\int\int f_a(v_x'\{v_x, w_x\})\, f_b(w_x'\{v_x, w_x\})\, v_x\; |\underline{v} - \underline{w}|\frac{\delta\sigma^{el}_{a:b}(|\underline{v} - \underline{w}|)}{\delta\Omega}\delta\Omega\partial^3 w \partial^3 v \;. \\ &- m_a \int\int\int f_a(\underline{v})\, f_b(\underline{w}) v_x\; |\underline{v} - \underline{w}|\frac{\delta\sigma^{el}_{a:b}(|\underline{v} - \underline{w}|)}{\delta\Omega}\delta\Omega\partial^3 w \partial^3 v \end{aligned}$$

The notation is a reminder that v_x' and w_x' are functions of v_x and w_x, related by the kinematics of the elastic collision. Consider that f_a and f_b can be written as a summation of delta-functions in velocity. We can obtain the contribution to the collision integral for the case when f_a and f_b correspond to single terms in the summation, $f_a = \varepsilon_a \delta(\underline{v}_a)$ and $f_b = \varepsilon_b \delta(\underline{w}_b)$. Then we can compute the full collision integral for arbitrary f_a and f_b by summing over the appropriately weighted delta function contributions. For the single delta-function choice of f_a and f_b,

$$R^{mt}_{b\to a} = m_a \varepsilon_a \varepsilon_b \int v'_x |\underline{v}' - \underline{w}'| \frac{\delta\sigma^{el}_{a:b}(|\underline{v}' - \underline{w}'|)}{\delta\Omega} \delta\Omega$$
$$- m_a \varepsilon_a \varepsilon_b v'_x |\underline{v} - \underline{w}| \int \frac{\delta\sigma^{el}_{a:b}(|\underline{v} - \underline{w}|)}{\delta\Omega} \delta\Omega \quad ,$$

and noting that $|\underline{v}' - \underline{w}'| = |\underline{v} - \underline{w}|$ for elastic collisions,

$$R^{mt}_{b\to a} = m_a \varepsilon_a \varepsilon_b |\underline{v} - \underline{w}| \int (v'_x - v_x) \frac{\delta\sigma^{el}_{a:b}(|\underline{v} - \underline{w}|)}{\delta\Omega} \delta\Omega$$

where $v'_x(\underline{\Omega})$ and $w'_x(\underline{\Omega})$ are a set of all possible a and b particle velocities pairs before collision that lead to velocities v_x and w_x after collision. But this is just a single elastic collision event described in reverse. Since the collision process is reversible, one can consider $v'_x(\underline{\Omega})$ and $w'_x(\underline{\Omega})$ to be the set of all possible a and b particle velocities pairs after a collision between particles with initial velocities v_x and w_x. Using (A.8) to substitute for $v'_x - v_x$ and the performing integration in azimuthal angle,

$$R^{mt}_{b\to a} = -\varepsilon_a \varepsilon_b \frac{m_a M_b}{m_a + M_b} (v_x - w_x) |\underline{v} - \underline{w}| 2\pi \int_0^\pi (1 - \cos\theta) \frac{\delta\sigma^{el}_{a:b}}{\delta\Omega} \sin\theta \, \partial\theta,$$

and with the definition of momentum transfer cross-section,

$$R^{mt}_{b\to a} = -\varepsilon_a \varepsilon_b \frac{m_a M_b}{m_a + M_b} (v_x - w_x) |\underline{v} - \underline{w}| \sigma^{mt}_{a:b}(|\underline{v} - \underline{w}|).$$

Summing over all delta functions comprising f_a and f_b leads to

$$R^{mt}_{b\to a} = -\frac{m_a M_b}{m_a + M_b} \int\int f_a(\underline{v}) f_b(\underline{w}) (v_x - w_x) |\underline{v} - \underline{w}| \sigma^{mt}_{a:b}(|\underline{v} - \underline{w}|) \partial^3 w \partial^3 v,$$

which is identical to the result obtained above.

For mixed binary collisions, we desire a value of ω^{el} such that $R^{mt}_{b\to a}$ derived from the BKG collision model agree with that obtained from the full collision integral, (B.2). From the BKG model,

$$\begin{aligned} R^{mt}_{b\to a} &= \omega^{el}_{a:b} m_a \int (M_{a:b} - f_a(\underline{v})) v_x \partial^3 v \\ &= \omega^{el}_{a:b} m_a \left(U_{x\,a:b} - U_{x\,a} \right) \end{aligned} \qquad \text{(B.3)}$$

$U_{x\,a:b}$ is defined in the BKG model as

$$U_{x\,a:b} = (m_a U_{x\,a} + M_b U_{x\,b})/(m_a + M_b).$$

Therefore (B.3) becomes

$$\begin{aligned} R^{mt}_{b\to a} &= \omega^{el}_{a:b} m_a \int (M_{a:b} - f_a(\underline{v}))v_x \partial^3 v \\ &= \omega^{el}_{a:b} n_a m_a \left(\frac{m_a U_{x\,a} + M_b U_{x\,b}}{m_a + M_b} - U_{x\,a} \right). \\ &= \omega^{el}_{a:b} \frac{m_a M_b}{m_a + M_b} n_a \left(U_{x\,b} - U_{x\,a} \right) \end{aligned} \qquad \text{(B.4)}$$

Equating (B.2) and (B.4) results in

$$\omega^{el}_{a:b} = \frac{1}{n_a \left(U_{x\,a} - U_{x\,b} \right)} \int\int f_a(\underline{v}) f_b(\underline{w})(v_x - w_x)\sigma^{mt}_{a:b} |\underline{v} - \underline{w}| \partial^3 w \partial^3 v. \qquad \text{(B.5)}$$

B.2 ω^{el} for Self -Collisions: Inferred from Temperature Isotropization Rate

From (A.45), the average change in the energy associated with motion along the x-axis of particle a colliding on particle b (both particles having mass m_a) is

$$\begin{aligned} \frac{1}{2} m_a \left(\left\langle v_x'^2 \right\rangle - v_x^2 \right) &= \frac{1}{2} m_a \left(w_x^2 - v_x^2 \right) \frac{1}{2} \frac{\sigma^{mt}}{\sigma^{el}} \\ &+ \frac{1}{2} m_a \left[\left(v_y - w_y \right)^2 + \left(v_z - w_z \right)^2 - 2\left(v_x - w_x \right)^2 \right] \frac{1}{8} \frac{\sigma^{vis}}{\sigma^{el}} \end{aligned} . \qquad \text{(B.6)}$$

For velocity distribution f_a $(= f_b)$, the rate of increase in the energy of the distribution function associated with particle motion along the x-axis is

$$\begin{aligned} R_{Tx} &= \frac{1}{2} m_a \int\int f_a(\underline{v}) f_a(\underline{w}) \left(w_x^2 - v_x^2 \right) \frac{1}{2} \sigma^{mt}_{a:a} |\underline{v} - \underline{w}| \partial^3 w \partial^3 v \\ &+ \frac{1}{2} m_a \int\int f_a(\underline{v}) f_a(\underline{w}) \left[\left(v_y - w_y \right)^2 + \left(v_z - w_z \right)^2 - 2\left(v_x - w_x \right)^2 \right] \frac{1}{8} \sigma^{vis}_{a:a} |\underline{v} - \underline{w}| \partial^3 w \partial^3 v \end{aligned} \qquad \text{(B.7)}$$

$$R_{Tx} = \frac{1}{2} m_a \int\int f_a(\underline{v}) f_a(\underline{w}) \left(w_x^2\right) \frac{1}{2} \sigma_{a:a}^{mt} |\underline{v} - \underline{w}| \partial^3 w \partial^3 v$$
$$- \frac{1}{2} m_a \int\int f_a(\underline{v}) f_a(\underline{w}) \left(v_x^2\right) \frac{1}{2} \sigma_{a:a}^{mt} |\underline{v} - \underline{w}| \partial^3 w \partial^3 v$$
$$+ \frac{1}{2} m_a \int\int f_a(\underline{v}) f_a(\underline{w}) \left[\left(v_y - w_y\right)^2 + \left(v_z - w_z\right)^2 - 2\left(v_x - w_x\right)^2\right] \frac{1}{8} \sigma_{a:a}^{vis} |\underline{v} - \underline{w}| \partial^3 w \partial^3 v \quad \text{(B.8)}$$

By symmetry, the first two integrals involving w_x^2 and v_x^2 cancel, leaving

$$R_{Tx} = \frac{1}{16} m_a \int\int f_a(\underline{v}) f_a(\underline{w}) \left[\left(v_y - w_y\right)^2 + \left(v_z - w_z\right)^2 - 2\left(v_x - w_x\right)^2\right] \sigma_{a:a}^{vis} |\underline{v} - \underline{w}| \partial^3 w \partial^3 v \quad \text{(B.9)}$$

For self-collisions, we desire a value of ω^{el} such that R_{Tx} derived from the BKG collision model agrees with (B.9). From the BKG model,

$$\begin{aligned} R_{Tx} &= \omega_{a:a}^{el} \frac{1}{2} m_a \int \left(M_{a:a} - f_a(\underline{v})\right) \left[2v_x^2 - v_r^2\right] \partial^3 v \\ &= \omega_{a:a}^{el} \frac{1}{2} m_a \int \left(M_{a:a} - f_a(\underline{v})\right) \left[2\left(v_x - U_x\right)^2 - v_r^2\right] \partial^3 v \\ &\quad + \omega_{a:a}^{el} \frac{1}{2} m_a \int \left(M_{a:a} - f_a(\underline{v})\right) 2\left[2v_x U_x - U_x^2\right] \partial^3 v \end{aligned} \quad \text{(B.10)}$$

$$\begin{aligned} R_{Tx} &= \omega_{a:a}^{el} \frac{1}{2} m_a \int f_a(\underline{v}) \left[v_r^2 - 2\left(v_x - U_x\right)^2\right] \partial^3 v \\ &\quad + \omega_{a:a}^{el} \frac{1}{2} m_a \int \left(M_{a:a} - f_a(\underline{v})\right) 2\left[2v_x U_x - U_x^2\right] \partial^3 v \\ &= \omega_{a:a}^{el} \frac{1}{2} m_a \int f_a(\underline{v}) \left[v_r^2 - 2\left(v_x - U_x\right)^2\right] \partial^3 v \\ &\quad + \omega_{a:a}^{el} \frac{1}{2} m_a 2\left[n_a U_x^2 - n_a U_x^2\right] \end{aligned} \quad \text{(B.11)}$$

$$R_{Tx} = \omega_{a:a}^{el} \frac{1}{2} m_a \int f_a(\underline{v}) \left[v_r^2 - 2\left(v_x - U_x\right)^2\right] \partial^3 v \quad \text{(B.12)}$$

Equating (B.9) and (B.12) results in

$$\omega_{a:a}^{el} = \frac{1}{8}\frac{\int\int f_a(\underline{v}) f_a(\underline{w})\left[\left(v_y - w_y\right)^2 + \left(v_z - w_z\right)^2 - 2\left(v_x - w_x\right)^2\right]\sigma_{a:a}^{vis}|\underline{v} - \underline{w}|\partial^3 w \partial^3 v}{\int f_a(\underline{v})\left[v_r^2 - 2\left(v_x - U_x\right)^2\right]\partial^3 v}.$$

(B.13)

For the case when f_a has rotational symmetry about the v_x axis, the velocities perpendicular to v_x can be written as

$$v_y = v_r \;;\; v_z = 0 \;;\; v_r^2 = v_y^2 + v_z^2$$
$$w_y = w_r \cos\gamma \;;\; w_z = w_r \sin\gamma \;;\; w_r^2 = w_y^2 + w_z^2$$

and (B.13) becomes

$$\omega_{a:a}^{el} =$$
$$\frac{2\pi}{8}\frac{\int\int f_a(\underline{v}) f_a(\underline{w})\left[v_r^2 + w_r^2 - 2v_r w_r \cos\gamma - 2\left(v_x - w_x\right)^2\right]\sigma_{a:a}^{vis}|\underline{v} - \underline{w}| w_r v_r \partial\gamma\, \partial w_x \partial w_r \partial v_x \partial v_r}{\int f_a(\underline{v})\left[v_r^2 - 2\left(v_x - U_x\right)^2\right]\partial^3 v}$$

(B.14)

where integration in γ is from 0 to 2π.

Appendix C: Procedure in KN1D to 'adjust' the normalization of the molecular source profile on the sides of the limiters (S_pH_2) arising from plasma neutralization to attain a net zero atom/molecule flux from wall

Consider the following picture of atomic and molecular fluxes:

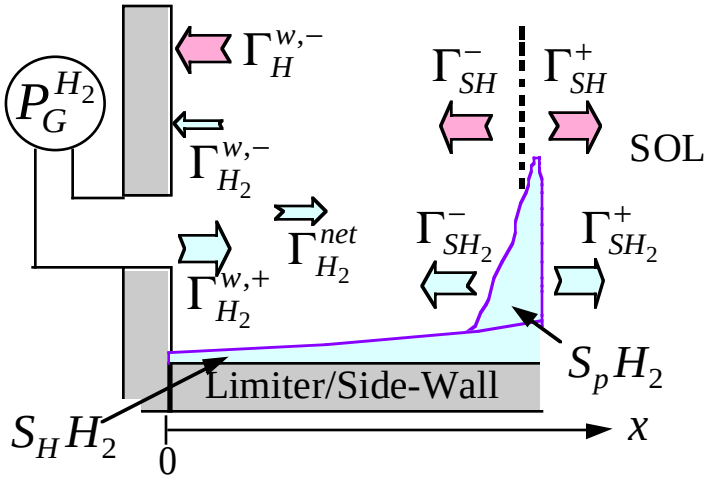

C.1 Molecular Fluxes

The molecular neutral pressure is measured by the ionization gauge ($P_G^{H_2}$). Owing to frequent collisions with the tubes and walls of the gauge, it is assumed that this pressure reflects the density of molecules in the gauge at room temperature, n_G. The flux of molecules leaving the gauge tube is therefore equal to the flux corresponding to a half-Maxwellian at the density, n_G, and wall temperature, T_w. This flux is presumed to be characteristic of the flux of molecules heading from all locations on the wall towards the plasma,

$$\Gamma_{H_2}^{w,+} = \frac{1}{4} n_G \bar{v} \; ; \; \bar{v} \equiv \sqrt{\frac{8\,kT_w}{\pi\, m_{H_2}}}. \qquad \text{(C.1)}$$

Plasma striking the side of the limiter (the single limiter surfaces here represents two limiters) yields a molecular neutral source profile, S_pH_2. Atoms striking the side of the limiter (and other 'pipes' connecting to the gauge location) yields a molecular neutral source profile, S_HH_2. The sum of these source profiles is designated as SH_2. The molecules born in the source are presumed to enter the volume as a half-Maxwellian distribution at the wall temperature with an average velocity vector that is normal to the limiter surface. As a result, half of the molecules initially proceed in the positive x

direction ($\Gamma^{+}_{S_pH_2}, \Gamma^{+}_{S_HH_2}$) and half of the molecules initially proceed negative x direction ($\Gamma^{-}_{S_pH_2}, \Gamma^{-}_{S_HH_2}$). These directed fluxes, if not attentuated, must balance the corresponding spatial integrals of the molecular sources,

$$\Gamma^{+}_{S_pH_2} = \Gamma^{-}_{S_pH_2} = \frac{1}{2}\int S_pH_2 \partial x$$
$$\Gamma^{+}_{S_HH_2} = \Gamma^{-}_{S_HH_2} = \frac{1}{2}\int S_HH_2 \partial x \quad . \qquad \text{(C.2)}$$

Most all of the molecules which head in the direction of the plasma, promptly undergo ionization, dissociation, and dissociative ionization. Very few are expected to experience elastic scattering or charge exchange. Consequently this flux converts into a source of atomic neutrals and ions. Some of the molecules heading in the direction of the wall may also be converted into atomic neutrals and ions. Let the fraction of this molecular flux that makes it to the wall be designated as ε so that

$$\Gamma^{w,-}_{H_2} = \varepsilon\left(\Gamma^{-}_{S_pH_2} + \Gamma^{-}_{S_HH_2}\right). \qquad \text{(C.3)}$$

The net molecular flux heading toward the plasma from the wall is therefore

$$\Gamma^{net}_{H_2} = \Gamma^{w,+}_{H_2} - \Gamma^{w,-}_{H_2} = \Gamma^{w,+}_{H_2} - \varepsilon\left(\Gamma^{-}_{S_pH_2} + \Gamma^{-}_{S_HH_2}\right),$$

$$\boxed{\Gamma^{net}_{H_2} = \Gamma^{w,+}_{H_2} - \frac{\varepsilon}{2}\int S_pH_2 \partial x - \frac{\varepsilon}{2}\int S_HH_2 \partial x \quad .} \qquad \text{(C.4)}$$

Note that $\Gamma^{w,+}_{H_2}$ is specified by the gauge pressure reading through Eq. (C.1).

C.2 Atomic Fluxes

The atomic hydrogen flux onto the wall can now be estimated. Atomic hydrogen is formed by molecular breakup. Through dissociative ionization, a small fraction of the molecular dissociation ($R^{H^+}_{dis}$) results in the formation of hydrogen ions rather than hydrogen atoms. The fraction of molecular dissociation resulting in atomic hydrogen products can be designated as $R^{H^0}_{dis}$, $R^{H^0}_{dis} + R^{H^+}_{dis} = 1.$

The dissociation process results in hydrogen products with Frank-Condon dissociation energies (~ 3 eV). Ignoring the fluid velocity of the molecular neutrals, the isotropic breakup of the molecules

results in an equal, oppositely directed flux of atomic hydrogen heading towards the plasma ($\Gamma^{+}_{S_pH}, \Gamma^{+}_{S_HH}$) and the wall ($\Gamma^{-}_{S_pH}, \Gamma^{-}_{S_HH}$).

Hydrogen atoms are formed from the interaction of five molecular fluxes with the plasma, $\Gamma^{w,+}_{H_2}$, $\Gamma^{+}_{S_pH}$, $\Gamma^{+}_{S_HH}$, $\Gamma^{-}_{S_pH}$ and $\Gamma^{-}_{S_HH}$. Accounting for the factors ε and $R^{H^0}_{dis}$, conservation of hydrogen nuclei yields the approximate relationship,

$$\Gamma^{-}_{SH} + \Gamma^{+}_{SH} = 2R^{H^0}_{dis}\left[(1-\varepsilon)\left(\Gamma^{-}_{S_pH_2} + \Gamma^{-}_{S_HH_2}\right) + \Gamma^{+}_{S_pH_2} + \Gamma^{+}_{S_HH_2} + \Gamma^{w,+}_{H_2}\right]. \quad \text{(C.5)}$$

Some fraction of the atomic flux, Γ^{+}_{SH}, becomes converted via charge exchange into a flux heading back to the wall. Some of the atomic flux (fraction $1-\delta$) hits the side-walls and does not make it to the wall. Defining an 'albedo' of the SOL plasma to this atomic hydrogen flux as α, the portion of the atomic hydrogen flux onto the wall is

$$\Gamma^{w,-}_{H} = \delta\left(\Gamma^{-}_{SH} + \alpha\Gamma^{+}_{SH}\right) \quad , \quad \text{(C.6)}$$

which from Eq. (C.5) with $\Gamma^{-}_{SH} = \Gamma^{+}_{SH}$ is

$$\Gamma^{w,-}_{H} = \delta(1+\alpha)R^{H^0}_{dis}\left[(1-\varepsilon)\left(\Gamma^{-}_{S_pH_2} + \Gamma^{-}_{S_HH_2}\right) + \Gamma^{+}_{S_pH_2} + \Gamma^{+}_{S_HH_2} + \Gamma^{w,+}_{H_2}\right]. \quad \text{(C.7)}$$

From Eq. (2),

$$\Gamma^{w,-}_{H} = \delta(1+\alpha)R^{H^0}_{dis}\left[\frac{2-\varepsilon}{2}\left(\int S_pH_2\,\partial x + \int S_HH_2\,\partial x\right) + \Gamma^{w,+}_{H_2}\right]. \quad \text{(C.8)}$$

C.3 Normalization of S_pH_2 Required for Atomic/Molecular Flux Balance

C.3.1 First-Guess Estimate of S_pH_2 normalization

The net flux of hydrogen molecules from the wall must balance 2 times the hydrogen atom flux onto the wall,

$$2\Gamma^{net}_{H_2} = \Gamma^{w,-}_{H} \quad . \quad \text{(C.9)}$$

From Eqs. (C.4) and (C.9),

$$2\Gamma_{H_2}^{w,+} - \varepsilon \int SH_2 \partial x = \delta(1+\alpha) R_{dis}^{H^0} \left[\frac{2-\varepsilon}{2} \int SH_2 \partial x + \Gamma_{H_2}^{w,+} \right]$$

$$\left[2 - \delta(1+\alpha) R_{dis}^{H^0} \right] \Gamma_{H_2}^{w,+} = \delta(1+\alpha) R_{dis}^{H^0} \left[\frac{2-\varepsilon}{2} \int SH_2 \partial x \right] + \varepsilon \int SH_2 \partial x$$

$$\left[2 - \delta(1+\alpha) R_{dis}^{H^0} \right] \Gamma_{H_2}^{w,+} = \left[\frac{2-\varepsilon}{2} \delta(1+\alpha) R_{dis}^{H^0} + \varepsilon \right] \int SH_2 \partial x$$

This requires the spatial integral of the molecular neutral source to satisfy,

$$\int S_p H_2 \partial x + \int S_H H_2 \partial x = \frac{2 - \delta(1+\alpha) R_{dis}^{H^0}}{\frac{2-\varepsilon}{2} \delta(1+\alpha) R_{dis}^{H^0} + \varepsilon} \Gamma_{H_2}^{w,+} \quad . \qquad \text{(C.10)}$$

For $\alpha \approx 0$, $R_{dis}^{H^0} \approx 1$, and $\varepsilon \approx 1$, $\delta \approx 1$, $\int S_H H_2 \partial x \approx 0$

$$\int S_p H_2 \partial x \approx \frac{1}{\frac{1}{2} + 1} \Gamma_{H_2}^{w,+} = \frac{2}{3} \Gamma_{H_2}^{w,+} \quad . \qquad \text{(C.11)}$$

This provides a reasonable first-guess estimate for the normalization of the $S_p H_2$ profile.

C. 3.2 Refinement of $S_p H_2$

After each iterative refinement of f_{H_2} and f_H from procedures **`Kinetic_H2`** and **`Kinetic_H`**, the mass balance of Eq. (C.9) can be tested, leading to a flux error of

$$E_H = 2\Gamma_{H_2}^{net} - \Gamma_H^{w,-} \quad . \qquad \text{(C.12)}$$

We want to adjust the normalization of $S_p H_2$ such that its spatial integral yields $E_H \approx 0$ in the next iteration. Let S_I represent the spatial integral of $S_p H_2$,

$$S_I \equiv \int S_p H_2 \partial x. \qquad \text{(C.13)}$$

From Eq. (C.12),

$$\frac{\partial E_H}{\partial S_I} = 2\frac{\partial \Gamma_{H_2}^{net}}{\partial S_I} - \frac{\partial \Gamma_H^{w,-}}{\partial S_I}$$

and using Eqs. (C.4) and (C.8)

$$\frac{\partial E_H}{\partial S_I} = -\varepsilon - \delta(1+\alpha)R_{dis}^{H^0}\frac{2-\varepsilon}{2} \quad . \qquad \text{(C.14)}$$

Using the results from the most recent iteration, parameters ε and $\delta(1+\alpha)R_{dis}^{H^0}$ can be estimated. From Eqs. (C.2) and (C.3),

$$\varepsilon = \frac{\Gamma_{H_2}^{w,-}}{\Gamma_{S_p H_2}^{-} + \Gamma_{S_H H_2}^{-}} = \frac{2\Gamma_{H_2}^{w,-}}{S_I + \int S_H H_2 \partial x} \quad , \qquad \text{(C.15)}$$

and from Eq. (C.8),

$$\delta(1+\alpha)R_{dis}^{H^0} = \frac{\Gamma_H^{w,-}}{\frac{2-\varepsilon}{2}\left(S_I + \int S_H H_2 \partial x\right) + \Gamma_{H_2}^{w,+}} . \qquad \text{(C.16)}$$

In order to make E_H closer to zero in the next iteration, S_I needs to be 'adjusted' such that

$$E_H + \frac{\partial E_H}{\partial S_I}\Delta S_I = 0 \quad , \qquad \text{(C.17)}$$

making use of Eqs. (C.12)-(C.16) and the values of $\Gamma_{H_2}^{w,-}$ and $\Gamma_H^{w,-}$ from the present iteration. Note that $\Gamma_{H_2}^{w,+}$ remains the same for all iterations, being constrained by the gauge measurement , Eq. (C.1).

References

[1] Research Systems Inc., Interactive Data Language (IDL®).

[2] Johnson, L.C. and Hinnov, E., Journal of Quantitative Spectroscopy & Radiative Transfer **13** (1973) 333.

[3] Janev, R.K., Elementary processes in hydrogen-helium plasmas : cross sections and reaction rate coefficients (Springer-Verlag, Berlin ; New York, 1987).

[4] Sawada, K. and Fujimoto, T., Journal of Applied Physics **78** (1995) 2913.

[5] Janev, R.K., et al., J. Nucl. Mater. **121** (1984) 10.

[6] Naval Research Laboratory, NRL Plasma Formulary.

[7] Janev, R.K., Atomic and molecular processes in fusion edge plasmas (Plenum Press, New York, 1995).

[8] Reiter, D., May, C., Baelmans, M., and Boerner, P., Elsevier. Journal of Nuclear Materials **241** (1997) 342.

[9] Fantz, U., Behringer, K., Gafert, J., and Coster, D., Elsevier. Journal of Nuclear Materials **266** (1999) 490.

[10] Bhatnagar, P.L., Gross, E.P., and Krook, M., Phys. Rev. **94** (1954) 511.

[11] Morse, T., Physics of Fluids **7** (1964) 2012.

[12] Hamel, B., Physics of Fluids **8** (1965) 418.

[13] Henry, A.F., Nuclear-reactor analysis (MIT Press, Cambridge, Mass., 1975).